CENPD - 269 - NP

EXTENDED BURNUP OPERATION of COMBUSTION ENGINEERING PWR FUEL

NUCLEAR POWER SYSTEMS

APRIL, 1982

POWER SYSTEMS
COMBUSTION ENGINEERING, INC.

LEGAL NOTICE

THIS REPORT WAS PREPARED AS AN ACCOUNT OF WORK SPONSORED BY COMBUSTION ENGINEERING, INC. NEITHER COMBUSTION ENGINEERING NOR ANY PERSON ACTING ON ITS BEHALF:

A. MAKES ANY WARRANTY OR REPRESENTATION, EXPRESS OR IMPLIED INCLUDING THE WARRANTIES OF FITNESS FOR A PARTICULAR PURPOSE OR MERCHANTABILITY, WITH RESPECT TO THE ACCURACY, COMPLETENESS, OR USEFULNESS OF THE INFORMATION CONTAINED IN THIS REPORT, OR THAT THE USE OF ANY INFORMATION, APPARATUS, METHOD, OR PROCESS DISCLOSED IN THIS REPORT MAY NOT INFRINGE PRIVATELY OWNED RIGHTS; OR

B. ASSUMES ANY LIABILITIES WITH RESPECT TO THE USE OF, OR FOR DAMAGES RESULTING FROM THE USE OF, ANY INFORMATION, APPARATUS, METHOD OR PROCESS DISCLOSED IN THIS REPORT.

CENPD-269-NP

EXTENDED-BURNUP OPERATION OF COMBUSTION ENGINEERING PWR FUEL

April 1982

Combustion Engineering, Inc.
Nuclear Power Systems
1000 Prospect Hill Road
Windsor, Connecticut 06095

ABSTRACT

This report describes the models presently in use by Combustion Engineering, Inc. (C-E) to calculate the performance of standard 14x14 and 16x16 fuel assembly designs to extended burnups (batch average discharge burnups up to 45 MWd/kg). The fuel performance parameters affected by increased burnup or residence time are described and the behavior phenomena governing the burnup dependence of these parameters are discussed. The models (or submodels) used by C-E to represent these fuel performance parameters are reviewed with emphasis placed on showing how burnup is included. Where applicable, a review of the current and anticipated data base supporting the models is made to demonstrate their adequacy to the target burnup value.

This report provides a basis for the generic licensing approval of C-E's fuel performance models for operation to extended burnups. By demonstrating the adequacy of the models used in analyzing fuel behavior at extended burnup, the licensing review of reload core analyses for extended-burnup fuel will be facilitated.

TABLE OF CONTENTS

Section			Page
ABSTRACT			ii
SUMMARY			x
1.	INTRODUCTION		1
	1.1	Background	1
	1.2	Report Objective and Scope	3
	1.3	Burnup Experience and Performance of C-E Fuel	5
	1.4	Extended-Burnup Research and Development Programs	10
		1.4.1 BG&E/C-E Extended-Burnup Program at Calvert Cliffs Unit 1	10
		1.4.2 EPRI/C-E Fuel Surveillance Program at Calvert Cliffs Unit 1	15
		1.4.3 EPRI/C-E Fuel Performance Evaluation in 16x16 Assemblies at Arkansas Nuclear One Unit 2	16
		1.4.4 DOE/AP&L/C-E High Burnup Program at Arkansas Nuclear One Unit 2	17
		1.4.5 DOE/OPPD/C-E High Burnup Program at Fort Calhoun	18
		1.4.6 EPRI/C-E/KWU Zircaloy Waterside Corrosion Program	18
		1.4.7 Studsvik OVER-RAMP Program	19
		1.4.8 Studsvik High Burnup SUPER-RAMP Program	20
		1.4.9 C-E/KWU Ramp Test Program in Petten	21
		1.4.10 DOE/C-E/KWU High Burnup Ramp Test Program at Petten	21
		1.4.11 BNWL High Burnup Effects Program	22
		1.4.12 Halden Program (IFA-427)	23
		1.4.13 DOE/C-E Licensing Assessment of PWR Extended-Burnup Fuel Cycles	24
	1.5	Organization of Report	25

TABLE OF CONTENTS (continued)

Section		Page
2.	FUEL ASSEMBLY DESCRIPTION	27
	2.1 Introduction	27
	2.2 Description of Structural Components	27
	2.3 Fuel Rod Description	32
	2.4 Burnable Poison Rod Description	33
3.	FUEL DESIGN BASES	36
	3.1 Introduction	36
	3.2 Functional Requirements	36
	3.3 Design Criteria	38
	3.3.1 Fatigue Damage	38
	3.3.2 Fuel Assembly Stress and Mechanical Loading	39
	3.3.3 Fuel Rod and Burnable Poison Rod Cladding Strain	39
	3.3.4 Fuel Assembly Holddown	40
	3.3.5 Mechanical Clearance	40
	3.3.6 Cladding Collapse	41
	3.3.7 Fuel and Poison Rod Internal Pressure	42
	3.3.8 Thermal-Hydraulic Design Criteria	43
	3.3.9 ECCS Acceptance Criteria	43
4.	FUEL PERFORMANCE TOPICS	44
	4.1 Fuel Rod	44
	4.1.1 Fatigue	44
	4.1.2 Cladding Corrosion	46
	4.1.3 Cladding Creep	57
	4.1.4 Cladding Collapse	59
	4.1.5 Embrittlement of Fuel Cladding	64
	4.1.6 Fission Gas Release	69

TABLE OF CONTENTS (continued)

Section		Page
	4.1.7 Fuel Thermal Conductivity	88
	4.1.8 Fuel Melting Temperature	91
	4.1.9 Fuel Swelling	92
	4.1.10 Fuel Rod Bow	95
	4.1.11 Fretting Wear	100
	4.1.12 Pellet/Cladding Interaction	104
	4.1.13 Cladding Deformation and Rupture	109
	4.1.14 Fuel Rod Growth	118
4.2	Fuel Assembly	122
	4.2.1 Guide Tube Wear	122
	4.2.2 Fuel Assembly Length Change	125
	4.2.3 Fuel Assembly Holddown	134
	4.2.4 Grid Irradiation Growth	136
	4.2.5 Spacer Grid Relaxation	139
	4.2.6 Corrosion of the Fuel Assembly Structure	140
	4.2.7 Burnable Poison Rod Behavior	146
5.	CONCLUSIONS	161
5.1	Overall Conclusions	161
5.2	Conclusions on Individual Fuel Performance Topics	163
	5.2.1 Fatigue	163
	5.2.2 Cladding Corrosion	164
	5.2.3 Cladding Creep	164
	5.2.4 Cladding Collapse	165
	5.2.5 Embrittlement of Fuel Cladding	165
	5.2.6 Fission Gas Release	165
	5.2.7 Fuel Thermal Conductivity	166
	5.2.8 Fuel Melting Temperature	166
	5.2.9 Fuel Swelling	167

TABLE OF CONTENTS (continued)

Section		Page
5.2.10	Fuel Rod Bow	167
5.2.11	Fretting Wear	167
5.2.12	Pellet/Cladding Interaction	168
5.2.13	Cladding Deformation and Rupture	168
5.2.14	Fuel Rod Growth	168
5.2.15	Guide Tube Wear	169
5.2.16	Fuel Assembly Length Change	169
5.2.17	Fuel Assembly Holddown	170
5.2.18	Grid Irradiation Growth	170
5.2.19	Spacer Grid Relaxation	171
5.2.20	Corrosion of the Fuel Assembly Structure	171
5.2.21	Burnable Poison Rod Behavior	171
6. REFERENCES		172

TABLES

Table		Page
1-1	Fuel Rod Topics	4
1-2	Fuel Assembly Topics	4
1-3	Fuel Performance Summary for C-E Reactors	8
1-4	Fuel Performance Statistics	9
2-1	Combustion Engineering Fuel Assembly Designs	30
4-1	Key Design Parameters, Operating Characteristics, and Fission Gas Release Results for Test Fuel Rods From Calvert Cliffs-1	75
4-2	The Correlation Data Base; FATES3 Predictions of Gas Release From OVER-RAMP Program Rods	78
4-3	Summary of C-E Fuel Inspection Programs Which Provided Data on Fretting Wear	103
4-4	Burnup Effects for Cladding Deformation and Rupture	112
4-5	Guide Tube Irradiation Growth Models	127
4-6	Guide Tube Axial Creep Models	128
4-7	Corrosion of BT03 Zircaloy-4 Structure After 4 Cycles	143
4-8	Burnable Poison Rod Details	148
4-9	Summary of Burnable Poison Rod Helium Release Data From C-E Sponsored Examinations	154

ILLUSTRATIONS

Figure		Page
1-1	Burnup Experience With C-E Zircaloy Clad Fuel Rods	6
1-2	Actual and Projected Batch Discharge Burnups (MWd/kg) of C-E Fuel Assemblies in Operating Reactors	11
1-3	Burnup Milestones for C-E Fuel Irradiation Tests	12
2-1	Overall Fuel Assembly Design	28
2-2	Fuel Assembly Structural Frame	29
2-3	Fuel Spacer Grid	31
2-4	Fuel Rod	34
2-5	Burnable Poison Rod	35
4-1	Design Curve for Cyclic Strain Usage of Zircaloy-4 at 700°F	47
4-2	Typical Composite Oxide Layer Thickness Trace for a Fuel Rod After 4 Cycles of Irradiation	50
4-3	Oxide Measurements From Calvert Cliffs-1 and Fort Calhoun	51
4-4	Maximum Oxide Layer Thickness of PWR Fuel Rods versus Burnup	52
4-5	Hydrogen Pickup of Zircaloy-4 in a PWR Environment	56
4-6	Effect of Test Variables on Fuel Rod Diametral Strain at Various Burnup Levels	60
4-7	Typical Probability Histogram for Fuel Rod Collapse	63
4-8	Yield Strength as a Function of Fluence for [ ], Irradiation Temperature 500°F to 650°F, Elevated Temperature Test	66
4-9	Uniform Elongation as a Function of Fluence for [ ] Zircaloy, Irradiation Temperatures 560-610°F	68
4-10	Percent Reduction of Area for Short-Transverse Specimens Irradiated to 4.3×10^{19} n/cm^2 (E>1 MeV)	70

ILLUSTRATIONS (continued)

Figure		Page
4-11	Ultimate Tensile Strength of Short-Transverse Specimens Irradiated to 4.3 x 10^{19} n/cm^2 (E>1 MeV)	71
4-12	Effect of Hydrogen Concentration on the Reduction of Area for Zircaloy-2 Irradiated to 10^{20}n/cm^2 (Ni)	72
4-13	Fission Gas Release Measured in Calvert Cliffs 1 Fuel Rods	76
4-14	Fission Gas Release From OVER-RAMP Rods	80
4-15	Predicted-Measured Gas Release versus Burnup	85
4-16	C-E Generic Model for Fractional Channel Closure in a 14x14 Design Fuel Assembly and Its Supporting Data Base	97
4-17	Confirmation of the C-E Generic Model for Fractional Closure in a 16x16 Design Fuel Assembly by Comparison With First Cycle Data From Arkansas Nuclear One, Unit 2	99
4-18	Peak Power versus Burnup for C-E/KWU PCI Ramp Experiments	108
4-19	Comparison of C-E Rupture Temperature and Burst Strain Models With PBF and FR-2 Experimental Results	117
4-20	Recent Fuel Rod Growth Measurements Compared to the C-E Zircaloy Fuel Rod Growth Model	121
4-21	Typical Probability Histogram for Fuel Assembly Length Change	130
4-22	Comparison of Arkansas Nuclear One Unit 2, End of Cycle 1 Assembly Length Changes to SIGREEP Predictions	132
4-23	Comparison of Arkansas Nuclear One Unit 2, End of Cycle 1 Shoulder Gap Changes to SIGREEP Predictions	133
4-24	Comparison of Measured Guide Tube and Spacer Grid Growth Strains	138
4-25	Swelling of Al_2O_3-B_4C	151
4-26	Shoulder Gap Closure Histograms for 16x16 Fuel Rods and Poison Rods	156
4-27	Effective Void Volume versus Fluence	158

SUMMARY

This report describes the fuel performance parameters affected by increased fuel burnup (or core residence time) and the behavior phenomena governing the burnup dependence of these parameters. The models (or submodels) used by Combustion Engineering, Inc. (C-E) to represent these parameters are reviewed with emphasis placed on showing how burnup is included in the analyses which incorporate these parameters. A review of the current and anticipated data base that support these models is made where appropriate to demonstrate the adequacy of the models up to batch average discharge burnups of 45 MWd/kg (maximum rod average burnups of 52 MWd/kg). In this manner, the report provides a basis for the generic licensing approval of C-E's fuel performance models for operation of 14x14 and 16x16 fuel assembly designs to these target burnup values.

The report is organized into five main sections. In Section 1, C-E's fuel performance experience is reviewed with emphasis on the relationship between increased burnup and fuel reliability. Each of C-E's extended-burnup research and development programs is briefly described with burnup milestones listed for the availability of data in several key fuel performance areas. Section 2 provides descriptions of C-E's 14x14 and 16x16 fuel assembly designs to acquaint the reader with the features of these designs and to establish references for the discussions of the various fuel performance parameters. In Section 3, the general performance and functional requirements of the fuel assembly are described with emphasis on those that are affected by extended burnup. Section 4 is the principal section of the report. It includes for each fuel performance parameter: (1) a discussion of the parameter with pertinent background information, (2) a description of the modeling of the parameter including the way in which burnup dependence is included, (3) the degree to which the parameter is affected by the extension of burnup (or core residence time), and (4) an evaluation of the adequacy of the model for extended burnup. A review of the current and anticipated data base is made in this section to the extent that it supports the operation of C-E fuel to extended burnup. Finally, the major conclusions of the report are presented in Section 5.

After a thorough review of the fuel performance parameters and behavior mechanisms affected by extended burnup, none have been found to exhibit any discontinuous effects or abrupt limitations as a function of burnup. The data obtained to date support this conclusion, and the development programs currently in place will supply further verification for both 14x14 and 16x16 fuel assembly designs to increasingly higher exposure levels. Since the fuel performance modeling described in this report accurately represents the observed data and exhibits a continuous behavior, it is felt to be an adequate representation to the target burnup values even in those cases where the data base is presently limited to lower burnup levels.

This report, together with the numerous references that are cited to provide the supporting details, form a complete set of the calculative models and methods used by C-E to analyze fuel performance. The models and methods discussed have either previously been deemed acceptable for conventional burnups or have recently been revised and submitted to the NRC for review. In a number of cases, recently acquired data from C-E's fuel demonstration and development programs are presented for the first time to provide support to higher exposure levels. These analytical methods are available for use for all extended-burnup applications involving C-E reload fuel. Since they conform to established licensing guidelines and/or requirements, and since existing guidelines and requirements are judged by both C-E and the NRC to be adequate for extended burnup, reload analyses for extended-burnup cycles can be accomplished within the current licensing framework. Furthermore, since C-E incorporates burnup dependent effects in each reload analysis, acceptable results from safety analyses will demonstrate acceptable performance at extended burnups. Thus, no special licensing effort beyond a straightforward extension of that already being accomplished for standard burnups is needed for extended-burnup reload cycles for batch average discharge burnups of up to 45 MWd/kg (maximum rod average burnups of 52 MWd/kg).

Section 1

INTRODUCTION

1.1 BACKGROUND

Over the past 20 years, there has been a steady increase in the average discharge burnup of PWR fuel from about 12 MWd/kg in 1962 to about 26 MWd/kg in 1982. If low enrichment initial core fuel is excluded from the data, then the present industry average discharge exposure is about 30 MWd/kg, which is more representative of the burnup of current PWR fuel cycle designs under equilibrium conditions (1-1). Increasing discharge burnup thus represents no major departure from current fueling practices, but rather is consistent with the historical trend of increased fuel exposure with time and irradiation experience.

The incentives for increasing fuel exposure are well documented (1-2) and affect all phases of the nuclear fuel cycle. For example, increasing the fuel discharge burnup from 30 to 45 MWd/kg would reduce uranium mining and milling requirements by 4 to 10%, depending on the reactor fueling strategy employed. Perhaps more important, considering the current lack of sufficient spent fuel storage and reprocessing capabilities, is the reduction in the quantity of spent fuel generated when the discharge burnup is increased. Since the amount of spent fuel is inversely proportional to its burnup, increasing discharge burnup from 30 to 45 MWd/kg would decrease the requirements for storage, transportation, and reprocessing by 33%. The requirement for fresh fuel fabrication would be similarly reduced for a like increase in discharge burnup. These reductions in fuel cycle requirements lead to more economical power generation costs as a result of lower fuel cycle costs which can be up to 12% lower than those without the extension of burnup.

Concurrent with the trend toward higher burnups is the desire for longer cycle lengths. Such cycles offer the potential for improved reactor availability and reduced radiation exposure of personnel due to less frequent refueling operations. The use of extended-burnup fuel facilitates longer cycles by

eliminating the fuel cost penalties (e.g., resulting from higher uranium and separative work requirements) that would otherwise occur if current burnup levels were retained. From a national perspective, the use of longer cycles is attractive because it reduces requirements for replacement power during refueling outages as a result of increased availability. Since this replacement power is typically obtained from oil-fired units, significant reductions in oil imports can be realized through the use of longer cycles. In addition, longer cycles reduce the number of licensing amendments which must be written, reviewed, and approved each year.

In recognition of the industry trend toward higher burnup, the Nuclear Regulatory Commission (NRC) held a series of generic meetings on the potential for extended-burnup operation of LWR fuel. All LWR fuel suppliers participated in these meetings as did the U.S. Department of Energy (DOE) and the Electric Power Research Institute (EPRI). The initial generic kickoff meeting was held on January 27, 1981. Following this kickoff meeting, which was open to all interested parties, individual proprietary meetings were held with each fuel supplier. Combustion Engineering (C-E) participated in such a meeting with the NRC on March 28, 1981. The basic objectives of these meetings were to present a forum where NRC could outline general licensing needs and concerns for extended-burnup operation and to receive feedback from the industry concerning related details such as extended burnup projections, test and demonstration program results, future R&D needs, and the identification of burnup-related phenomena (1-3).

After reflecting upon the information presented and discussed in the generic meetings, the NRC concluded that "a considerable amount of information exists and that extended-burnup operation is justifiable" (1-4). Furthermore, the NRC believes that present licensing requirements as described by the Code of Federal Regulations, the Regulatory Guides, and the Standard Review Plan (SRP) "are adequate for extended-burnup considerations" (1-4); therefore, what is needed is a review of present design methods and safety analyses to assure their validity over the target extended-burnup range. The NRC further stated that the information presented in the generic meetings which would support the conclusion that extended burnup operation is justifiable has not been

documented in a consistent and systematic manner to allow an orderly review. It was therefore suggested that a topical report be prepared to formally present C-E's extended-burnup experience, methods, and test data for the purpose of providing a basis for the generic approval of the operation of C-E fuel to extended burnup (1-4).

1.2 REPORT OBJECTIVE AND SCOPE

The objective of this topical report is to provide a basis for the generic licensing approval of C-E's fuel performance models for operation of 14x14 and 16x16 fuel assembly designs up to batch average discharge burnups of 45 MWd/kg (maximum rod average burnups of 52 MWd/kg). To this end, the fuel performance parameters or topics affected by increased burnup or residence time are described and the behavior phenomena governing the burnup dependence of these parameters are discussed. The models (or submodels) used by C-E to represent these parameters are reviewed with emphasis placed on showing how burnup is included in the analyses which incorporate these parameters. Where applicable, a review of the current and anticipated data base supporting these models is made to demonstrate their adequacy to the target burnup values. Extensive use of references is made so as not to repeat in detail analyses and data previously reported.

This topical report focuses on the behavior of the fuel performance parameters or topics listed in Tables 1-1 and 1-2. Shown in these tables are the fuel performance topics judged by C-E to be burnup dependent and/or important in determining the behavior of fuel at extended burnup. Both 14x14 and 16x16 fuel assembly designs are discussed to document the generic fuel performance modeling capability of C-E to extended burnups. Where applicable, steady state, power ramping, and transient conditions are included in the discussions of the burnup behavior, modeling characteristics, and data base for these fuel performance topics.

A principal element in achieving the above stated objective of this topical report consists of demonstrating the adequacy of the models (or submodels) used in analyzing fuel behavior at extended burnup. Accomplishing this objective

TABLE 1-1

FUEL ROD TOPICS

1. Fatigue
2. Cladding Corrosion
3. Cladding Creep
4. Cladding Collapse
5. Embrittlement of Fuel Cladding
6. Fission Gas Release
7. Fuel Thermal Conductivity
8. Fuel Melting Temperature
9. Fuel Swelling
10. Fuel Rod Bow
11. Fretting Wear
12. Pellet/Cladding Interaction
13. Cladding Deformation and Rupture
14. Fuel Rod Growth

TABLE 1-2

FUEL ASSEMBLY TOPICS

1. Guide Tube Wear
2. Fuel Assembly Length Change
3. Fuel Assembly Holddown
4. Grid Irradiation Growth
5. Spacer Grid Relaxation
6. Corrosion of the Fuel Assembly Structure
7. Burnable Poison Rod Behavior

will facilitate the licensing review of reload analyses for extended-burnup fuel. Analytical methods previously deemed to be acceptable for conventional burnups will be available for use for extended-burnup applications. Since, as referenced above, the NRC feels that present licensing requirements are adequate for extended burnup, review of reload analyses for extended-burnup cycles can be accomplished under the same ground rules and requirements as are currently used. Furthermore, since Combustion Engineering incorporates burnup dependent effects in each reload analysis, acceptable results from safety analyses will demonstrate acceptable performance at extended burnups.

1.3 BURNUP EXPERIENCE AND PERFORMANCE OF C-E FUEL

As of January 1, 1982, Combustion Engineering had eight nuclear power plants in operation. Palisades was C-E's first plant, starting commercial operation in January 1972. The first fuel batch incorporating C-E's 14x14 fuel assembly design was irradiated in Maine-Yankee, starting in November 1972. The first plant to use C-E's 16x16 fuel assembly design was Arkansas Nuclear One Unit 2, which began operation in December 1978. In total, C-E has fabricated and put into operation 73 separate fuel batches, consisting of 3325 fuel assemblies or about 597,000 fuel rods. Figure 1-1 is a profile of these rods showing their achieved burnup and operational status. Clearly, a large number of fuel rods have achieved significant burnups, and this has been done with excellent fuel rod performance at all eight operating plants.

The data plotted on the upper half of this figure represent fuel rods currently in operation, and those below the abscissa represent discharged rods. The number of fuel rods discharged in the range of 32 to 36 MWd/kg is a clear indication that these burnups are typical for fuel committed from 5 to 10 years ago. The fuel management plans and associated enrichments were designed for these performance levels during the early to mid-1970s, and the statistics shown in Figure 1-1 show a successful accomplishment of these design objectives. Current plans call for batch average discharge burnups in the range of 35-45 MWd/kg with fuel enrichments of 3.5 to 4.2 wt% U-235. As fuel of this design completes its four to five-year residences in operating plants, summaries of the type shown in Figure 1-1 will reflect the gradual upward shift in discharge burnup.

FIGURE 1-1

BURNUP EXPERIENCE WITH C-E ZIRCALOY CLAD FUEL RODS

STATUS - DECEMBER 1, 1981

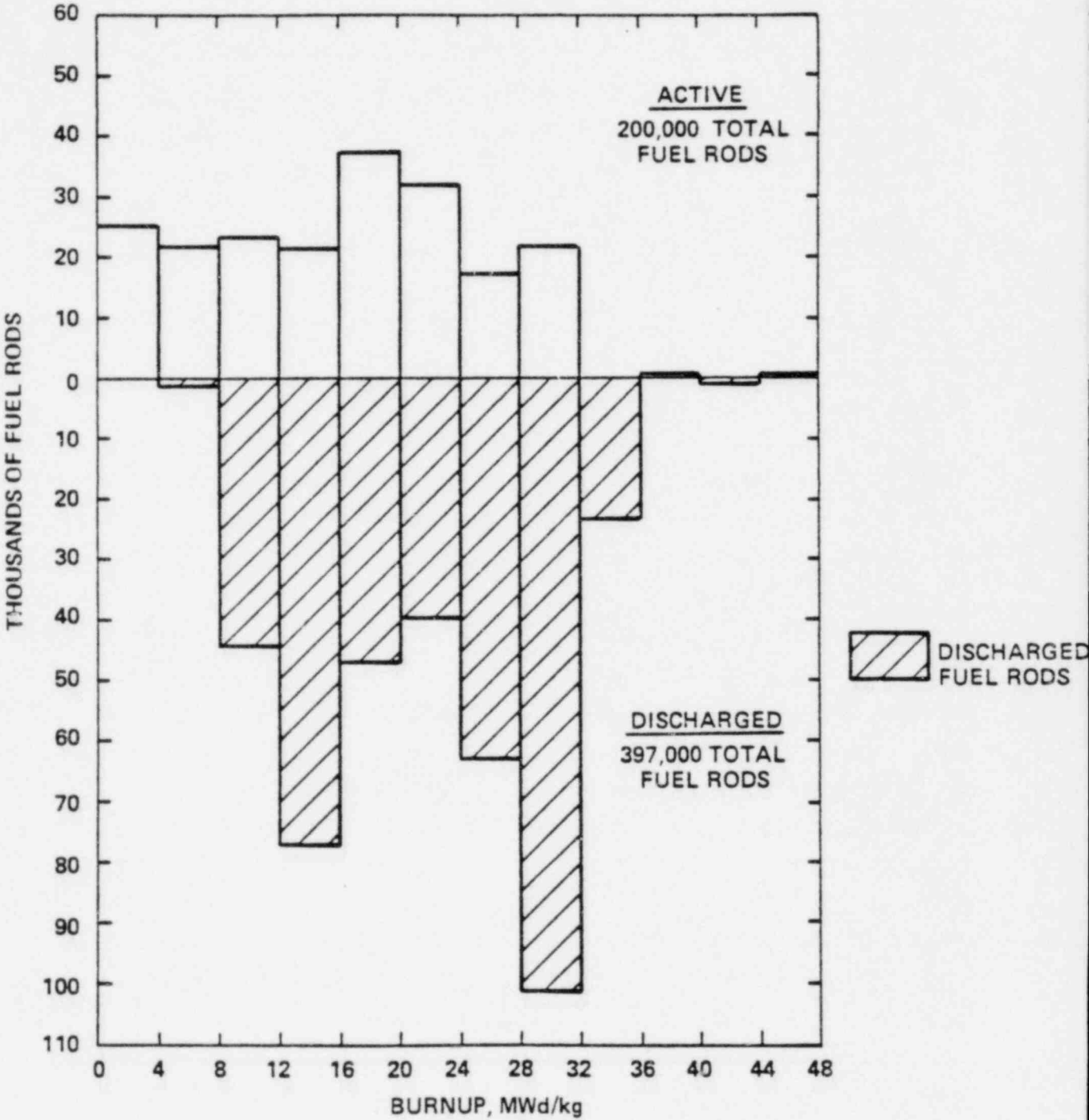

Reactor availability for C-E's operating plants has been above the national average and the fuel performance for these plants is currently at a reliability level of 99.99% (based on plant I-131 activity). A breakdown of this excellent fuel performance by operating plant is shown in Table 1-3. C-E's experience with the operation of PWR fuel rods has shown a reduced frequency of fuel failure with increased burnups. The primary reason for the improved performance at higher burnups is the reduced linear heat ratings associated with the fuel that has accumulated the higher burnup.

Data from all eight of C-E's plants has been evaluated to assess any relationship of fuel failure to burnup level. In most cases, it was necessary to rely on the activity levels of the coolant as an indicator of fuel failures, since sipping of the fuel assemblies has been generally unnecessary. The background level of coolant activity that normally occurs in PWRs is associated with some nominal level of leaking rods from 0 to 5 in number. In cases where the iodine levels changed to some higher level, the escape rate coefficient was used to estimate the number of failed rods. In those cases where sipping was performed, examinations of the fuel assemblies permitted a more direct count of the number of failed rods. Table 1-4 shows the estimated number of failed rods resulting from the operation of fuel in various cycles and the burnup range for the various cycles. Although the data are somewhat limited at higher burnups, the trend is dramatic. Approximately 0.047% of those fuel rods operating in their first cycle developed a leak before the end of that cycle. In the second cycle, that percentage falls to 0.0082%, and in those rods operating a third or higher cycle, the percentage improves almost another order of magnitude to 0.0011%. C-E believes that this operating experience supports the operation of fuel to higher exposures without increasing the number of fuel failures.

Lead test assembly programs (to be discussed in Section 1.4) are being continued to add confidence to the reliable operation of PWR fuel to extended burnups. The decline in linear heat ratings which accompanies the higher burnup assemblies is the primary reason to expect very low incidence of fuel failure at higher burnups. The experience cited above supports this, and the statistical confidence associated with this observation will increase gradually as the data base is expanded.

TABLE 1-3

FUEL PERFORMANCE SUMMARY FOR C-E REACTORS
(STATUS DECEMBER 1, 1981)

REACTOR	CURRENT FUEL CYCLE	B.O.C. DATE	E.O.C. DATE	CURRENT CYCLE BURNUP MWd/kg[b] CORE AVG.	CURRENT CYCLE BURNUP MWd/kg[b] PEAK BATCH AVG.	1981 EQUILIBRIUM CONDITIONS % CORE POWER	1981 EQUILIBRIUM CONDITIONS I-131 μCi/mg	FUEL ROD RELIABILITY (%)
Arkansas-2	2	7/2/81	9/82[a]	11.7	17.5	100	[redacted]	[redacted]
Calvert Cliffs-1	5	12/21/80	4/82[a]	17.7	38.1	100		
Calvert Cliffs-2	4	3/10/81	10/82[a]	13.0	27.1	100		
Fort Calhoun[e]	6	6/8/80	9/18/81	21.9	45.3[c,d]	95		
Maine Yankee	6	8/12/81	7/82[a]	14.6	26.6[c]	97		
Millstone-2	4	10/20/80	1/82[a]	21.8	31.4[c]	100		
Palisades[e]	4	5/24/80	8/28/81	21.4	35.3[c,d]	100		
St. Lucie-1[e]	4	5/7/80	9/8/81	21.1	35.7[d]	100		

(a) Projected end-of-cycle date

(b) Estimate, December 1, 1981

(c) C-E fuel in mixed core

(d) End-of-Cycle reported burnup

(e) Core in refueling, data are for end of previous cycle

(f) Composite reliability of fuel supplied by C-E and another fuel vendor

TABLE 1-4

FUEL PERFORMANCE STATISTICS

STATUS December 1, 1981

CYCLE OF EXPOSURE

	1	2	3	4 or 5
Fuel Assembly Burnup Range (MWd/kg)	0-20	13-20	22-35	34-46
Number of Fuel Rods				
Discharged	397,000	266,000	121,000	5,960
Operating	200,000	137,000	58.000	176
Total	597,000	403,000	179,000	6,486
Estimated Number of Leaking Fuel Rods	280	33	2	---
Percent Leaking Fuel Rods	0.047%	0.0082%	0.0011%	---

Before beginning a discussion of extended-burnup research and development (R&D) programs, it is beneficial to review the projected discharge burnups of C-E fuel assemblies in operating reactors. Figure 1-2 shows such a projection for six C-E reactors for the ten-year period starting in 1980. All values after about 1983 are speculative since firm plans after this date are subject to reactor operating schedules and utility energy requirements. As can be seen from this figure, the projected batch average discharge burnups increase gradually from about 30 MWd/kg to approximately [ ] MWd/kg over the decade shown. In all cases, the reactor operating schedules tentatively call for 18-month refueling intervals with a typical fuel assembly remaining in core for three such long cycles.

1.4 EXTENDED-BURNUP RESEARCH AND DEVELOPMENT PROGRAMS

Combustion Engineering has underway a wide range of analytical and experimental programs aimed at understanding and verifying the performance of both standard and advanced fuel designs to extended burnup. The objective of these programs is to provide the technology required to design, license, fabricate, and successfully operate C-E fuels to extended burnup. The programs include evaluations of basic fuel performance phenomena such as pellet/cladding interaction, external waterside corrosion of Zircaloy and fission gas release, as well as high burnup fuel testing in which demonstration assemblies are irradiated for four and five cycles in commercial power reactors to confirm their anticipated acceptable performance to extended burnups. Figure 1-3 provides an overview of the extended-burnup programs in which C-E is participating. Shown in this figure are the principal fuel performance areas covered and the dates at which various burnup milestones will be achieved. A brief summary of these programs is given in the following sections.

1.4.1 Baltimore Gas and Electric (BG&E)/C-E Extended Burnup Program at Calvert Cliffs Unit 1 (1-5, 1-6)

The overall objectives of this program are (1) to provide a technical basis for the design, licensing, and operation of standard fuel to extended burnups, and (2) to conduct a demonstration which investigates alternate fuel designs

FIGURE 1-2
ACTUAL AND PROJECTED BATCH DISCHARGE BURNUPS (MWd/kg) OF C-E FUEL ASSEMBLIES IN OPERATING REACTORS

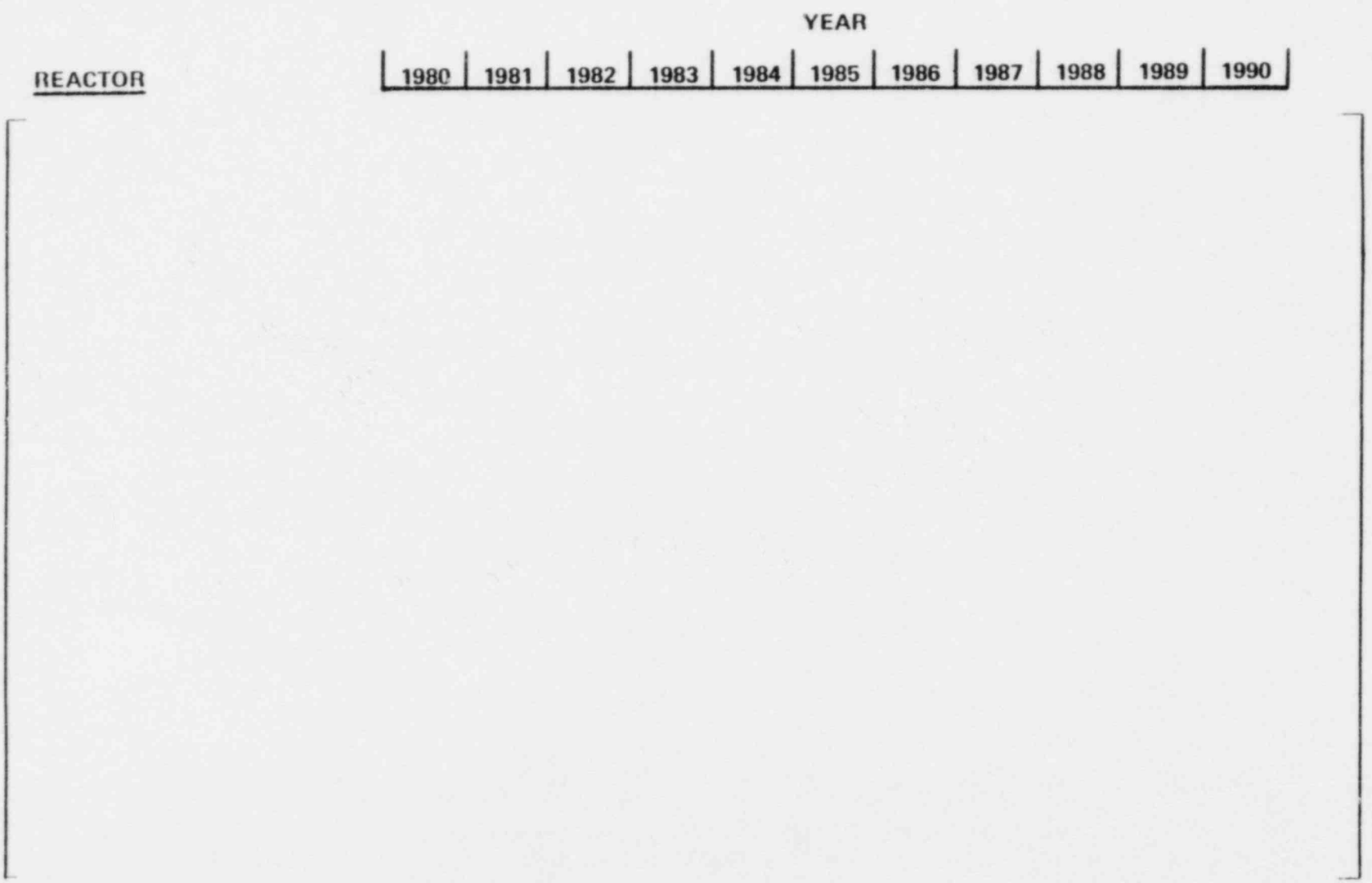

FIGURE 1-3
BURNUP MILESTONES FOR C-E FUEL IRRADIATION TESTS
(MWD/KG)

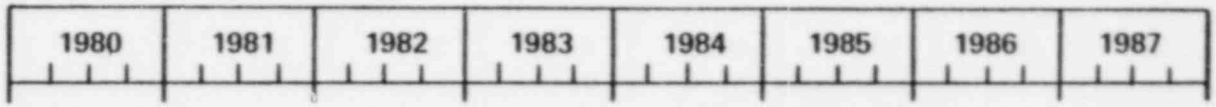

FIGURE 1-3 (Continued)
BURNUP MILESTONES FOR C-E FUEL IRRADIATION TESTS
(MWD/KG)

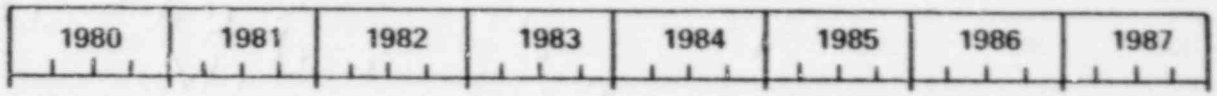

FIGURE 1-3 (Continued)
BURNUP MILESTONES FOR C-E FUEL IRRADIATION TESTS
(MWD/KG)

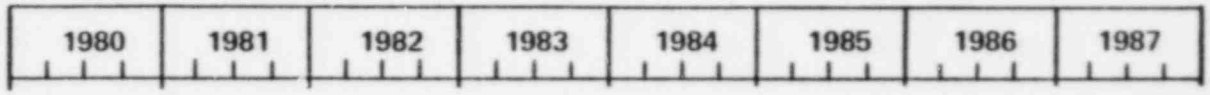

and provides data for future application to reloads for Calvert Cliffs reactors. This development program consists of two complementary subprograms: SCOUT and PROTOTYPE.

[

]

The evaluation of alternate fuel rod designs is facilitated by obtaining performance data on a statistically significant number of full length rods. This objective will be accomplished by [

]

1.4.2 EPRI/C-E Fuel Surveillance Program at Calvert Cliffs Unit 1 (1-7, 1-8, 1-9, 1-10)

EPRI and C-E have been participating in a joint fuel performance program since 1975 in Calvert Cliffs-1 operated by BG&E. The objective of this program is to obtain fuel performance data on C-E 14x14 test fuel rods that have systematic variations in the initial as-fabricated parameters such as fuel pellet porosity distribution, pellet length-to-diameter ratio, pellet density, rod internal pressure, initial cladding properties, and cladding with and without an ID coating of graphite. The project scope emphasizes the acquisition of data in three categories:

- mechanical stability data that include axial growth of fuel rods and fuel assemblies, fuel rod creep, and fuel rod bow;
- thermal performance data that include fission gas release measurements and evaluation of fuel microstructural changes; and
- cladding corrosion measurement data.

A total of 60 test fuel rods were fabricated and characterized for the program. The test rods were installed into three characterized, reconstitutable assemblies which were placed in Calvert Cliffs-1 as part of the initial core loading. Test rods are to be irradiated for a maximum of five operating cycles and examined at poolside after each refueling outage. After each of the first four cycles, a number of test fuel rods are examined at a hot-cell facility.

Data from poolside and hot cell examinations of four-cycle rods have been obtained to a maximum assembly average burnup of 43 MWd/kg (peak rod average burnup of 46 MWd/kg). Poolside examination of data for five-cycle fuel rods will be available in mid-1982. These data will extend the burnup range for the standard C-E 14x14 fuel design to 55 MWd/kg (peak rod average).

1.4.3 EPRI/C-E Fuel Performance Evaluation in 16x16 Assemblies at Arkansas Nuclear One Unit 2 (1-7, 1-11)

The joint EPRI/C-E Fuel Performance Evaluation Program in Arkansas Nuclear One Unit 2 is designed to generate a statistically significant data base on the performance of the first C-E fuel assemblies designed with a 16x16 lattice array of rods. The program includes the irradiation of six well-characterized standard 16x16 fuel assemblies, two each intended for one, two and three cycles of operation, respectively. Each assembly contains fifty precharacterized standard fuel rods. The rods are removable and distributed within the assemblies such that they will experience a spectrum of operating histories. Ten rods per assembly contain precharacterized fuel pellets in predetermined locations such that they will experience a range of power histories. The characterization data obtained in this program was extensive and included assembly length, assembly width, and channel width; fuel rod length and

diameter; pellet densities for representative pellet lots; and extensive measurements of cladding mechanical properties.

These assemblies were loaded into the reactor late in 1978 with planned interim and final poolside inspections after one and three cycles, respectively. These inspections will provide performance data to burnups of approximately 40 MWd/kg (peak rod average) in the areas of irradiation induced growth (assembly and fuel rod), channel closure, cladding creep, and external corrosion. The characterized assemblies have been examined after one operating cycle (April 1981) with lead rod average burnups of approximately 15.3 MWd/kg. Following the examination, these assemblies were returned to the core for Cycle 2 operation.

1.4.4 DOE/AP&L/C-E High Burnup Program at Arkansas Nuclear One Unit 2 (1-12, 1-13)

The primary goal of this DOE-sponsored program being conducted at the Arkansas Nuclear One Unit 2 reactor, which is operated by Arkansas Power & Light Co. (AP&L), is to demonstrate the extended burnup operation of C-E's 16x16 fuel assembly design. The program consists of fuel performance demonstrations for discharge exposures equivalent to batch average burnups up to 53 MWd/kg along with fuel management and safety analyses to support the implementation of low leakage fuel management and extended burnup for possible future implementation. Current fuel designs will be irradiated to a peak rod average exposure of 52 MWd/kg which is equivalent to a batch average burnup of 43 MWd/kg. Poolside and hot-cell examinations will be performed for fuel which has been irradiated for three and four cycles to obtain fuel performance data. Of particular interest will be the effects of extended burnup on pellet clad interactions, external corrosion, fuel dimensional stability and fuel rod internal pressure. The results from the post-irradiation fuel examinations will be used to evaluate fuel performance limits for current fuel designs.

To extend the peak rod average burnup to 64 MWd/kg (equivalent batch average burnup equal to 53 MWd/kg), advanced fuel design concepts are being developed. Concepts such as annular pellets, graphite lubricant between the pellet and

clad, and fuel with large grain sizes will be evaluated by including demonstration rods in two assemblies (along with current design rods) for subsequent irradiation. Hot-cell and poolside inspection of the rods are planned after various cycles of operation. These results will be used to assess current models which predict fuel performance and behavior and to verify the satisfactory performance of the advanced designs in a PWR.

1.4.5 DOE/OPPD/C-E High Burnup Program at Fort Calhoun (1-14, 1-15)

The principal goals of this DOE-sponsored program conducted in cooperation with Omaha Public Power District (OPPD) are to demonstrate the extended-burnup operation of C-E's 14x14 fuel assembly design and to demonstrate an improved low leakage fuel management technique. The program consists of extending the discharge exposure of the standard assemblies containing modern nondensifying fuel to an average of 52 MWd/kg with a peak rod value of 56 MWd/kg. Poolside and hot cell examinations will be carried out for fuel assemblies exposed to three, four and five cycles of irradiation. Fuel rods containing modern nondensifying fuel will be examined to characterize fuel performance up to the above listed burnups. In particular, fission gas release data will be measured for comparison with the behavior predicted by gas release models.

1.4.6 EPRI/C-E/KWU Zircaloy Waterside Corrosion Program (1-16, 1-17)

This program, jointly sponsored by EPRI, C-E, and KWU of Germany was initiated in October 1978 to study waterside corrosion of Zircaloy clad fuel rods. The waterside corrosion rate of Zircaloy cladding in PWRs is such that it has not limited operating strategies or impacted design limits. However, the longer in-core residence time associated with increasing fuel discharge burnups may result in an increase in the corrosion rate of the Zircaloy cladding. Therefore, the broad objectives of this project are to (1) obtain a data base on Zircaloy corrosion for an anticipated range of corrosion rates, (2) characterize the physical and chemical properties of the corrosion films in this operating regime, and (3) develop an analytical correlation that predicts the in-reactor corrosion of Zircaloy-4 in PWR environments. The primary goal of the program is to provide detailed experimental and theoretical bases from which to confirm the corrosion performance of current design fuel rods to extended burnups.

The six major tasks of the program are (1) a state-of-the-art review, (2) the acquisition of film thickness data, (3) a characterization of the corrosion film, (4) the measurement of the thermal conductivity of the corrosion film, (5) the development of correlations for Zircaloy-4 corrosion in PWR environments, and (6) the extension of the resulting corrosion correlation to other reactors (optional). The resulting data base and corrosion model will be used to define safe operating margins for PWR fuel of current and advanced design operating to high exposures.

1.4.7 Studsvik OVER-RAMP Program (1-18, 1-19)

C-E was one of 11 organizations which sponsored a test program conducted by AB Atomenergi of Sweden aimed at the ramp behavior of PWR fuel rods. This program was completed in 1980.

The specific aims of the research project were:

(1) to investigate the fuel pellet/cladding interaction (PCI) mechanism,
(2) to study the influence of major fuel physical parameters on pellet/cladding interaction, and
(3) to experimentally evaluate the effect of ramp rate on the propensity to fail.

Twenty-four (24) of the 40 rods included in the ramp testing, which was performed at the R2 reactor between 1977 and 1979, were supplied by C-E and KWU. These rods were pre-irradiated for one, two or three cycles in the Pathfinder test assembly in the Obrigheim reactor. Rods representative of C-E's standard design were included.

The OVER-RAMP test results, combined with similar results from the Petten ramp test program (cf. Section 1.4.9) confirm that the linear heat rating required to cause PCI failure is higher than that achieved in lead rods for normal operation of C-E plants. The test results also show that although once-burned fuel has a slightly higher threshold to PCI failure, fuel irradiated two cycles and three cycles both show similar thresholds to peak rod burnups of 32 MWd/kg. The effects of higher burnup therefore may reach an early saturation relative to this failure mechanism. Confirmation of this C-E belief in a

limited dependency on burnup is expected from the results of the high burnup ramp test programs which are discussed in Sections 1.4.8 and 1.4.10.

1.4.8 Studsvik High Burnup SUPER-RAMP Program (1-20)

The Studsvik SUPER-RAMP program is an international cooperative program. The program was established to study the performance of LWR fuel rods which have undergone power ramps in the R2 test reactor in Studsvik, Sweden, following normal irradiation to high burnup in commercially operated power reactors. PWR and BWR subprograms are included in the overall scope. These are essentially follow-on programs to the recently concluded PWR OVER-RAMP and BWR INTER-RAMP programs comprising standard burnup fuel rods. The PWR subprogram will include ramp tests of 24 rods provided by C-E, KWU and Westinghouse. The PWR subprogram objectives are:

- to experimentally establish the PCI failure threshold of standard type PWR test fuel rods on fast power ramping at burnup levels between 30 and 45 MWd/kg,

- to investigate whether or not a change in failure propensity or failure mode is obtained as compared to the failure behavior at lower burnup levels (as determined from the OVER-RAMP program), and

- to establish the possible increase in PCI failure power levels for candidate PCI remedy design fuel rods at selected burnup levels.

The PWR test matrix includes standard design fuel rods as well as modified fuel designs consisting of Gd_2O_3 added to the fuel, annular fuel and fuel with large grain size (undoped). Other major design variables include rod prepressurization, gap size and cladding thickness-to-diameter ratio.

The SUPER-RAMP program was initiated in early 1980 and is scheduled for completion by the end of 1982.

1.4.9 C-E/KWU Ramp Test Program in Petten (1-21)

The objective of this experimental program is to define the potential limits where fuel rods can operate with insignificant risk of failure due to PCI. The mechanisms leading to PCI failure are being studied to determine their sensitivity to such operational parameters as peak power level, power step size, power ramp rate and time at power. The program started in 1973 when Kraftwerk Union (KWU) began pre-irradiating fuel rod segment strings (as part of the Pathfinder Program) in the Obrigheim reactor. C-E first provided fuel and cladding components for such rod segments the following year as part of the C-E/KWU Joint Program Agreement. Thus far, approximately 120 rod segment strings, comprising 840 total rod segments, have been irradiated through 1 to 4 reactor cycles. C-E has provided the fuel and cladding for approximately 130 of these rod segments.

Ramp tests under this program were first performed at Petten in 1976 to determine PCI failure thresholds. Since then, 99 ramp tests have been completed involving the PWR rod segments from Obrigheim. The peak rod average burnup of the segments tested to date is 30 MWd/kg; future ramp tests will examine PCI failure thresholds for burnups in excess of this value.

1.4.10 DOE/C-E/KWU High-Burnup Ramp Test Program at Petten (1-22)

The overall objective of this jointly sponsored program is to investigate the power ramp behavior of PWR type fuel under fast power ramp conditions. The work scope includes (1) ramp testing in Petten of 20 fuel rod segments having three or four cycles of exposure in a PWR and (2) reporting the results of previous ramp tests performed at Petten on similar fuel rod segments at lower burnup levels.

The objectives and ramp test sequences proposed for various parts of the program are divided into four areas as follows:

(1) confirm the defect threshold (below which no ramp failures occur) of high burnup standard fuel rods for unrestricted reactor operation,

(2) investigate the conditions for defect-free reactor operation to high rod power exceeding the defect thresholds previously established,
(3) investigate the effects of fuel pellet geometry on ramp behavior of high burnup fuel rods, and
(4) investigate the influence of additional low power irradiation on further ramp behavior.

Background data for 68 tests performed previously at Petten will be supplied as part of the program. These data will include rod segment design information, pre-irradiation and pre-ramp characteristics, power reactor (Obrigheim/Pathfinder) irradiation conditions and results, and post-ramp PIE data.

The twenty new tests to be conducted under this program will extend the available data to higher levels of burnup than previously available. Twelve of the segments to be ramped will have burnups in excess of 30 MWd/kg and eight will have burnups in excess of 40 MWd/kg. Included among these tests are fuel rod segments having modified designs to determine if such designs improve power ramp behavior. The ramp tests are being performed in the time period 1981-1983, and the final results are expected to be available in 1984.

1.4.11 BNWL High Burnup Effects Program (1-23)

The BNWL High Burnup Effects Program is being sponsored by the following five major participants or participant groups: EPRI, DOE, U.S. Nuclear Fuel Vendors, Japanese Nuclear Industry and European Nuclear Industry. The program's primary objective is to obtain well characterized data on the effects of fuel temperature and burnup on fission gas release in current design LWR fuel rods. Data will be collected from the open literature, from fuel rods provided by program participants, and from the irradiation of rods in the BR-3 reactor in Belgium. A part of the program has been specifically organized to address conservative fuel design requirements related to fission gas release for licensing of UO_2 fuel at extended burnups. In this part, characterized fuel rod segments irradiated to three moderately high burnup levels under low power/low fuel temperature conditions in a power reactor will be subjected to short-term irradiations at higher controlled temperature conditions. The short-term irradiation conditions will extend to what is considered to be the worst

case design limit conditions for licensing calculations. This type of test, which is referred to as an irradiation bumping test, will provide fission gas release data on rods that have been exposed to realistic linear heat generation rates and fuel temperature histories in a commercial reactor during most of their life, and which could conceivably be exposed to worst case design limits near the end of their life.

The program is being carried out in three separate tasks. Task 1 was completed in May 1979 and included an updated evaluation of the state of technology and an assessment of the utility of data reported in the literature for developing a fission gas release correlation applicable at high burnup. Over 450 data points were identified and evaluated.

Task 2 will involve the examination, fission gas sampling, and continued irradiation of fuel rod segments that have already achieved significant burnup levels so that the needed high burnup data will be obtained relatively rapidly. Twenty-one of the 33 PWR rods in the program will be supplied by C-E and KWU from the Pathfinder assembly irradiation in Obrigheim. Fuel rod design variables include fuels of different grain size and variation in level of pre-pressurization. Fuel rods with peak pellet burnup levels from 20 to 54 MWd/kg are currently available for destructive analyses. Also, selected rod segments will be reirradiated to achieve peak burnups of about 40 MWd/kg.

Task 3, a parameter effects study, is designed to provide well characterized data on the effects of fuel temperature, burnup, power history and different fuel characteristics (e.g., varying fuel grain size) on fission product behavior with emphasis on fission gas release. Thirty-six PWR rods will be fabricated for irradiation in the BR-3 reactor. Fuel rod design parameters will include fuel of varying grain size, varying pellet length-to-diameter ratio, and annular pellets. The peak pellet burnup to be achieved is expected to be 73 MWd/kg.

1.4.12 Halden Program (IFA-427) (1-24)

The Halden Reactor Project has a unique capability for measuring fuel rod

operating parameters during irradiation. This capability is being used to provide information of particular interest to extended-burnup fuel performance. Since joining the Halden Project, C-E has been involved in the irradiation of several test rigs to study the dynamics of fuel densification, rod internal pressure, and fuel temperature. These parameters are measured on a continuous basis by thermocouples and transducers. Fuel densification is measured by determining the change in fuel stack length.

One test rig, IFA-427, went into operation in June 1975 and has accumulated a lead rod exposure in excess of 45 MWd/kg. The rods in this rig are being punctured to obtain fission gas release data at extended burnup. These data should be available in 1982.

1.4.13 DOE/C-E Licensing Assessment of PWR Extended Burnup Fuel Cycles (1-25)

C-E recently completed a study sponsored by DOE which assesses the licensability of PWR fuel with batch average discharge burnups up to about 50 MWd/kg. This assessment constituted a simulation of the licensing process without the detailed calculations necessary to apply for a reload fuel license. All important current licensing issues impacted by fuel burnup were addressed, primarily to determine if appropriate and sufficient data would be available from DOE and other industry sponsored demonstration programs to support a timely licensing process. The technical disciplines addressed included nuclear design, fuel performance, safety-related reactor performance, and the ex-core fuel cycle process steps of fabrication, transportation, fuel handling and storage. The major conclusions of this assessment were that:

- no technical problems are expected as a result of irradiating PWR fuel to extended burnups;

- no discontinuous effects or abrupt limitations up to discharge burnups of 50 MWd/kg have been observed from the experience obtained to date, nor are any expected;

- current research, demonstration and development programs address the major licensing considerations associated with the implementation of extended burnup fuel; and

- there appears to be no significant current safety or licensing issue that precludes the use of extended-burnup fuel on technical bases.

The objectives of the research and development programs summarized above are aimed at obtaining the operating experience and fuel performance data needed to confirm the anticipated acceptable performance of C-E fuel to extended burnups. By participating in these programs, C-E will be able to support in an orderly approach the utilities' operation of C-E fuel to the target exposure values.

1.5 ORGANIZATION OF REPORT

As discussed in Section 1.2, this extended-burnup topical report will focus on evaluating C-E's models (or submodels) of various fuel performance parameters to determine which are a function of burnup and to what target exposure supporting data exist or are being developed. The report starts in Section 2 with a description of C-E's 14x14 and 16x16 fuel assembly designs. This description is given to acquaint the reader with the features of C-E's fuel designs and to establish references with respect to which discussions of the fuel performance parameters can be made.

In Section 3, the bases of the fuel assembly design are presented. The general performance and functional requirements of the fuel assembly are described with emphasis on those that are deemed to be related to extended burnup.

Section 4 is the principal section of the report. It includes for each fuel performance parameter or topic (cf. Tables 1-1 and 1-2) the following:

(1) a general discussion of the parameter and any pertinent background information,
(2) a description of the modeling of the parameter including the way burnup is accounted for,
(3) the degree to which the parameter is affected by the extension of burnup or residence time, and
(4) an evaluation of the adequacy of the model for extended burnup.

Within this framework, a review of the current and anticipated data base is made to the extent that it supports operation of C-E fuel to extended burnup. The level of qualification of the models (or submodels) with respect to extended burnup is also given.

Finally, in Section 5, the major conclusions of the topical report are presented. The implication of the burnup dependent modeling of the various fuel performance parameters on reload core safety analysis is discussed.

Section 2

FUEL ASSEMBLY DESCRIPTION

2.1 INTRODUCTION

The Combustion Engineering fuel assembly consists of fuel rods, burnable poison rods (optional), guide tubes, spacer grids, and upper and lower end fittings. Figure 2-1 shows a schematic of a typical fuel assembly design. The five guide tubes, the spacer grids, and the two end fittings form the structural frame of the assembly, which functions to maintain the fuel and poison rods in the proper geometrical array (see Figure 2-2). Specific assembly dimensions are summarized on Table 2-1 for the standard fuel designs.

The sections below provide a brief description of the fuel assembly components. A more complete design description is available in the FSARs (e.g., Section 4.2 of Reference 2-1 and Section 3.3 of Reference 2-2).

2.2 DESCRIPTION OF STRUCTURAL COMPONENTS

The fuel assembly spacer grids (see Figure 2-3) are fabricated from preformed Zircaloy or Inconel strips (the bottom spacer grid material is Inconel) interlocked in an egg crate fashion and welded together. C-E has used these materials for all fuel assemblies it has supplied to the nuclear industry.

The spacer grids maintain the fuel rod array by providing positive lateral restraint to the fuel rods but only frictional restraint to axial fuel rod motion. The Zircaloy spacer grids are fastened to each of the five guide tubes by welding at eight locations, four on the upper face of the grid and four on the lower face of the grid, where the spacer strips contact the guide tube surface. The lowest spacer grid (Inconel) is not welded to the guide tubes due to material differences. It is supported by an Inconel 625 skirt which is welded to the spacer grid and to the perimeter of the lower end fitting.

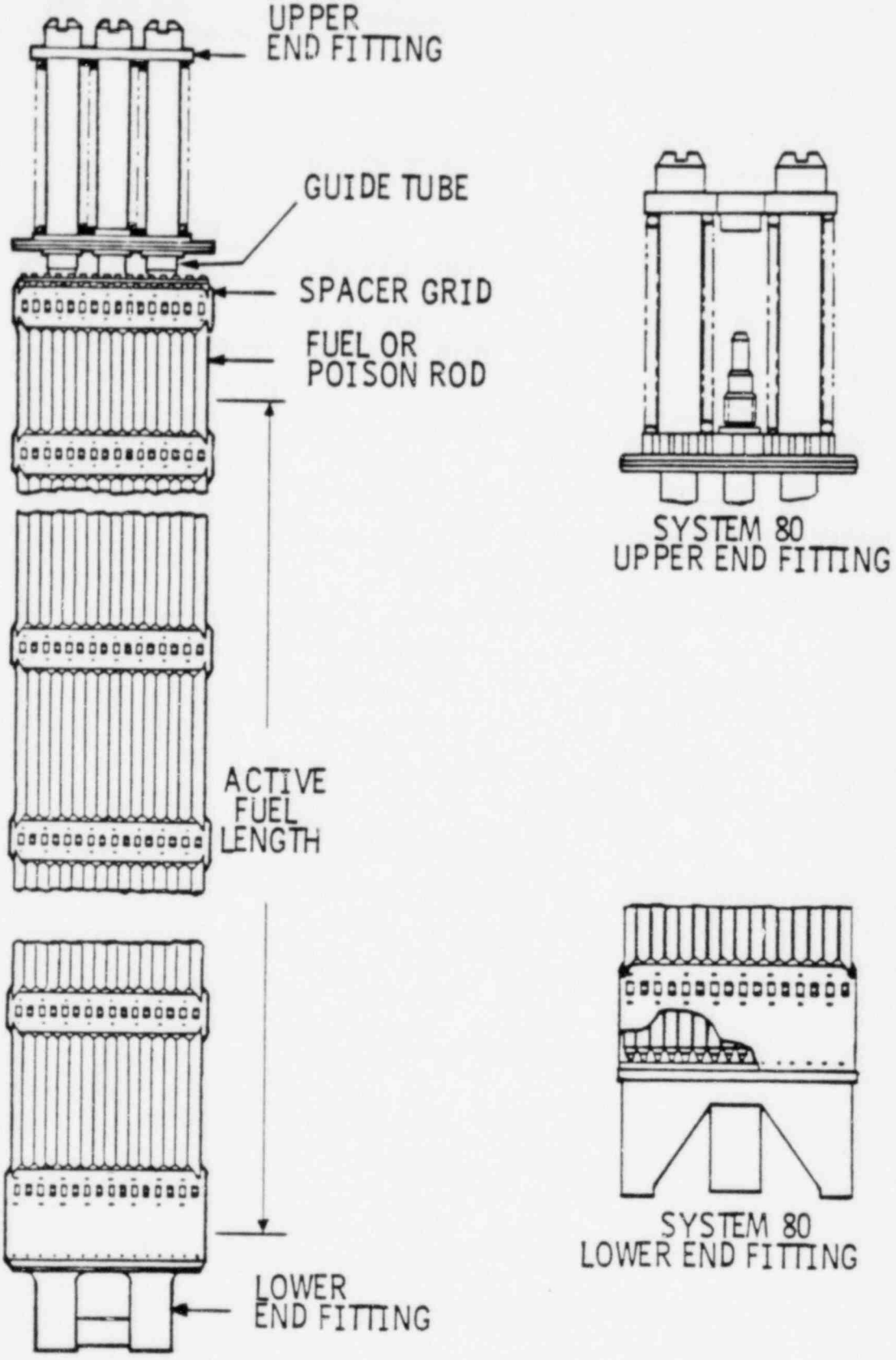

FIGURE 2-1
OVERALL FUEL ASSEMBLY DESIGN

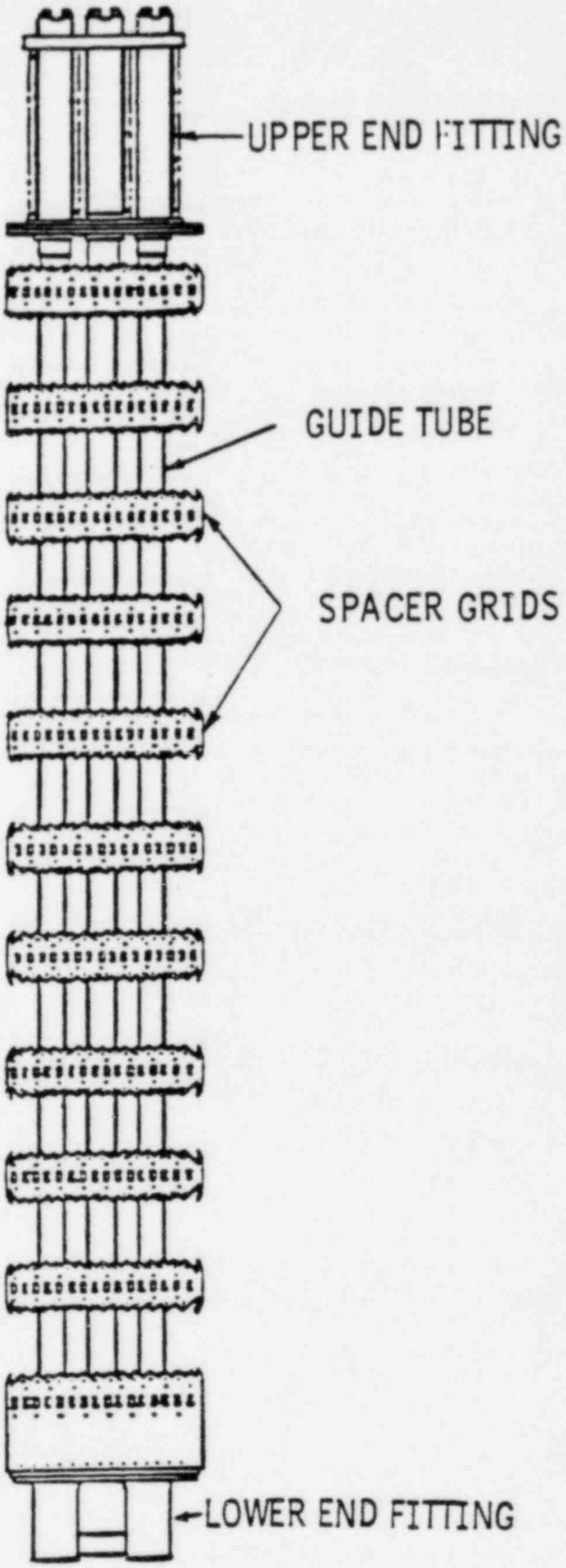

FIGURE 2-2
FUEL ASSEMBLY STRUCTURAL FRAME

TABLE 2-1

COMBUSTION ENGINEERING FUEL ASSEMBLY DESIGNS

Parameter	14x14 Design	16x16 Design
Rods per Assembly	176	236
Rod Pitch (inches)	0.580	0.506
Rod Diameter (inches)	0.440	0.382
Active Length (inches)	136.7	150, 136.7*
Stack Height Density (g/cm^3)	10.046	10.061
Fuel Clad I.D. (inches)	0.384	0.332
Fuel Pellet O.D. (inches)	0.3765	0.325
Number of Spacer Grids per Assembly	8 Zircaloy, 1 Inconel	9 Zircaloy, 1 Inconel*
		11 Zircaloy, 1 Inconel**
		10 Zircaloy, 1 Inconel***

Notes:

* St. Lucie Unit 2

** Arkansas Nuclear One Unit 2

*** San Onofre Units 2 and 3, Waterford 3, System 80 plants

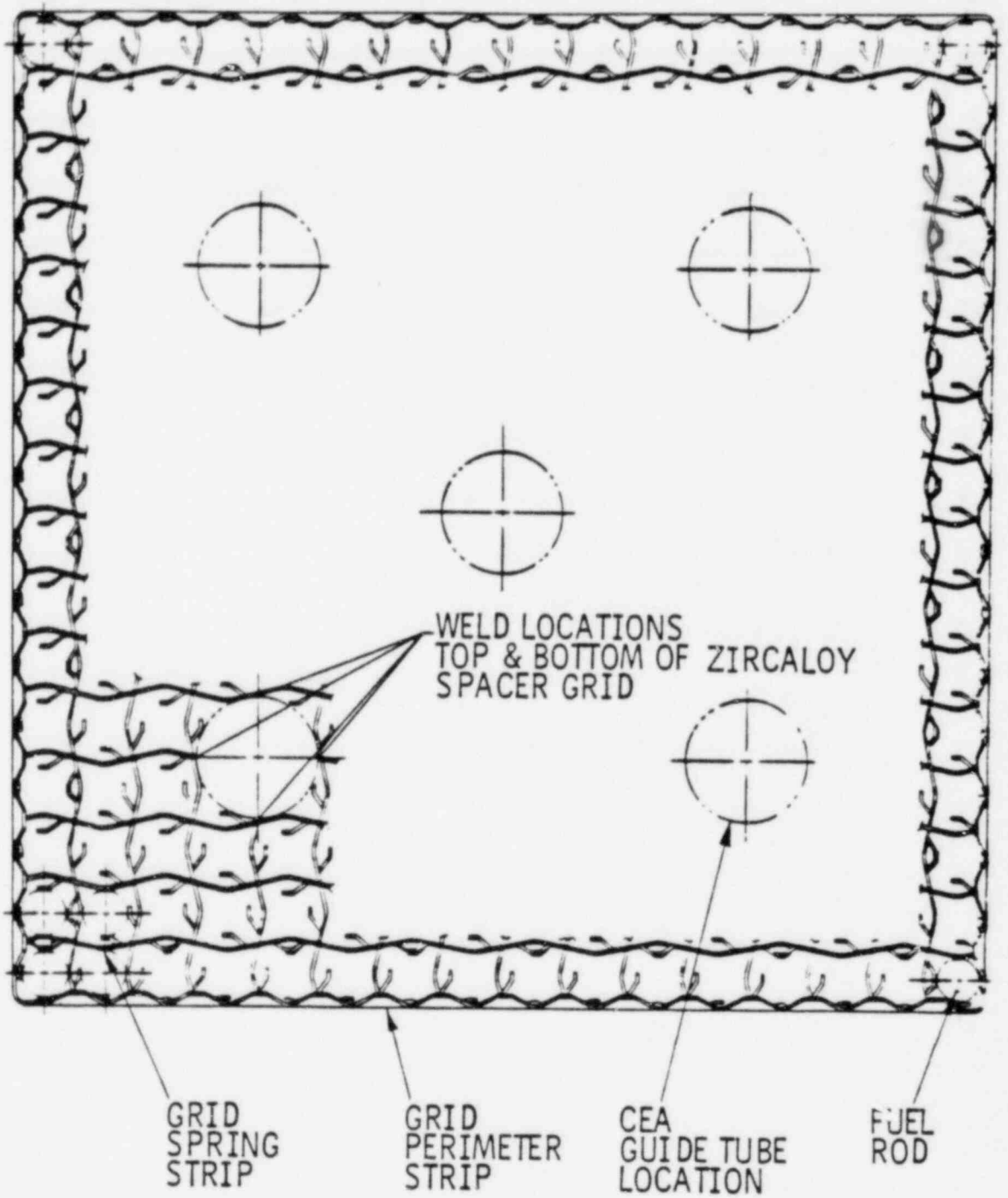

FIGURE 2-3

FUEL SPACER GRID

The guide tubes are seamless Zircaloy tubes with threaded connections at their ends. The guide tubes act in conjunction with the grids and end fittings to provide a rigid frame structure for support of the fuel rods and poison rods. They also serve as the guidance path for the control rods and as a locating feature for the neutron source and in-core instrumentation.

The upper end fitting consists of two cast 304 stainless steel plates, machined 304 stainless steel posts and helical Inconel X-750 springs. The end fitting attaches to the guide tubes to serve as an alignment and locating device and has features to permit lifting of the fuel assembly. The lower cast plate locates the top ends of the guide tubes and is designed to prevent excessive axial motion of the fuel rods. The Inconel springs are of conventional coil design. They provide the holddown force which resists the upward force on the fuel assembly due to hydraulic drag.

The lower end fitting is a 304 stainless steel casting consisting of a plate with flow holes and a support leg at each corner that aligns the lower end of the fuel assembly with the core support structure alignment plate. For plants that have the in-core instrumentation designed for insertion from the bottom of the fuel, the lower end fitting includes a center post for guidance of the instrument.

The fuel assembly design enables reconstitution, i.e., removal and reinsertion of fuel rods in an irradiated fuel assembly. The threaded joints which mechanically attach the upper end fitting to the guide tubes are torqued and locked during service but may be removed to provide access to the fuel rods. The upper end fitting is stored in a remote location during the rod removal operation. The upper end caps of the fuel rods are designed to enable grappling of the fuel rod for purposes of removal and handling. The fuel rod lower end caps are conically shaped to ensure proper reinsertion within the fuel assembly grid cage structure.

2.3 FUEL ROD DESCRIPTION

The fuel rod components consist of slightly-enriched UO_2 cylindrical ceramic pellets, a round wire Type 302 stainless steel compression spring, and an

alumina spacer disc located at each end of the fuel column. These components are encapsulated within a Zircaloy tube that is seal welded to Zircaloy end caps. The fuel rods are internally pressurized with helium during assembly to provide a good heat transfer medium and to preclude clad collapse during the design life of the fuel. A magnetic force weld is used to make the end cap closures. The fuel rod is pictured in Figure 2-4.

The fuel cladding is cold worked and stress-relief-annealed Zircaloy-4 tubing. The UO_2 pellets are dished and chamfered at both ends in order to better accommodate thermal expansion and fuel swelling. The compression spring located at the top of the fuel pellet column maintains the column in its proper position (e.g., prevents the formation of gaps in the column) during handling and shipping. The fuel rod plenum, which is located above the pellet column, provides space for axial thermal differential expansion of the fuel column and accommodates the initial helium loading and released fission gases.

2.4 BURNABLE POISON ROD DESCRIPTION

Fixed burnable neutron absorber (poison) rods may be included in selected fuel assemblies to reduce the beginning-of-life reactivity and/or the moderator temperature coefficient of reactivity. They replace fuel rods within selected lattice locations. The actual number of poison rods required depends upon the specific application. The poison rod cladding and end caps are identical to those in fuel rods, but the pellet column contains burnable poison pellets and spacer pellets instead of fuel pellets. The poison material is alumina with uniformly dispersed boron carbide particles within a specified size range. The balance of the column, typically the top and bottom several inches of the active core height, consists of alumina or Zircaloy spacer pellets. The burnable poison rod plenum spring is designed to produce a smaller preload on the pellet column than that in a fuel rod because of the lighter material in the poison pellets. The poison rod is pictured in Figure 2-5.

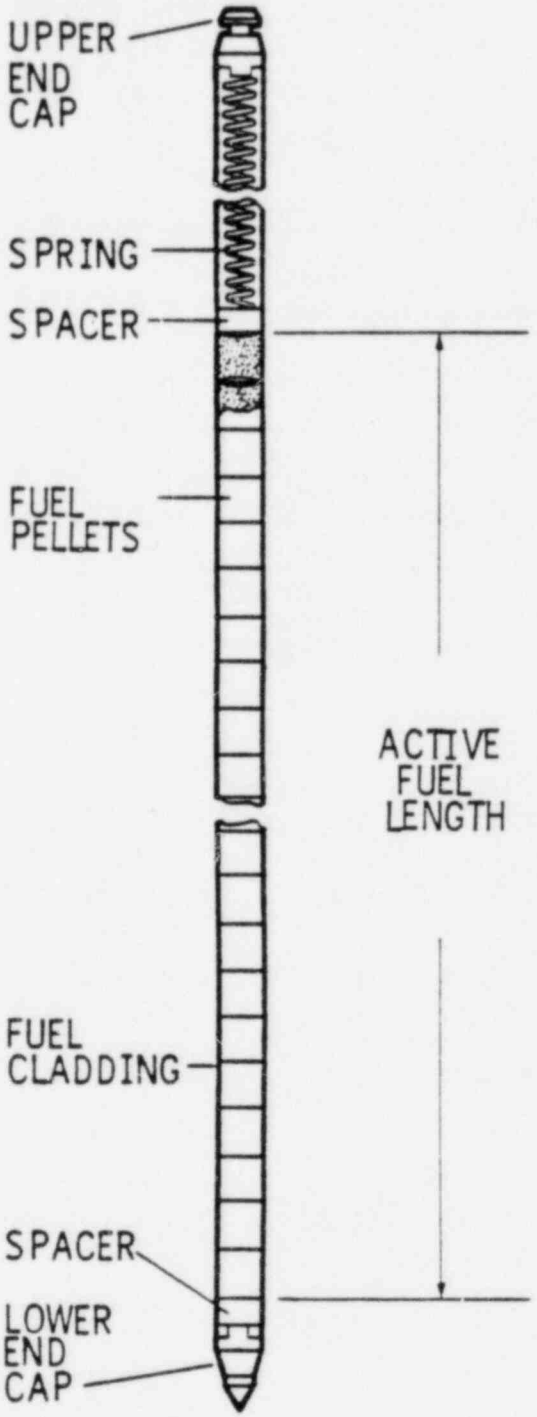

FIGURE 2-4
FUEL ROD

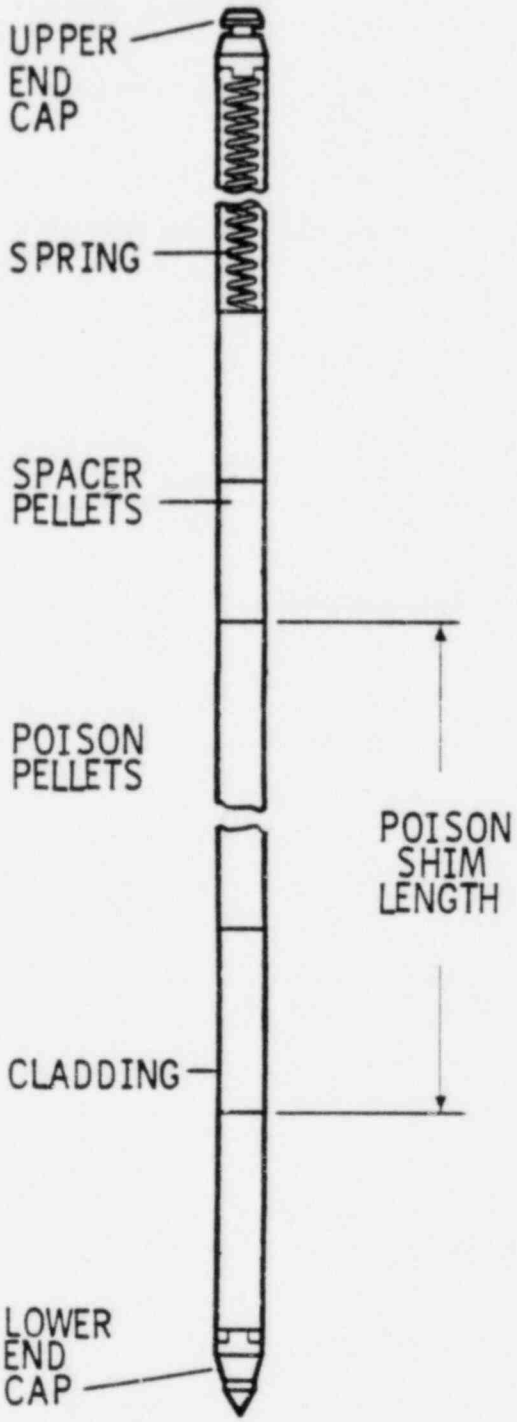

FIGURE 2-5
BURNABLE POISON ROD

Section 3

FUEL DESIGN BASES

3.1 INTRODUCTION

The fuel assembly design bases are prepared to ensure that the design will achieve its thermal performance objectives reliably and safely throughout its service life. Reliability is provided by using conservative structural criteria for the mechanical components. Safety is assured by demonstrating that the design satisfies conservative structural and thermal criteria such that:

(a) the fuel assembly is not damaged as a result of normal operation and anticipated operational occurrences,

(b) the fuel assembly damage under accident conditions is never so severe as to prevent control rod insertability when required, and

(c) core coolability is maintained for design basis transients.

Reference 3-1 defines "not damaged" as no fuel rod failure, assembly dimensions remaining within operational tolerances, and functional capabilities not being reduced below those assumed in safety analyses. Coolability is defined as the fuel assembly retaining its rod bundle geometry with adequate coolant channels to permit removal of residual heat after accidents.

The functional requirements of the fuel assembly components are discussed in Section 3.2, and specific design criteria are provided in Section 3.3.

3.2 FUNCTIONAL REQUIREMENTS

The fuel assembly components must satisfy certain requirements while sustaining the chemical, thermal, hydraulic, and irradiation-induced effects of the reactor environment up to the discharge burnup.

Functional requirements for the fuel assembly structure are listed below.

(a) The fuel assembly structure must support and locate the fuel rods axially and radially such that adequate spacing is maintained for nuclear and hydraulic considerations and so that a coolable core configuration is maintained for all design conditions.

(b) The fuel assembly structure must support the fuel and burnable poison rods such that no unacceptable wear occurs at contact points under all normal flow and temperature conditions.

(c) The fuel assembly structure must support, locate and maintain alignment of the control elements such that the control element assemblies (CEAs) move as required for both insertion and withdrawal under all design conditions without incurring excessive wear at contact points.

(d) The assembly design must be such that the magnitude and range of stresses, during steady state and transient operating conditions, are values which will not result in unacceptable fuel damage.

(e) The assembly structure must accommodate instrumentation, a neutron source and/or flow restrictors, if required.

Functional requirements for the fuel rod are as follows:

(a) The fuel rods must support and locate the fuel pellets so that no unacceptable changes in fuel pellet position occur and so that a coolable configuration is maintained under all design conditions.

(b) The fuel rods must be designed to contain the fuel pellets and the fission products generated by operation of the fuel with no rod mechanical failures under normal operation and anticipated operational occurrences.

The functional requirements for the burnable poison rod are stated below.

(a) The burnable poison rods must support and locate the burnable poison pellets so that no unacceptable changes in pellet position occur under all design conditions.

(b) The burnable poison rods must contain the burnable poison pellets and gaseous products produced by the poison material with no rod mechanical failures under normal operation and anticipated operational occurrences.

3.3 DESIGN CRITERIA

To ensure that the fuel assembly design will satisfy the general performance requirements described in Section 3.1 and the functional requirements listed in Section 3.2, specific design criteria have been established. The following sections list the design criteria currently used by C-E and reference the sections of this document which discuss the effect of extended burnup on either the criteria or the models which are used to evaluate the criteria. In all cases, these criteria are considered conservative. In the future, C-E may wish to revise some of these criteria that it feels are overly conservative for current fuel designs. In the meantime, the design criteria listed below will continue to be used until alternate criteria are requested and approved for application to C-E fuel.

The design criteria which are discussed below have been applied previously in the licensing and analysis of C-E fuel designed for standard burnup levels. Thus, these criteria have been approved for fuel designs intended for operation to batch average discharge burnups of approximately 33 MWd/kg. Combustion Engineering has reviewed these design criteria under the general guidelines established in Reference 3-1 and has concluded that the criteria are burnup independent, just as the general guidelines upon which they are based, and therefore they are applicable to the extended burnups addressed by this document (i.e., up to a batch average burnup of 45 MWd/kg).

3.3.1 Fatigue Damage

Fatigue is the term applied to the damage which occurs in a material each time it is stressed and unstressed. Repeated application of cyclic stress levels above a certain value, known as the endurance limit, will eventually produce a fatigue failure. Materials testing is used to establish both the endurance limit and the critical number of cycles at given cyclic stress levels above the endurance limit. Methods exist to account for the cumulative damage which occurs when several different stress levels are applied to a component during its lifetime.

The criterion on the cumulative fatigue damage is:

> The cumulative strain cycling usage, defined as the sum of the ratios of the number of cycles in a given effective strain range ($\Delta\varepsilon$) to the permitted number (N) at that range, will not exceed 0.8.

The methods and assumptions used to calculate the fuel rod cladding strain range are discussed in Section 4.1.1. The correlation between strain and the permitted number of cycles is also presented in Section 4.1.1.

3.3.2 Fuel Assembly Stress and Mechanical Loading

Stress levels and mechanical loading of fuel assembly structural components, fuel rods, and poison rods must be limited in order for the designs to satisfy the requirements listed in Sections 3.1 and 3.2. The stress limits for each of the fuel assembly components are discussed in Section 4.2 of Reference 3-2. The mechanical loading limits are discussed in Section 9.0 of Reference 3-3.

Because the effect of irradiation is to increase yield strength and tensile strength, unirradiated material properties are used for conservatism to establish the stress limits and loading capabilities. Therefore, the topic of material strength of the structural components of extended burnup fuel will not be discussed further in this report. Section 4.1.5 documents the irradiation effects on the fuel cladding strength.

3.3.3 Fuel Rod and Burnable Poison Rod Cladding Strain

Cladding tensile strain occurs when the fuel pellet or burnable poison pellet unrestrained diameter would be larger than the inner diameter of the cladding. This will occur when the combination of cladding creepdown and pellet swelling have closed the diametral gap between the pellets and cladding. The subsequent increase in pellet diameter that produces tensile strain of the cladding can be due to either further irradiation swelling of the pellet material or additional thermal expansion from local power increases. Permanent (unrecoverable) strain of the cladding takes place if the stress produced in the cladding by the pellet diameter increase exceeds the yield strength of the cladding, or if the stress remains in the cladding long enough for creep to occur.

The criterion applied to cladding strain is:

> The net unrecoverable circumferential strain shall not exceed 1% as predicted by computations considering cladding creep and fuel or poison pellet swelling effects.

The cladding strain limit is discussed in Section 4.1.5. Cladding creep models are described in Section 4.1.3. Fuel pellet and poison pellet swelling models are presented in Sections 4.1.9 and 4.2.7, respectively.

3.3.4 Fuel Assembly Holddown

The fuel assembly must be restrained from liftoff due to the high drag forces created by coolant flow. Axial motion could lead to wear and fretting damage of the rods and structural components.

The criterion on assembly holddown is:

> The combination of the fuel assembly wet weight and holddown spring force must maintain a net downward force on the fuel assembly during all normal and anticipated transient flow and temperature conditions.

Two burnup-related phenomena will affect the assembly holddown force. Fuel assembly length, discussed in Section 4.2.2, changes as the Zircaloy guide tubes creep and grow under stress and irradiation. The holddown springs themselves are subject to stress relaxation under temperature and irradiation. Relaxation modeling is described in Section 4.2.3.

3.3.5 Mechanical Clearance

Proper clearances must be provided between mechanical components in order to ensure: the proper interface between the fuel and reactor internals; the ability to insert and remove fuel assemblies without excessive force; the

proper functioning of the system which absorbs the kinetic energy from scramming control rods; and the accommodation of fuel rod, poison rod, and fuel assembly length change.

The criterion for mechanical clearance is:

> Adequate clearances must be maintained between the fuel assembly structural components and the reactor support structure, fuel rods, poison rods, and control element assembly to ensure functionability during the fuel assembly lifetime.

The sections of this report which deal with topics related to clearance are those on fuel rod irradiation growth (Section 4.1.14), fuel assembly length change (Section 4.2.2), spacer grid irradiation growth (Section 4.2.4), and poison rod irradiation growth (Section 4.2.7).

3.3.6 Cladding Collapse

Collapse is the term applied to a condition of elastic instability where a slightly oval cladding tube will suddenly "flatten" into a vacant space between pellets in the fuel or poison pellet column. The conditions leading to collapse are long term phenomena since collapse occurs only after the cladding has crept into the oval shape from its nearly circular shape at beginning of life. The driving force for the creep is supplied by the differential pressure on the fuel rod cladding.

The criterion for preventing cladding collapse is:

> The fuel rods and burnable poison rods will be initially pressurized with helium to an amount sufficient to prevent gross cladding deformation under the combined effects of external pressure and long term creep. The cladding design will not rely on the support of fuel or poison pellets or the plenum spring to prevent gross deformation.

Cladding collapse modeling is discussed in Section 4.1.4.

3.3.7 Fuel and Poison Rod Internal Pressure

The internal pressure in fuel or poison rods increases with increasing burnup when all other conditions are the same (e.g., constant fuel temperature). With increased burnup, the total internal pressure, due to the combined effects of the initial helium fill gas and the gases released from the fuel or poison pellets, can approach values comparable to the external coolant pressure. The predicted fuel and poison rod internal pressures will be consistent with the following criteria:

(a) the primary stress in the cladding resulting from differential pressure will not exceed the design stress limits (cf. Section 3.3.2), and

(b) the internal pressure will not cause the cladding to creep outward from the pellet surface while operating at the design peak linear heat rate for normal operation.

The criteria discussed above do not limit fuel or poison rod internal pressure to values less than the primary coolant pressure, and the occurrence of positive differential pressures would not adversely affect normal operation if appropriate criteria for cladding stress, strain, and strain rate were satisfied.

The fuel and poison rod internal pressures are predicted analytically as a function of their burnup dependent parameters to ensure compliance with the design criteria. For fuel and poison rods, internal rod pressures are a function of a variety of burnup dependent parameters which determine the amount of gas (fill gas and released gas) present in the rod internal void volumes and the size of those internal void volumes (plenum, annular space between fuel and clad, etc.). These parameters include fission gas release (Section 4.1.6), fuel swelling (Section 4.1.9), fuel thermal conductivity (Section 4.1.7), cladding creep (Section 4.1.3), and cladding irradiation growth (Section 4.1.14) in fuel rods; and gas release, cladding creep, pellet swelling and cladding irradiation growth (Section 4.2.7) in poison rods.

3.3.8 Thermal-Hydraulic Design Criteria

Avoidance of thermally or hydraulically induced fuel damage during normal steady state operation and during anticipated operational occurrences is the principal thermal-hydraulic design basis. To satisfy this design basis, design criteria on minimum departure from nucleate boiling ratio (DNBR), and fuel melting have been established. The predicted minimum DNBR and peak fuel temperature will be consistent with the following criteria:

(a) The minimum DNBR shall be such as to provide at least a 95% probability with 95% confidence that departure from nucleate boiling (DNB) does not occur on a fuel rod having that minimum DNBR during steady state operation and anticipated operational occurrences. A penalty is imposed on DNBR to account for fuel rod bow. Fuel rod bow is burnup dependent, and the effect of extended burnup is discussed in Section 4.1.10.

(b) The peak temperature of the fuel shall be less than that required for incipient melting during steady state operation and anticipated operational occurrences. The melting point is 5080°F for unirradiated UO_2 fuel and decreases with burnup. The burnup dependence of the fuel melting point at extended burnup is discussed in Section 4.1.8.

3.3.9 ECCS Acceptance Criteria

The fuel assembly design, in combination with the Emergency Core Cooling System (ECCS) design, is required to conform to acceptance criteria on peak cladding temperature, maximum cladding oxidation, maximum hydrogen generation, and maintenance of coolable core geometry and long term cooling during a LOCA (see Section 6.3.3 of Reference 3-2). Fuel performance during a LOCA is dependent on many parameters. Some of the important fuel rod parameters affected by extended burnup are cladding corrosion (Section 4.1.2), irradiation growth (Section 4.1.14), fuel fission gas release (Section 4.1.6), and fuel swelling (Section 4.1.9). These parameters contribute to the fuel rod response during the event and are considered in demonstrating compliance to the acceptance criteria. These effects are discussed in Section 4.1.13.

Section 4

FUEL PERFORMANCE TOPICS

4.1 FUEL ROD

The fuel performance topics (or parameters) that are associated with individual fuel rods are discussed in this section. A list of these topics was given in Table 1-1 and includes those that are related to the behavior of individual fuel pellets (e.g., fuel swelling, fuel thermal conductivity), the behavior of cladding under both typical and atypical environmental conditions (e.g., cladding oxidation, cladding deformation and rupture), and the combined effects of these working in concert (e.g., pellet/cladding interaction, irradiation growth). The ordering of these topics is arbitrary and has no particular significance. Fuel performance topics that are associated with the overall fuel assembly and/or its structural components are discussed in Section 4.2.

4.1.1 Fatigue

Fuel rod cladding fatigue is a complex process which is dependent on many variables, including power history, initial pellet and cladding dimensions, level of fuel rod prepressurization, fuel and cladding creep properties, and neutron exposure history. The current method of calculating fatigue damage conservatively accounts for each of these factors in a time history analysis. The resulting fatigue damage has a large margin to the criterion listed in Section 3.3 for standard fuel cycles, and it is expected to remain large for extended-burnup cycles.

4.1.1.1 Modeling of Fatigue Damage

The cyclic strain of the fuel rod cladding which accompanies changes in power level can be divided into three periods during the fuel lifetime. During the first period, there is a finite gap between the fuel pellet and cladding, even during full power operation. Changes in the fuel rod power level affect the cladding strain only through the change in rod internal pressure. The strain ranges produced during this period of time are small and result in negligible fatigue damage.

The second period begins when a sufficient amount of cladding creepdown and fuel swelling has occurred to bring the pellet into direct contact with the cladding at full power. As the burnup progresses, there will be an increasing amount of cladding elastic strain for a given change in power level. The increase in elastic strain is due to the fact that the pellet and cladding remain in contact over a wider range of power levels as fuel swelling continues. The elastic strain produces elastic stress in the cladding. For the cladding creep model described in Section 4.1.3, the elastic stress results in permanent tensile strain as the time at contact continues.

Eventually, the variability of elastic strain becomes small for a given change in power level. During this third period, the elastic stresses produced by contact result in enough outward creep of the cladding during times of contact to nearly balance the amount of fuel swelling. Thus, there is no change in the zero power gap, and the power level at which the pellet and cladding come into contact is essentially the same for each power cycle.

The current method for fatigue analysis accounts for power dependent and time dependent phenomena by using rod internal pressure, cladding diameter, and pellet diameter change models that are described in Reference 4-1. The cladding is assumed to conform to the predicted diameter of the pellet during periods of contact (elastic compression and hot pressing of the pellet are ignored). Conservative assumptions are used to select the starting dimensions and properties of the fuel rod chosen for analysis. For the initial design analyses, daily power cycling between ten percent and one hundred percent power is assumed throughout life. Fifty reactor heatups and cooldowns are also represented. Once the fuel has been partially irradiated, fatigue margin is calculated (e.g., for reload cycle verification) using actual past power histories and assumed daily load cycling for future operation.

The method for fatigue analysis results in a series of cladding strain range values covering the fuel lifetime. The cumulative fatigue damage fraction is determined by summing the ratios of the number of cycles in a given strain range to the permitted number in that range. The permitted number of cycles in any strain range is based on the method of universal slopes developed by Manson (4-2), and has been adjusted to provide a strain cycle margin for the

effects of uncertainty and irradiation. Figure 4-1 shows the relationship between strain and allowable cycles previously submitted to the NRC in Reference 4-3. The resulting fatigue damage fraction is compared to the 0.8 limit listed in Section 3.3.

4.1.1.2 Effect of Extended Burnup

The total number of fatigue cycles depends on reactor operation and residence time, not on fuel burnup. While longer residence times with the assumption of continued daily power cycling would tend to increase calculated fatigue damage, the increased damage is typically offset in the analysis by the use of actual plant operating history for previous exposure. Realistically, extended burnup will only result in a few additional power cycles on the fuel.

4.1.1.3 Evaluation of Fatigue

The method used to calculate fatigue damage will remain applicable for extended burnup operation since the individual components of the method (e.g., cladding creep, fuel swelling) are shown to be modeled adequately in other sections of this report. Using the above described models and assumptions, design analyses are expected to continue to demonstrate wide margins to fatigue failure.

4.1.2 Cladding Corrosion

The waterside corrosion of Zircaloy fuel cladding in pressurized water reactors (PWRs) has never restricted operating strategies or impacted design limits. Extending the discharge burnup will, however, result in longer fuel in-reactor residence times which will increase corrosion. In addition to fuel residence time, the amount of corrosion is dependent upon local heat flux and coolant temperature, as well as the chemistry of the primary coolant.

C-E has an ongoing program to study the waterside corrosion of Zircaloy clad fuel rods. Part of this program is jointly sponsored with EPRI and KWU (4-4, 4-5), and examines the corrosion performance of KWU fuel. C-E's waterside corrosion program also includes the DOE/OPPD/C-E program in Fort Calhoun (4-6) and the EPRI/C-E program in Calvert Cliffs-1 (4-7) in which C-E

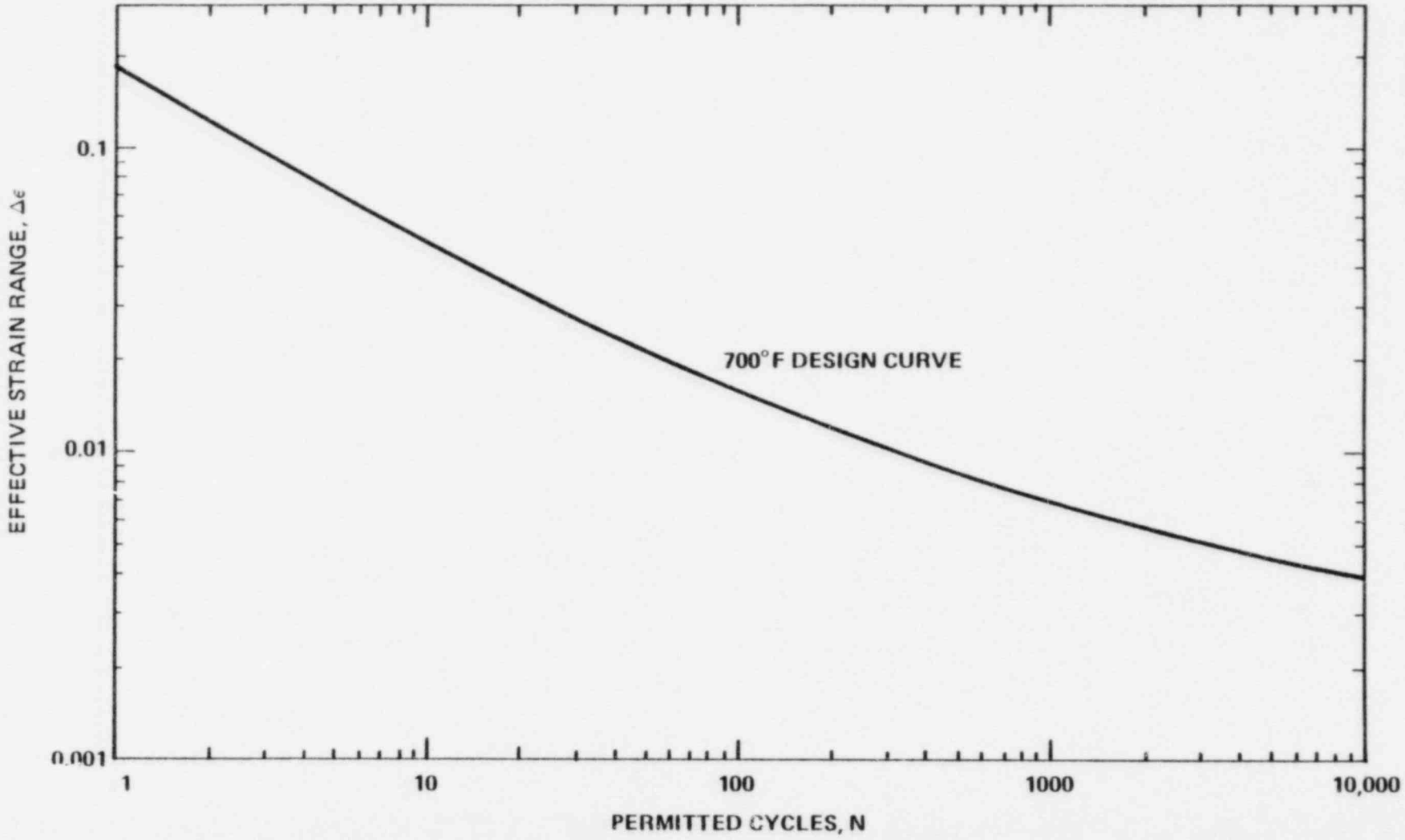

FIGURE 4-1
DESIGN CURVE FOR CYCLIC STRAIN USAGE OF ZIRCALOY-4 AT 700°F

14x14 fuel will be examined after extended burnups of up to 55 MWd/kg. C-E also has a program, jointly sponsored with DOE and AP&L, in Arkansas Nuclear One Unit 2 (4-8) to investigate waterside corrosion of C-E 16x16 fuel. It is the purpose of this section to briefly review fuel rod corrosion behavior and to discuss the current status of these ongoing corrosion programs in the context of achieving extended fuel burnups.

4.1.2.1 Corrosion Behavior

Zircaloy Corrosion Reaction. The Zircaloy corrosion reaction in pure high temperature water or steam is written as:

$$Zr + 2H_2O \rightarrow ZrO_2 + 2H_2.$$

Part of the hydrogen diffuses through the oxide layer into the metal. The amount of hydrogen absorbed in the metal, expressed as a percentage of the total amount produced during the corrosion reaction, is called the "pickup fraction". Zircaloy-4 has a smaller hydrogen pickup fraction during corrosion than does Zircaloy-2, although the corrosion kinetics of the Zircaloys are similar.

General Corrosion . Autoclave isothermal corrosion tests show that the oxide initially developed is a smooth, continuous black or gray-black, lustrous, adherent film which is protective in nature. After extensive exposure, the film may become mottled, then gray, and finally tan while retaining its adherence to the underlying metal. Under heat transfer conditions, the appearance of the oxide also changes as the exposure increases. One-cycle PWR fuel rods with about 300 days of exposure normally develop a thin black oxide along their entire length. Rods exposed for multiple cycles have a different surface appearance. In the lower third of these fuel rods, the oxide layers are thin and black with a spotted transition region in the middle of the rod, developing into a gray oxide in the upper part of the rod. The oxide then changes to black in the plenum (nonfueled) region. The transition from black to gray occurs at an oxide layer thickness between 5 and 10 μm. Oxide layers with thicknesses greater than 10 μm (0.4 mil) have a gray coloration. Generally, the oxide layer thickness associated with a gray/tan film is greater than that associated with a black film.

The axial variation in oxide layer thickness is illustrated in Figure 4-2. These measurements were made using a nondestructive eddy-current technique (4-4). Generally, the corrosion layer thickness increases with axial position from the bottom of the rod. This reflects the increase in rod surface temperature and the temperature at the metal oxide interface; the latter controlling the extent of corrosion. There are local minima at the grid positions. This reduced affinity at the grid positions for corrosion is due to the lower local temperature caused by an increase in both coolant velocity and local turbulence as well as a local depression in power at the grids.

C-E data on corrosion of Zircaloy fuel rod cladding from two PWRs are presented in Figure 4-3; the oxide layer thickness at the peak temperature position of the fuel rod is given as a function of rod burnup up[ ] Some of the published data from other pressurized water reactors (4-4 , 4-5) are presented in Figure 4-4. Included are data obtained from the EPRI/C-E/KWU Waterside Corrosion Program. This fuel was irradiated in five KWU pressurized water reactors. These rods were irradiated from one to four reactor cycles and had achieved rod average burnups of up to 44 MWd/kg. Large scatter exists in the data as is evident in Figure 4-4. Some of this scatter from reactor to reactor can be attributed to differences in the thermal hydraulics (e.g., inlet temperature, system pressure, coolant flow rate), as well as differences in power history which will influence the clad surface temperature. The trends in oxide layer thickness shown in Figures 4-3 and 4-4 illustrate that no abrupt increase in corrosion rate has been observed at extended burnups.

The modeling of corrosion is still under development (4-4 , 4-5). Some of the effects believed to be important are discussed below together with more recent observations.

Phenomenologically, isothermal corrosion has an approximately cubic dependence on time in the temperature range 250-400 °C. At a weight gain of approximately 30 to 40 mg/dm^2 (which corresponds to an oxide layer thickness of 2.0 to 2.7 µm, since for ZrO_2, 1 µm = 15 mg/dm^2), there is a transition in the corrosion kinetics from the cubic relationship to a linear relationship with

FIGURE 4-2
TYPICAL COMPOSITE OXIDE LAYER THICKNESS TRACE FOR A FUEL ROD AFTER 4 CYCLES OF IRRADIATION

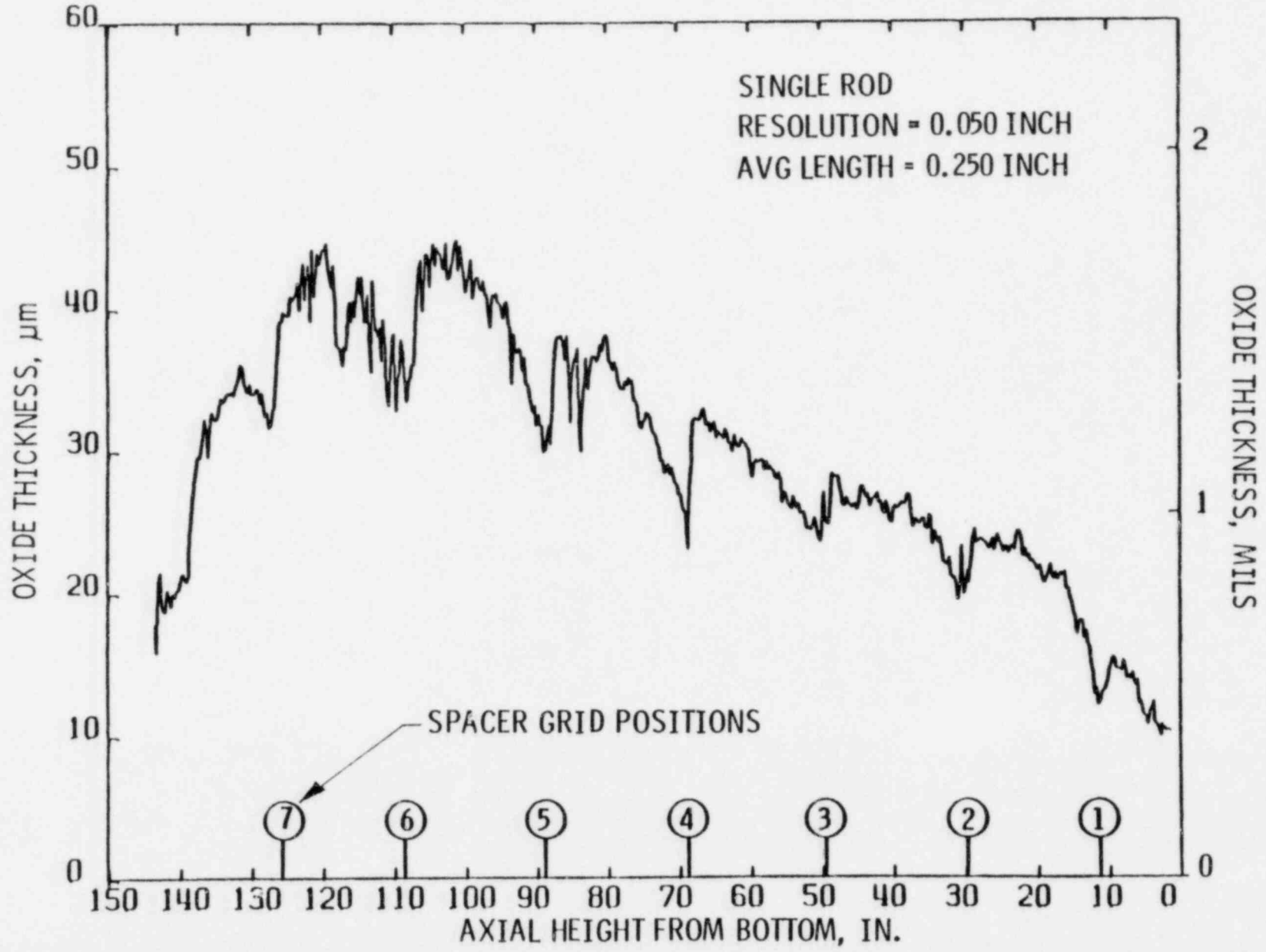

FIGURE 4-3
OXIDE MEASUREMENTS FROM CALVERT CLIFFS-I AND FORT CALHOUN

FIGURE 4-4

MAXIMUM OXIDE LAYER THICKNESS OF PWR FUEL RODS VERSUS BURNUP

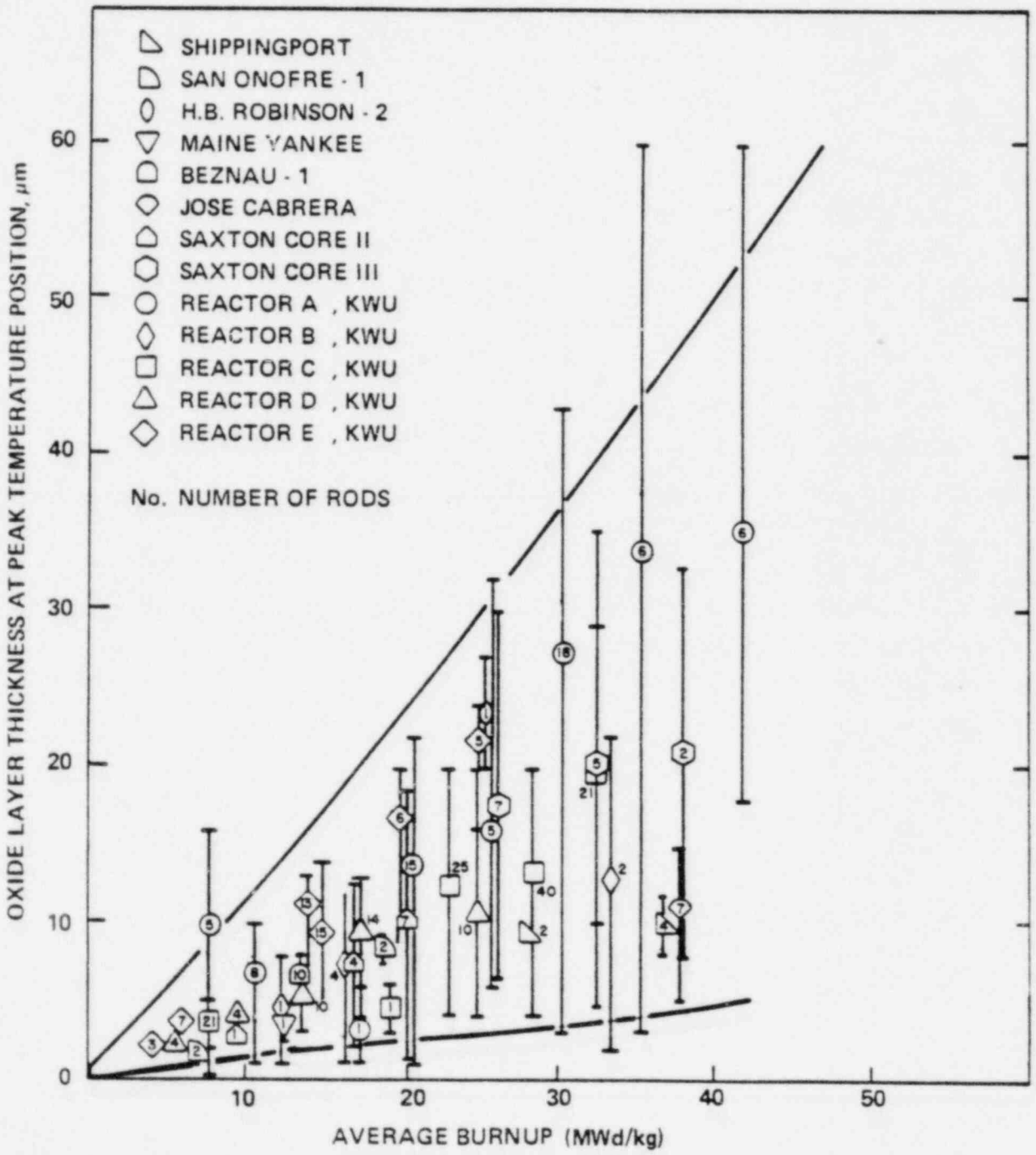

time. One school of thought assumes that the linear posttransition corrosion behavior is actually a cyclic repeat of the pretransition kinetics which, when averaged over the sample surface area, results in a mean linear rate. However, it is also possible that a protective layer at the metal interface with a more or less constant thickness controls the rate of corrosion in the posttransition region.

Under conditions of heat flux, there is a temperature gradient across the oxide layer. It is believed that the corrosion rate is controlled by the temperature at the metal/oxide interface, the correlation of which is sensitive to the oxide thermal conductivity. A review of thermal conductivity data shows that it could be in the range 0.15 to 6.3 W/m°K. In view of the large uncertainty, measurements were made by the UKAEA as part of the joint EPRI/C-E/KWU Waterside Corrosion Program. Thermal diffusivity measurements were conducted on irradiated tubular samples which were large enough to minimize any damage to the oxide during preparation. Based on these measurements as well as on experimental determinations of the oxide specific heat and use of the unirradiated oxide film density, it is estimated that the thermal conductivity is 1.45 W/m°K. Some measurements of the density of irradiated ZrO_2 suggest that the density is reduced by irradiation from 4.8 g/cc to 4.29 g/cc. If this is the case, the thermal conductivity for irradiated material is 1.30 W/m°K.

Zircaloy waterside corrosion appears to be some what greater in-reactor than ex-reactor. In early analyses (4-4 , 4-5), it was concluded that corrosion varied from reactor to reactor and, in the case of Reactor A from KWU, there was a cycle by cycle increase in enhancement. Some of the possible reasons for this in-reactor enhancement of waterside corrosion include:

- radiation effects in the oxide layer,
- radiolysis of water,
- coolant chemistry and local boiling effects, and
- modification of the oxide layer chemistry.

In addition, some reactors exhibit a crud deposit on the surface of fuel rods which can enhance corrosion by increasing the metal/oxide interface temperature.

Post irradiation autoclave corrosion tests were performed as part of the EPRI/C-E/KWU Waterside Corrosion Program to define the effect of prior reactor exposure on the subsequent out-of-reactor corrosion behavior, i.e., the memory effect. The initial post irradiation autoclave corrosion rate was similar to the in-reactor rate and continuously decreased with time to the rate expected from a model based on the ex-reactor data. Times in excess of 140 days at 280 °C were required for the corrosion memory effect to disappear. These observations suggest that the reactor environment, as well as changes in the nature of the oxide film, are involved in the enhancement of corrosion.

Optical metallography and scanning electron microscopy were used to characterize the microstructure of the oxide films. The microcrack appearance and spacing, as well as the subgrain size and distribution, were similar for oxides formed in-reactor as well as ex-reactor. The average microcrack spacing was about 2 to 3 μm and increased with total oxide thickness. The crack spacing at the water/oxide interface was always larger than the average oxide crack spacing.

Secondary ion mass spectroscopy and other techniques were utilized to obtain the relative impurity concentration and profile in the oxide film. None of the current oxide layer chemical composition data suggest modifications to the oxide layer chemistry which may be responsible for the in-reactor enhancement of corrosion.

X-ray diffraction analysis showed that the irradiated and unirradiated oxides were predominantly monoclinic in structure. The data reveal irradiation induced line broadening implying an increase in the density of defects. Thus far, the physical examination of the oxide film has failed to reveal why there is an enhancement in corrosion and why it varies from reactor to reactor. It is surmised that differences in coolant chemistry, materials used in the primary system, and crud formation could be affecting corrosion.

In summary, waterside corrosion is a complex process which is influenced by many factors; these are currently being investigated. One of the more important variables controlling the rate of formation of the oxide layer is the temperature at the oxide layer interface. The ongoing C-E waterside corrosion

programs are expected to develop more data on the parameters which control the variability in behavior from plant to plant and to identify measures to minimize its extent.

Hydrogen Pickup. During the corrosion process, hydrogen is evolved and a fraction of this hydrogen reacts with the cladding (i.e., the "pickup fraction"). Metallographic techniques were used to estimate the hydrogen content in cladding by comparing the hydride distribution in a sample with known visual standards. These data, presented in Figure 4-5, agree well with the Saxton quantitative hydrogen analysis data (4-5 , 4-9 , 4-10). Hydrogen pickup for Zircaloy-4 corroding in a PWR environment is lower than the 20 to 30% anticipated from out-of-pile tests. For samples with a weight gain greater than about 30 to 40 mg/dm^2 (which corresponds to an oxide layer thickness of 2.0 to 2.7 μm), the hydrogen pickup fraction was found to be less than 16%. The thinner oxides had a higher pickup fraction than the thicker oxides. For heavier oxides of 20 μm or more, the pickup fraction is 10%. Thus, a pickup fraction of 10% may be used to calculate the hydrogen inventory in the cladding at higher burnups.

4.1.2.2 Effect of Extended Burnup

The corrosion rate is dependent on the temperature at the metal/oxide interface, which in turn depends on the oxide thickness formed as well as the heat flux, and the oxide layer thermal conductivity. As the oxide layer thickness increases for a constant power, the temperature at the metal/oxide interface increases, driving up the corrosion rate. This, in turn, increases the oxide layer thickness further. Thus, at higher burnups and longer residence times when oxide layers are thicker, the corrosion rate will increase unless the decrease in power is sufficient to offset the effect of the increase in oxide layer thickness. Corrosion thus appears to be sensitive to those parameters which will increase the temperature at the metal/oxide interface such as heat flux, thermal conductivity, thermal hydraulic condition, oxide already formed, as well as other parameters such as residence time, coolant chemistry and possibly irradiation damage.

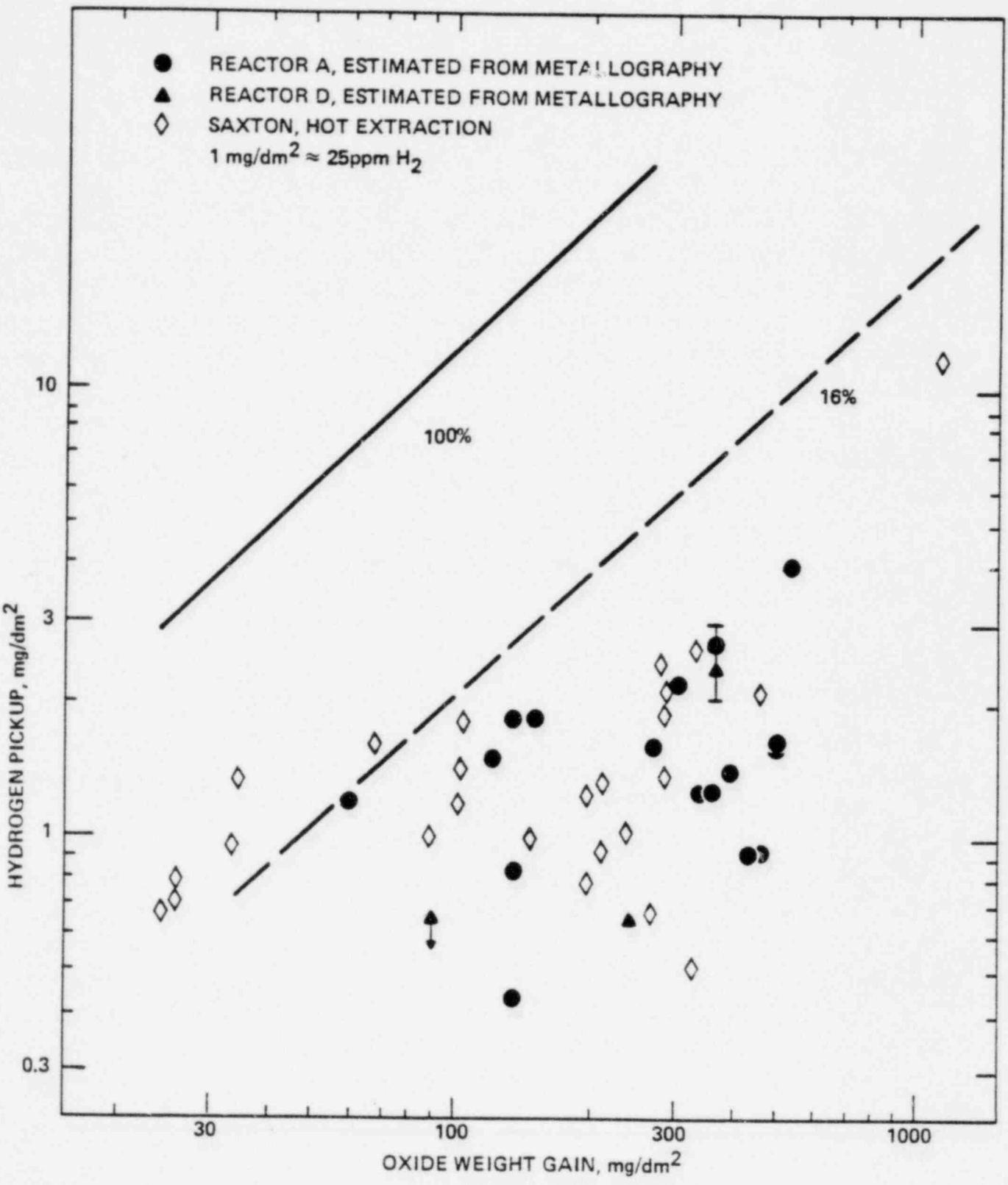

FIGURE 4-5

HYDROGEN PICKUP OF ZIRCALOY-4 IN A PWR ENVIRONMENT

4.1.2.3 Evaluation of Cladding Corrosion

The data which are currently available have been presented in Section 4.1.2.1. Thus, there is an experimental basis with which to project general corrosion for C-E plants. Data available to date indicate that fuel cladding waterside corrosion can vary significantly from reactor to reactor and even from cycle to cycle. The ongoing EPRI/C-E/KWU Waterside Corrosion Program is expected to develop data on the factors which control the variability in waterside corrosion behavior and to identify measures to minimize its extent. The available data indicate no sigificant increase in the rate of corrosion with burnup. This appears to be due to the decrease in power of fuel that has accumulated high burnup. The lower power level offsets the effect of increased oxide thickness. C-E has several irradiation test programs in place which will provide experimental confirmation of the extended-burnup performance of C-E fuel. These programs will monitor corrosion and allow the model predictions to be verified to burnups in excess of 55 MWd/kg for both 14x14 and 16x16 fuel assembly designs.

4.1.3 Cladding Creep

During normal reactor operation, the fuel cladding is subjected to stresses which cause it to slowly deform or creep. While the high temperature coolant pressure tends to decrease the cladding diameter, fission gas release and fuel swelling after fuel cladding contact tends to slow this creepdown process. The observed creep behavior is the net result of these competing processes. Apart from the stress and temperature, which are the two important factors contributing to the creep phenomenon, the neutron environment also enhances creep. The effect of extended-burnup operation on the diametral creep of fuel cladding is discussed in this section. Axial creep effects are included in the empirical fuel rod growth correlation discussed in Section 4.1.14.

4.1.3.1 Modeling of Creep

The creep rate is a function of neutron flux, temperature and applied stress. The in-reactor creep model (4-1), used by C-E (prior to fuel/cladding contact), is as follows:

Equation (1) describes the cladding diametral creep in the initial stages of the in-reactor exposure prior to the establishment of contact between fuel pellets and cladding. Once the cladding touches the pellets, subsequent dimensional changes of the fuel rod are controlled by several factors including the cladding creep; fuel pellet densification, swelling, and fragmentation; fission gas release; thermal expansions of the fuel pellets and cladding; and the axisymmetric stress state between pellets and cladding. This cladding creep model is incorporated into FATES3 (4-11).

4.1.3.2 Effect of Extended Burnup on Cladding Creep

The fuel rod dimensional behavior is complex after contact. Contact between fuel pellet and cladding is anticipated early in life at relatively low burnups between 10 and 20 MWd/kg. The fuel rod dimensional behavior during extended burnup will be affected by cladding creep, fuel pellet creep, fuel pellet fragmentation and densification, fission gas release, fuel swelling, thermal expansion of cladding and fuel, and power density. However, the cladding creep behavior and mechanisms for extended-burnup operation are expected to be the same as those for normal-burnup operation. The application of the creep model, described in the previous section, to extended-burnup operation is therefore valid.

4.1.3.3 Evaluation of Creep

Diametral creep measurements are available for several fuel rods from Calvert Cliffs-1 test fuel assemblies after 1, 2, 3 and 4 reactor cycles (4-12) through (4-14). For all the measurements, the diametral strain has not changed significantly from the end of the first irradiation cycle to the end of the fourth irradiation cycle. A typical example is given in Figure 4-6. These data demonstrate that for current C-E fuel rod designs [ ] the net diametral change is almost constant after the end of the first cycle of irradiation. Thus, for the Calvert Cliffs-1 test assemblies, the diametral creepdown is self-limiting after the end of the first irradiation cycle (burnup approximately 19.4 MWd/kg) and remains constant up to an average burnup of 43 MWd/kg. The cladding diameter is not expected to change significantly during extended-burnup operation to a burnup of about 50 MWd/kg. The cladding creep model is judged to be applicable to the range of burnups covered by this topical.

4.1.4 Cladding Collapse

The fuel rod cladding tubes always have a minor degree of variation from a perfectly circular cross section with uniform wall thickness. When subjected to a net external pressure in the reactor, bending stresses are produced as a

FIGURE 4-6
EFFECT OF TEST VARIABLES ON FUEL ROD
DIAMETRAL STRAIN AT VARIOUS BURNUP LEVELS

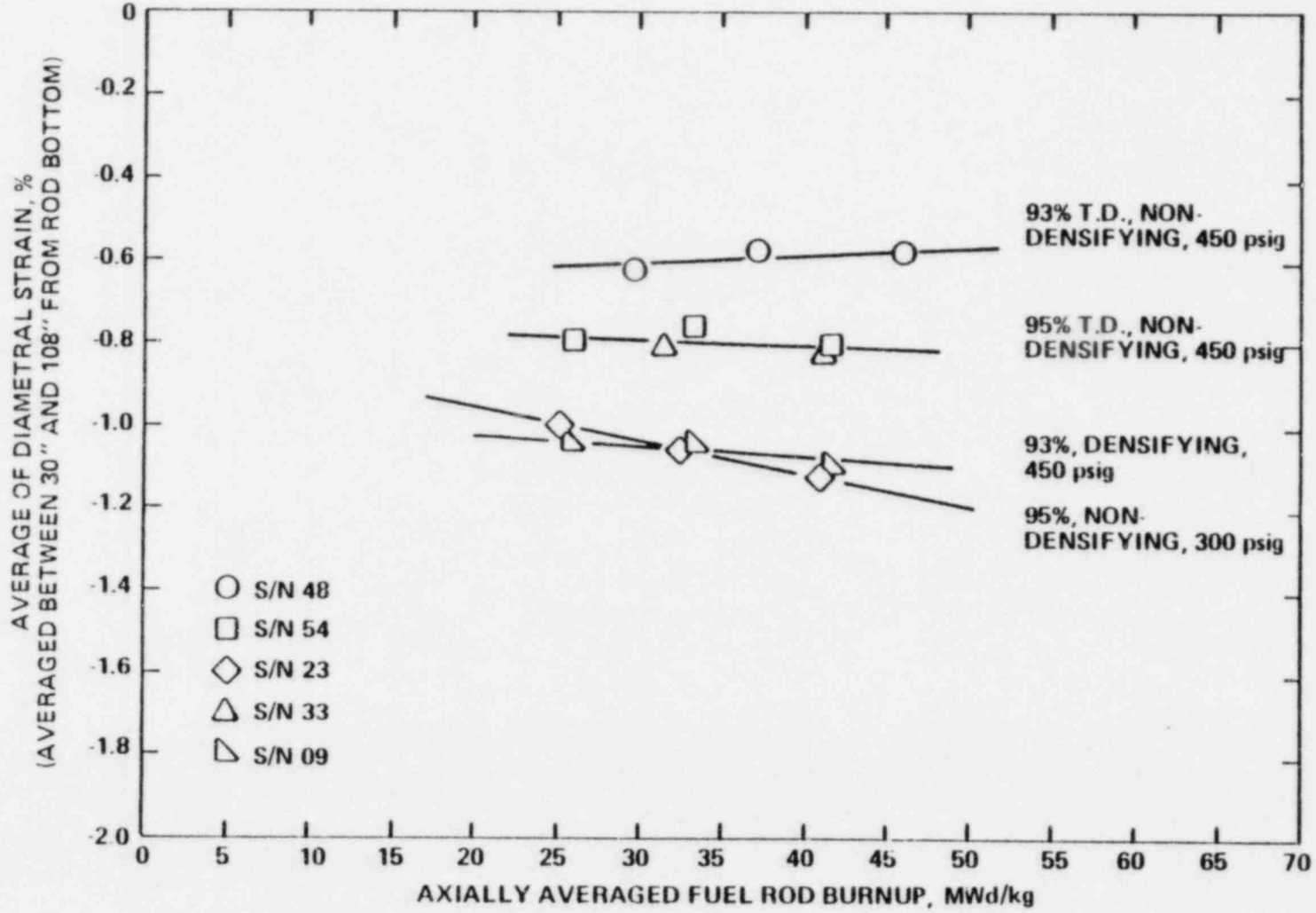

result of the slightly imperfect geometry. Under the high temperature and neutron flux conditions in the reactor, the Zircaloy cladding creeps in response to the bending stresses. The resulting creep strain increases the deviation from the circular shape, thereby increasing the bending stresses. This process continues at an increasing rate until contact is made with the fuel pellets or, if a significant axial gap exists in the pellet column, until an unstable condition is reached and the cladding "collapses" into a flattened shape.

No significant axial gaps have ever been observed in Combustion Engineering's modern design fuel which has prepressurized fuel rods and stable, "nondensifying" fuel pellets. The gaps would be evidenced by large local ovalities of the fuel rod cladding, by a distinct region of atypical crud deposition around the cladding circumference, or by atypical signals during gamma scanning. None of these effects has been observed during the extensive post-irradiation examination programs conducted on both 14x14 and 16x16 fuel designs. The prepressurized, stable fuel will be used in C-E fuel designed for extended burnup.

4.1.4.1 Modeling of Cladding Collapse

The current methods of evaluating cladding collapse resistance are described in References 4-15 and 4-16. Reference 4-15 describes a method which utilizes the CEPAN computer code to predict creep deformation and collapse time of Zircaloy fuel cladding containing initial ovality. Although significant gaps have not been observed, the method assumes a gap in the pellet column exists at the most unfavorable elevation in the fuel rod. No credit is taken for the support offered by the pellets at the edges of the gap. The original method of selecting input to CEPAN resulted in a deterministic combination of worst case cladding as-built dimensions and assumed worst case operating conditions during the fuel lifetime. The NRC has concluded that CEPAN provides an acceptable analytical procedure for determining the minimum time to collapse for C-E Zircaloy clad fuel. If this minimum collapse time exceeds the fuel lifetime, then collapse resistance has been demonstrated.

Since the probability of all of the adverse cladding dimensions and fuel rod operating conditions occurring simultaneously in any given fuel rod is extremely remote, an improved methodology described in Reference 4-16 results in a more reasonable degree of conservatism by statistically determining the effects of uncertainties in cladding dimensions. This methodology utilizes the SIGPAN computer code, which combines the CEPAN computer code with the SIGMA stochastic simulation computer code (Reference 4-17) to generate a probability histogram of cladding collapse times based on random combinations of as-built cladding dimensions. [

]

Reference 4-16 was submitted to the NRC in September 1981, and approval is expected in 1982. The method described in the reference is intended to be used for all future collapse analyses.

4.1.4.2 Effect of Extended Burnup

Since cladding collapse is a creep-related phenomenon, the longer residence times associated with extended-burnup fuel will increase the amount of creep of unsupported cladding. The increased creep strain will be accounted for in the analysis of the ability of the fuel rod design to resist cladding collapse, unless it can be demonstrated that there will be no significant axial gaps in the fuel rod pellet columns.

4.1.4.3 Evaluation of Cladding Collapse

Although early experience with densifying UO_2 fuel pellets indicated that cladding collapse could result in fuel failure, improvements in fuel design, notably the development of stable fuel pellet types, have essentially

FIGURE 4-7

TYPICAL PROBABILITY HISTOGRAM FOR FUEL ROD COLLAPSE

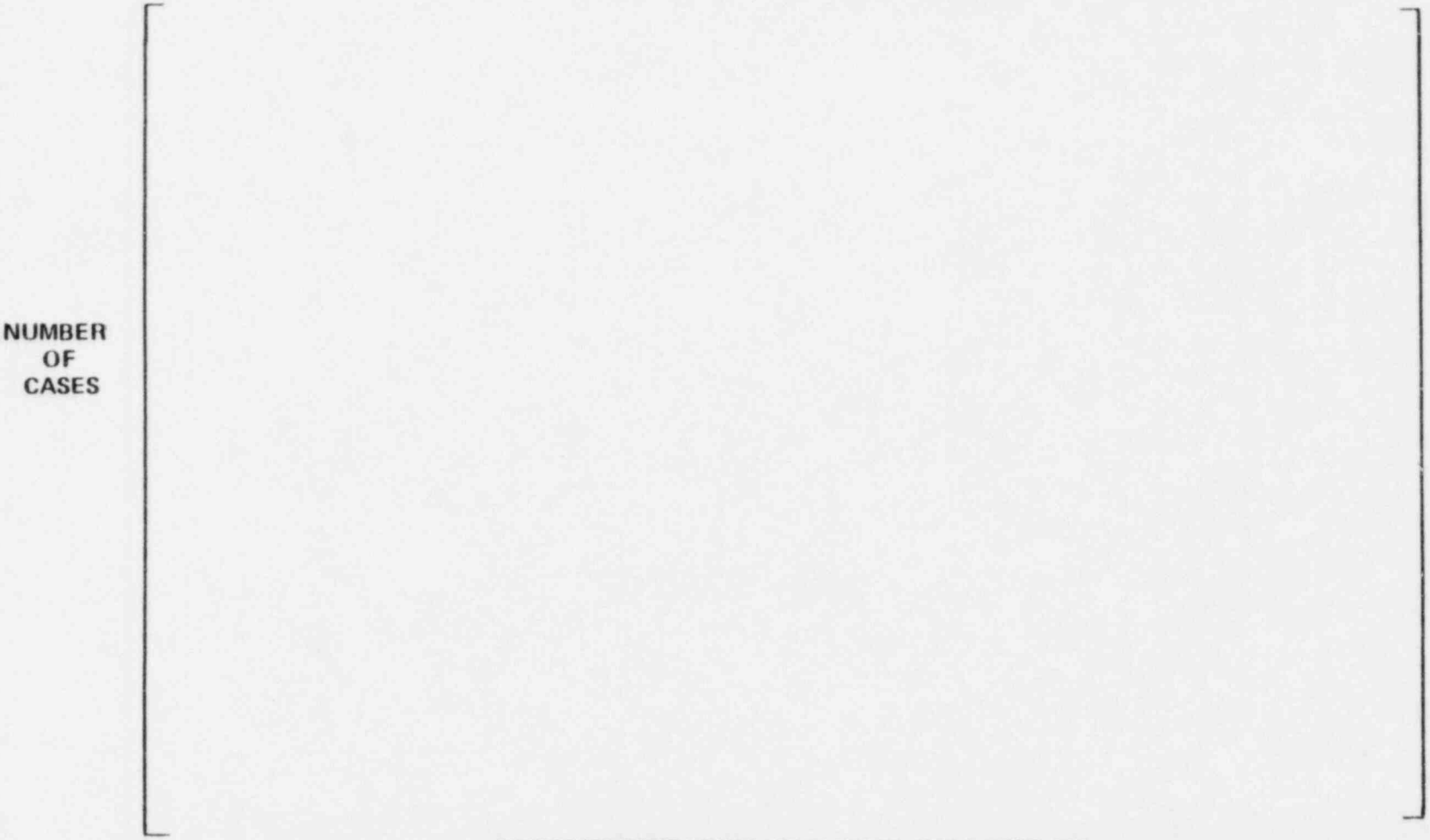

eliminated this potential problem. Current commercial fuel pellets have shown through operating performance that significant axial gaps do not form in the fuel pellet column. Without the occurrence of gaps of sufficient length, cladding collapse cannot occur and, as a consequence, the cladding will remain stable and will not be subject to high local strains from this effect. Furthermore, there is no evidence to indicate that continued operation of fuel rods having cladding in oval contact with the fuel pellet column is detrimental. Nevertheless, C-E will continue to use the cladding collapse criterion given in Section 3.3.6 until justification is provided to eliminate this criterion.

The predicted time for creep collapse is a function of cladding as-built properties and plant specific operating history. Because of this, no specific limits can be provided for the collapse resistance of C-E designs. C-E will continue to follow the past practice of calculating the collapse time for each resident batch prior to the startup of each reactor cycle.

The criterion for collapse will be that the most limiting rod in the core will have at least a 95% probability that its predicted time to collapse exceeds the reactor operating time during its residence. The SIGPAN model will be used to demonstrate that this criterion has been satisfied.

4.1.5 Embrittlement of Fuel Cladding

Exposure of Zircaloy to fast neutron irradiation causes the material to become embrittled. Specifically, the material yield strength and ultimate strengths increase while the ductility decreases. The effect is nonlinear and is manifested early in the irradiation exposure and tends to reach saturation levels fairly rapidly. In addition, Zircaloy cladding reacts with water to form a zirconium dioxide (ZrO_2) layer on the outer surface of the fuel rod; hydrogen is produced in the reaction and some is absorbed by the metal and may cause embrittlement. The fuel rod design criteria related to strength and ductility were discussed in Sections 3.3.2 and 3.3.3, respectively.

4.1.5.1 Modeling of Embrittlement

[

]

4.1.5.2 Effect of Extended Burnup

Extending fuel burnups will increase the cladding integrated neutron fluence and will also increase the hydrogen concentration in the cladding. Since the material elevated-temperature yield strength increases with fluence and is unaffected by hydrogen level as discussed in Section 4.1.5.3, it is concluded that an increase in burnup will cause the material yield strength to increase further, raising the margin over the unirradiated yield strength.

The material ductility at 650 °F is slightly reduced initially by irradiation but then remains relatively constant. [

]

4.1.5.3 Evaluation of Embrittlement

Influence of Irradiation on Mechanical Properties. The fuel cladding used by C-E is in the [ ] (4-3). The increase in elevated-temperature yield strength due to irradiation is illustrated in Figure 4-8 (cf. References 4-18 through 4-21). Most of the

FIGURE 4-8
YIELD STRENGTH AS A FUNCTION OF FLUENCE FOR[ ]
IRRADIATION TEMPERATURE 500F TO 650F ELEVATED TEMPERATURE TEST

irradiation-induced hardening occurrs by about 2×10^{21} nvt (E > 1 MeV) or approximately 12.5 MWd/kg. The fluence dependence of the [ ] is illustrated in Figure 4-9. The data (4-22) suggest that for [ ]

Influence of Hydrogen on Mechanical Properties . Hydrogen, which is absorbed by Zircaloy through corrosion with the primary coolant, remains in solution in the Zircaloy until the terminal solid solubility of hydrogen is exceeded. At 300°C (572°F), the solubility limit is approximately 100 ppm. Amounts in excess of the solubility limit will precipitate as zirconium hydride platelets.

[ ]

FIGURE 4-9
UNIFORM ELONGATION AS A FUNCTION OF FLUENCE FOR [ ] ZIRCALOY, IRRADIATION TEMPS. 560-610°F

[redacted]

4.1.6 Fission Gas Release

The calculation of fission gas release is an integral part of the fuel performance calculations involving the temperature distribution and internal pressure of fuel rods. The release of fission product gases plays an important role in the calculation of gas conductivity and therefore affects the transfer of heat from the UO_2 pellets to the cladding. C-E submitted a model for these calculations to the NRC in 1974 (4-1) and has recently revised that model in a submittal in July 1981 (4-11).

The dependence of fission gas release on burnup has, until recently, not been fully understood. Recent advances in modeling, aided by better experiments, have shown a relative absence of burnup dependence to rod-averaged burnups of 46 MWd/kg in the lower temperature range and somewhat more burnup enhancement for rods which achieve temperatures above about 1400 °C. Some of the experiments which have helped C-E's modeling efforts are discussed in this report as they have provided the basis for the treatment of burnup in C-E's FATES3 computer code (4-11). Data on the release of fission gases during normal steady state operation are available to 46 MWd/kg. For operation

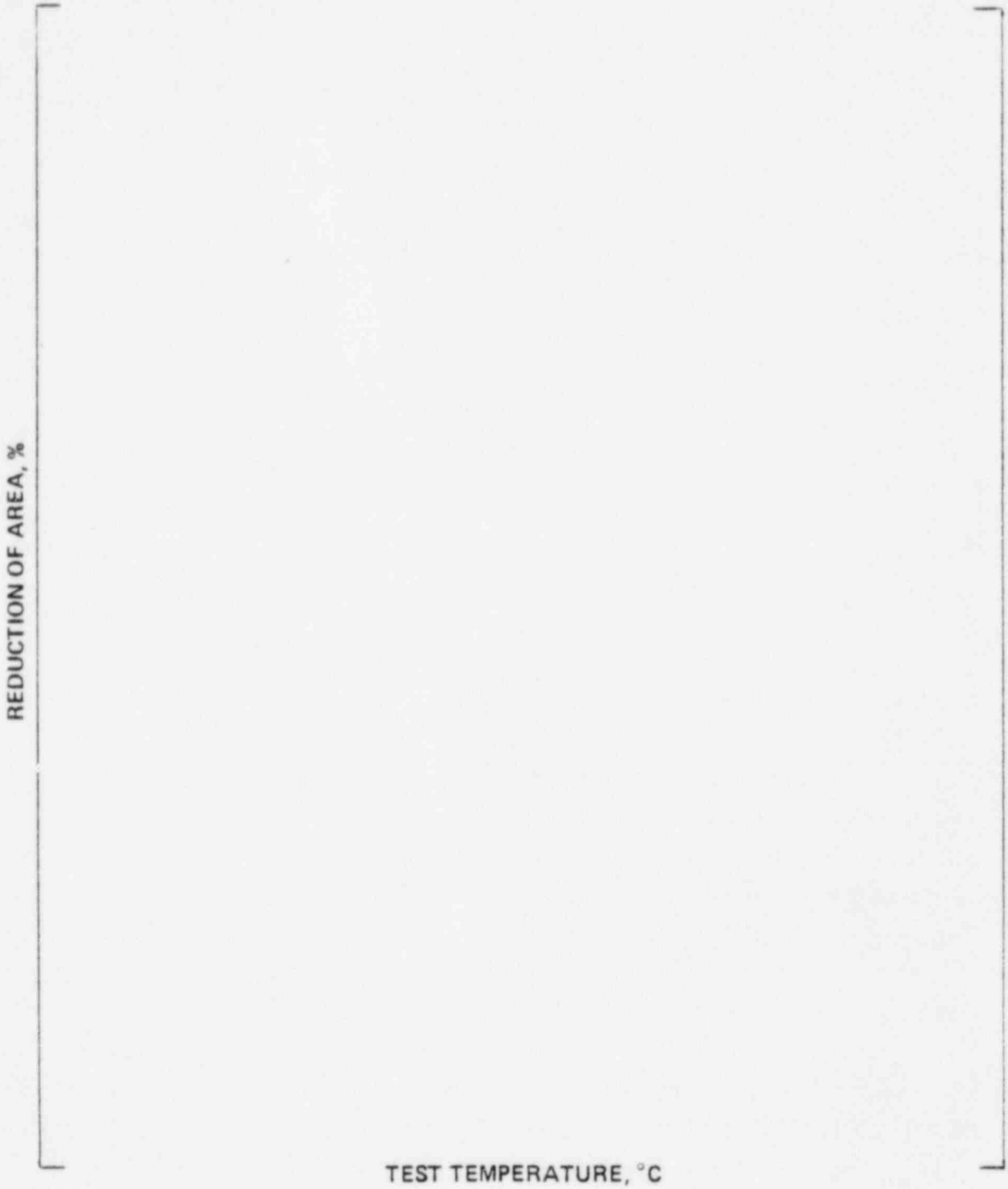

FIGURE 4-10
PERCENT REDUCTION OF AREA FOR SHORT-TRANSVERSE SPECIMENS IRRADIATED TO 4.3×10^{19} n/cm^2 (E > 1 MeV)

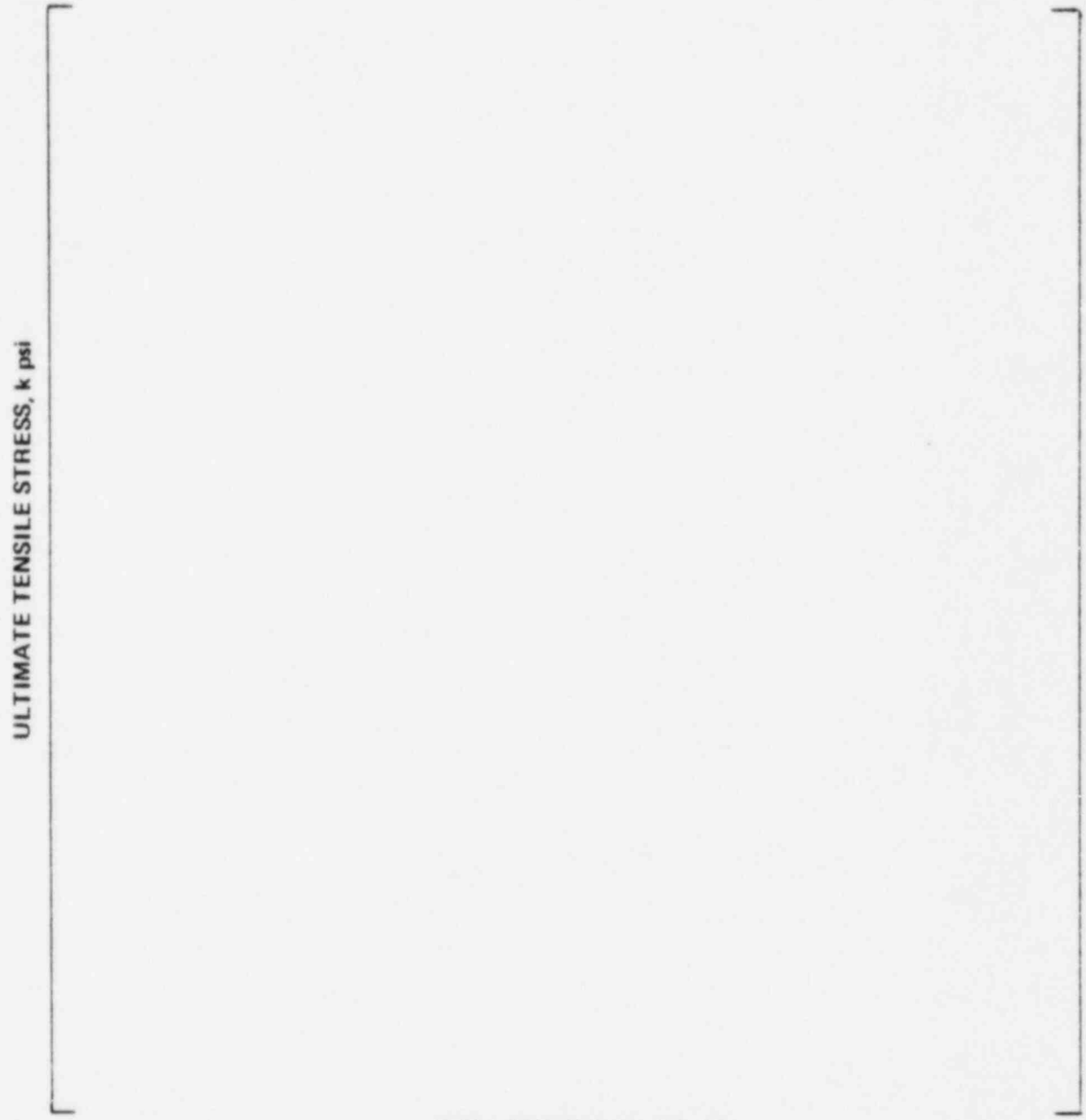

FIGURE 4-11
ULTIMATE TENSILE STRENGTH OF SHORT-TRANSVERSE SPECIMENS IRRADIATED TO 4.3×10^{19} n/cm^2 (E > 1 MEV)

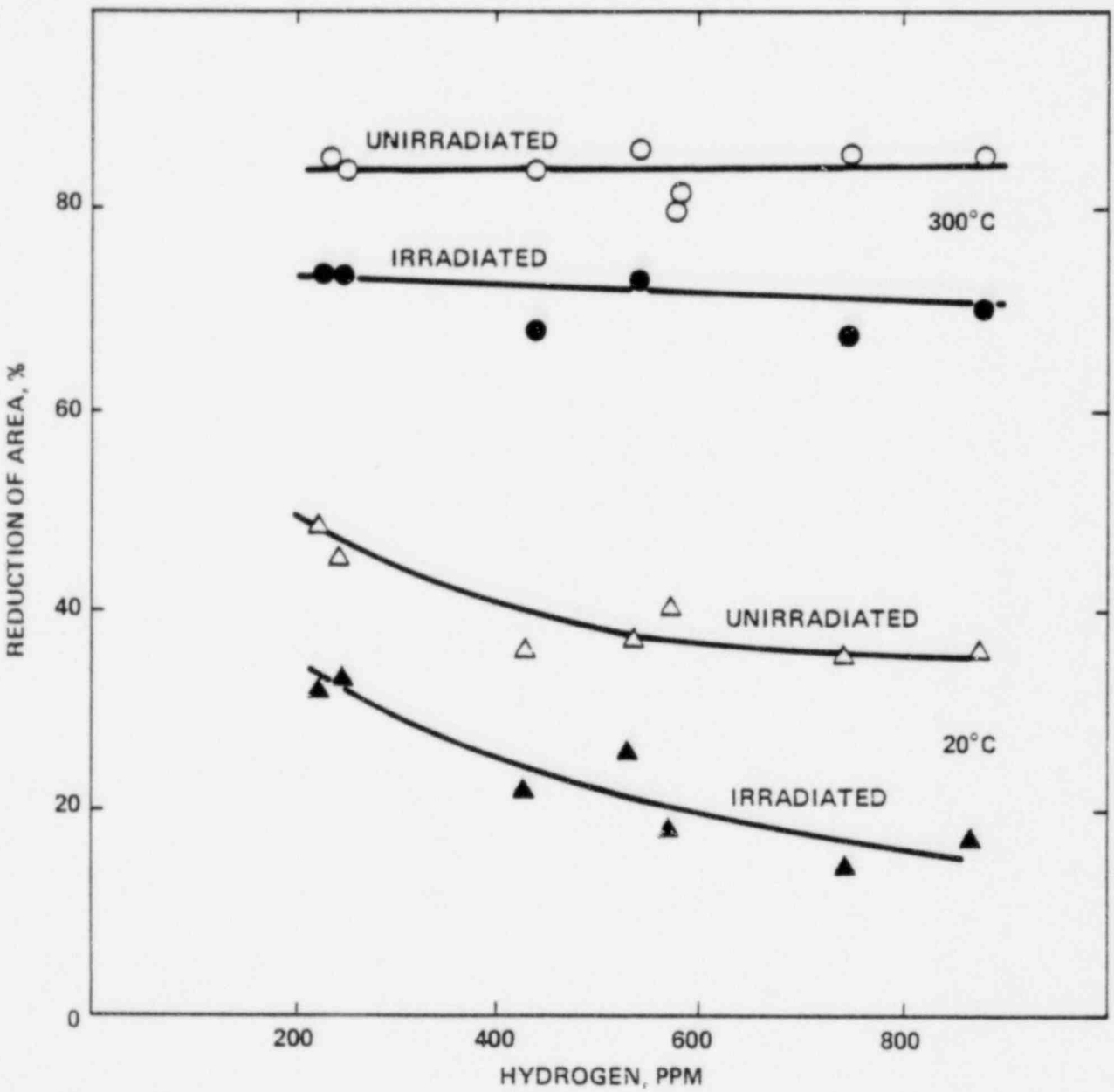

FIGURE 4-12
EFFECT OF HYDROGEN CONCENTRATION ON THE REDUCTION OF AREA FOR ZIRCALOY-2 IRRADIATED TO 10^{20} n/cm^2 (Ni)

typical of anticipated operational occurrences, the data from ramp tests up to 31 MWd/kg are reported, and the trends shown provide an improved basis for the modest extrapolation to higher levels of burnup.

4.1.6.1 Modeling of Fission Gas Release and Effect of Extended Burnup

Current Status of C-E's Fission Gas Model . The C-E Fuel Evaluation Model, submitted and approved in 1974, included an empirical model for the release of fission gases which reflected some dependence on burnup. As the irradiation time increased to 3 years, the calculated value of fission gas release would approach the full value of the temperature-dependent release. The more recent model, submitted in July 1981, is under review by the NRC at this time. Its form is significantly different from the previous one and will be fully described in this section. In addition to a more direct treatment of burnup, the new model reflects a continuous dependence on temperature and the local grain size of the UO_2 pellet.

Experimental Data on Gas Release . In 1975, C-E launched an effort to improve the available data on the release of fission gases from UO_2. A program, co-sponsored by EPRI and C-E, was initiated at the Calvert Cliffs-1 reactor to study the behavior of PWR fuel rods in an operating reactor (cf. Section 1.4.2). These rods contained systematic variations in design, pellet microstructure, pellet density, and rod internal pressure.

A unique feature of the program at Calvert Cliffs-1 is that it has allowed the effects of different design variables, including fuel type, to be evaluated in well-characterized test rods irradiated under nearly identical operating conditions in a power reactor. Consequently, performance comparisons among the fuel types can be made without the uncertainties attached to different operating conditions and irradiation environments. This is an important consideration for any experiment if it is to provide high quality fission gas release data that is suitable for modeling purposes or mechanistic evaluations.

Thus far, test fuel rods have been irradiated for four operating cycles at Calvert Cliffs-1 and have received detailed examinations at poolside during

each of the refueling outages. The results of these examinations have been reported by Bessette et al., (4-29) and Ruzauskas et al., (4-30,4-31).

After each cycle, a number of the test rods were selected for additional examination at a hot cell facility. Results from the first three cycles have been reported to the NRC in detail as part of the FATES3 Report (4-11). The fourth cycle data are now available and are included here along with the earlier results.

A total of eighteen full length rods, six containing an early densifying type of UO_2 fuel pellets and twelve of the more representative, nondensifying types of UO_2 fuel pellets are listed in Table 4-1. The important design parameters and the key data regarding operating parameters are shown for each of the test rods. The fission gas release values in Table 4-1 are plotted against the rod-averaged burnup in Figure 4-13. Putting aside the data point from the single densifying fuel rod containing argon for the moment, a review of these data indicates that the gas release of the 3- and 4-cycle rods was low, less than 1%, regardless of differences in fuel types. This is consistent with the behavior observed previously in the 1- and 2-cycle rods. Also, the fractional fission gas release does not exhibit an appreciable burnup dependence up to 45.8 MWd/kg. Over the range of burnup thus far, slightly more gas release is observed in rods containing fuel Type V, which had the higher enrichment. This difference is consistent with the higher heat ratings and the greater as-fabricated open porosity of the fuel used in these rods.

The higher gas release measured for Rod NBD144, which contained 5% argon mixed with helium, resulted from a higher temperature of operation through the entire irradiation history compared to the temperatures of comparable fuel rods containing only helium. A reduction in gap conductance due to the presence of argon was mainly responsible for the higher temperatures. In addition, Rod NBD144 was a peripheral rod in the assembly and operated at somewhat higher heat ratings (especially in the third and fourth cycles) compared to other rods fabricated with fuel of the same enrichment but located in the interior of the assembly (e.g., Rod 09). C-E's fuel rods currently in service and being manufactured for future use, are pressurized only with helium and use pellets of the nondensifying type.

Table 4-1

Key Design Parameters, Operating Characteristics, and Fission Gas Release Results for Test Fuel Rods From Calvert Cliffs-1

Fuel Rod Numbers[a]	01	05	11	12	09	NBD 144	50	51	53	54	60	23	33	46	47	39	42	48
Fuel Parameters	← DENSIFYING →						← NON-DENSIFYING →							← NON-DENSIFYING →				
Type	← I →						II	II	II	II	III	IV	IV	← V →				
% TD	← 93 →						95	95	95	95	93	95	95	← 93 →				
Wt. % U-235	← 2.45 →						← 2.45 →					← 2.33 →		← 2.82 →				
Poreformer	← NONE →						PVA	PVA	PVA	PVA	MMA	S-K	S-K	← PVA →				
Initial Grain Size, μm	← 2.5 →						4	4	4	4	7	4	4	← 15 →				
Open Porosity, % of Pellet Volume	← 0.1 →						1.3	1.3	1.3	1.3	2.2	0.35	0.35	← 3.7 →				
Operating Parameters																		
Number of Cycles	1	2	3	3	4	4	1	2	3	4	3	4	4	1	2	3	3	4
Peak LHGR, kw/ft, (in Cycle 1)	← 9.1 →						← 9.1 →					8.8	8.8	← 11.1 →				
Rod and Time-Averaged LHGR, kw/ft																		
Cycle 1	5.5	5.5	5.5	5.5	5.5	5.6	5.5	5.5	5.5	5.5	5.5	5.3	5.3	6.3	6.3	6.3	6.3	6.4
2	---	5.1	5.1	5.0	4.9	5.4	---	5.0	5.1	5.0	5.0	4.9	4.9	---	5.3	5.3	5.4	5.5
3	---	---	4.3	4.4	4.4	4.0	---	---	4.3	4.3	4.4	4.4	4.4	---	---	4.7	4.6	4.5
4	---	---	---	---	3.7	4.0	---	---	---	3.7	---	3.8	3.8	---	---	---	---	3.9
Rod-Averaged Burnup at Discharge, GWd/mtU	18.7	25.8	33	33	41.4	42.2	18.7	25.8	33	41.4	33	40.9	40.9	21.6	29.1	37	37	45.8
Fission Gas Release, %[b]	0.27	0.34	0.36	0.35	0.36	1.45	0.33	0.35	0.33	0.55	0.59	0.37	0.28	0.71	0.64	0.71	0.72	0.93

[a] Common Design Parameters (Nominal)

Fuel Column Length, inches 136.7
Fuel Rod Length, inches 147
Fuel Pellet OD, inches 0.3795

Cladding ID, inches 0.388
Fuel Rod OD, inches 0.440
Pellets Dished at Both Ends

Initial Fill Gas Pressure - 450 psig Except Rods 23 and 39 which had 300 psig @ 20C

Initial Fill Gas Composition - Helium Except Rod NBD-144 which had 5% Argon - 95% Helium

[b] Assumes a Production Rate of 30 Atoms of Xe + kr/100 Fissions and 200 MeV/Fission

FIGURE 4-13

FISSION GAS RELEASE MEASURED IN CALVERT CLIFFS-1 FUEL RODS

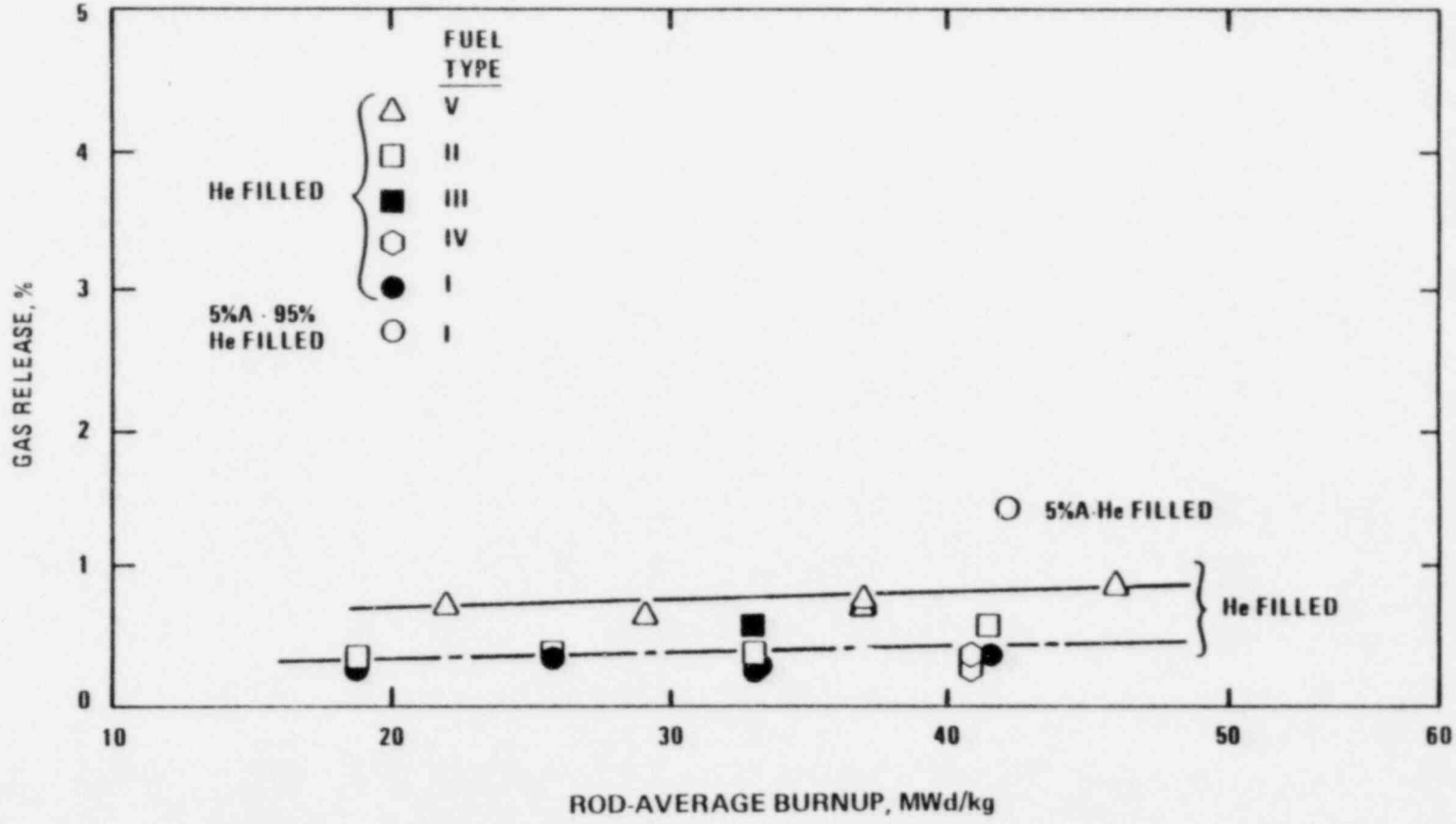

All of the fuel rods which were filled with only helium exhibited a rather consistent level of gas release (below 1%) and showed a relative absence of burnup enhancement. The duty cycle for these test rods was tracked rather closely, and the associated thermal history accounted for in the use of these data to benchmark the FATES3 model in the range of normal operating conditions. More detail on this experiment is available in the FATES3 Topical Report (4-11) and in a paper by Pati et al. (4-32)

The potential increase in fission gas release for higher linear heat ratings which accompany certain postulated events is treated using FATES3. The best source of data on fission gas release in UO_2 fuel rods for these conditions is a series of ramp tests conducted to study pellet/cladding interaction. Rodlets which are ramped, but do not perforate, are examined in a hot cell and are punctured to determine percent fission gas release. Since the rodlets achieve their burnup in a PWR and later get transferred to a test reactor for controlled operation to higher heat ratings, the time at which maximum heat ratings are achieved is known. The relatively low heat ratings associated with the base irradiation and the measurements taken on companion rods without power ramps make it possible to determine the amount of release which accompanies the ramp test. The post-ramp metallography and other examinations conducted as part of the tests provides data to benchmark temperature and to determine internal void volumes of the rodlets.

Twenty-five rodlets tested in the R-2 Reactor at Studsvik in Sweden, after base irradiation in either Obrigheim or the BR-3 Reactor in Belgium, were used by C-E to develop the model for fission gas release in FATES3. An independent set of 10 rodlets tested in the HFR Petten Reactor were used as part of the data base for independent checking of the C-E model.

Of the 25 rodlets tested at Studsvik, 17 were designed and fabricated by C-E and KWU, and the balance by Westinghouse. All of these rodlets were pre-pressurized, and are representative of modern PWR fuel designs, which among other things avoids the uncertainties of high densification. Table 4-2 lists the 25 rodlets, their peak linear heat ratings upon ramping, the rod-averaged burnup achieved and two values for fission gas release (measured and predicted). The range of burnup values for these ramped rodlets extends to 31 MWd/kg and the linear heat ratings extend to 16.2 kW/ft. With the exception of

Table 4-2

The Correlation Data Base

FATES3 Predictions of Gas Release From Over-Ramp Program Rods

Rod Number	Initial Grain Size, μm	Ramp Peak LHGR, kW/ft[a,b]	Rod Averaged Burnup, MWd/kg	% Gas Release	
				Measured	Predicted
[					]

[a

b

]

a few overpredictions in the case of the highest burned, Type F rodlets, the correspondence of experiment and prediction is very good.

The overall trends shown by the Studsvik data are best viewed by referring to Figure 4-14 which plots the percent fission gas released during the ramp against the terminal level of linear heat ratings achieved in the ramp test. A hold time of 48 hours at the ramp terminal level was used in these tests. A series of straight lines represents points of a common design at a given level of burnup. The initial grain size of the fuel is shown on each set of data.

It is apparent from Figure 4-14 that fission gas release is low at ramp terminal power levels below 10.5 kW/ft for all fuel types. This observation is consistent with the behavior observed for commercial rods which have experienced normal irradiation in power reactors. A review of the power histories of these rods during the base irradiations has indicated that the gas released during the base irradiation is expected to be small relative to the release measured after the power ramps at the R-2 Reactor.

The fuel rod designs tested varied from short segmented rods (about 40 cm long) irradiated in the KWO Reactor to rods of longer lengths (about 100 cm long) irradiated in the BR-3 Reactor. Since a significant part of the fuel column in the longer fuel rods experienced local ramp terminal powers below 10.4 kW/ft, the fission gas release shown in Figure 4-14 for these rods has been adjusted. Specifically, this adjustment ignores the fission gas inventory for the portion of the fuel column below 10.3 kW/ft in the determination of the percentage of fission gas released during the ramp. Therefore, all of the data points in Figure 4-14 represent the release of fission gas from fuel ramped to local terminal powers above this linear heat rate.

Figure 4-14 demonstrates that the main variables which affect fission gas release are rod power (fuel temperature), fuel burnup and fuel grain size. For a given fuel type and burnup, fission gas release is strongly dependent on power (fuel temperature). A burnup dependence of gas release is evident by comparing release values of 6 μm grain size fuel at two reported levels of burnup. In the range of ramp terminal powers of 13.4 to 14.9 kW/ft, fuel pre-irradiated to higher burnup (~ 24 MWd/kg) releases more gas on a percentage

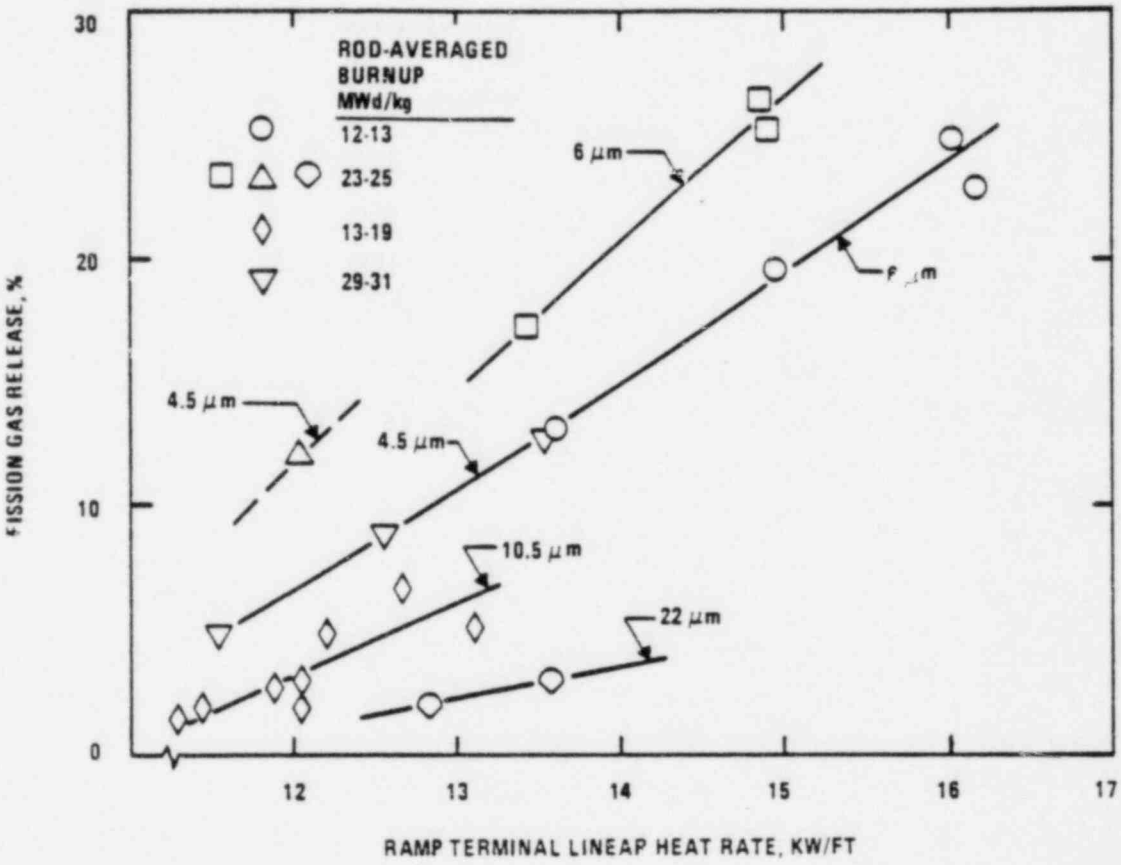

FIGURE 4-14

FISSION GAS RELEASE FROM OVER-RAMP RODS

basis than fuel at the lower burnup (~ 13 MWd/kg). Since the inventory of generated fission gas increases with burnup, increasingly more fission gas atoms will be released to degrade the gap conductance, thus contributing to higher fuel temperatures and larger percentage releases. This is in addition to any burnup enhancement occurring between these burnups.

The above trend of increased percentage release between 12 and 24 MWd/kg appears to be reversed when the burnup extends beyond 24 MWd/kg. For example, neglecting the small difference in grain size between 4.5 and 6 μm, a small reduction in gas release on a percentage basis is indicated when the release values observed at ~ 24 MWd/kg are extrapolated to lower powers at which data are available on fuel with ~ 30 MWd/kg. An improved gap conductance with increasing burnup beyond the onset of fuel cladding contact may be considered as a factor affecting the apparent burnup dependence in the above sets of data. The improvement in gap conductance may occur due to higher contact pressure at the fuel cladding interface which outweighs the degradation effect of increased gas release on a total atoms released basis. Therefore it is possible to hypothesize that, at a given power level, the fuel temperature is reduced sufficiently at ~30 MWd/kg compared to fuel temperatures at ~ 24 MWd/kg such that any detrimental burnup effect is overcome by a beneficial effect of lower temperatures.

The pronounced effect of grain size is apparent from a comparison of the release values of different fuel types having a common level of burnup. For example, at a burnup level of approximately 25 MWd/kg, and at a ramp terminal power level of 13.7 kW/ft, the fuel of 22 μm grains shows a factor of six lower gas release compared to the fuel of 6 μm grains. The data from the fuel with an intermediate grain size of 10.5 μm follow the same trend. Despite its significantly lower burnup at identical ramp terminal powers, the fuel with 10.5 μm grain size released two to three times more gas than the fuel with 22 μm grain size.

Description of C-E's Current Model. The empirical model for gas release which is used in FATES3 was developed primarily from the data obtained from Calvert Cliffs-1 and from Studsvik. In the model, gas release is calculated by

following the local inventory of retained fission gas in the fuel. At each axial region of the fuel column, the fuel is divided into ten rings of equal thickness and the local inventory of fission gas is followed in each of these rings. Local fuel temperature, burnup, grain size and irradiation history are variables affecting the inventory of retained fission gas in the following manner:

[ ]

The percent of generated fission gas that is released, F, is calculated from:

[ ]

The functional relationships assumed in Equations (1) and (2) are based on an inspection of the shapes of the experimentally determined curves of the retained inventory of fission gas in small UO_2 fuel samples at high burnups (cf. Reference 4-33 and 4-34). The specific values of the constants in the expresssion for K, given by Equation (2) have been arrived at by correlating the gas release predictions of the overall gas release model, when employed in

the FATES3 code, to the experimental data obtained from the steady state irradiation of commercial fuel rods in Calvert Cliffs-1 (4-35,4-36) and from ramp tests performed at Studsvik as part of the Over-Ramp Program (cf. Section 1.4.7) which included C-E segmented commercial fuel rods irradiated in Obrigheim (4-37). The maximum inventory obtained by applying Equation (3) is equivalent to the release predicted by the low temperature gas release model developed by the ANS 5.4 Committee (4-38).

Fission gas release that is accompanied by grain growth (via grain boundary sweeping) is accounted for in the model by an additional term which depletes the fission gas previously retained in the volume of fuel which is swept by moving grain boundaries. The local inventory of fission gas that remains in each ring of fuel after a local grain growth from G_i to G_f is given by:

[

]

The kinetics of grain growth are followed in each fuel ring [

]

[

]

As suggested by the Ainscough grain growth model (4-40), the grain size does not saturate with the use of Equation (6). However, the dynamic grain size in the C-E adaptation of Equation (6) is forced to saturation, based on the assumption that for each temperature there is a limiting grain size regardless of the starting grain size. This is accomplished by the following expression:

[ ]

The model described above accounts for the effects of temperature, burnup, and grain size. A more detailed description of the model and its characteristics can be found in C-E's Topical Report which submitted the fission gas release model along with other improvements to FATES (4-11).

Comparison of Model to Experimental Data . In addition to the experimental data used to develop FATES3, a series of independent data from several experiments was used to evaluate the predictability of the model. Several factors were involved in the selection of these data, but the most important criteria were the ranges of linear heat rating and burnup represented and the similarity of the test rod designs to the intended application of FATES3.

The normal operating range for PWRs is covered and exceeded by a combination of results from Calvert Cliffs-1, Obrigheim, and from the data reported by Bellamy and Rich (4-41). The higher linear heat ratings associated with ramp tests is covered by data from Over-Ramp and from Petten. Although the discussion here emphasizes the comparison of these experiments with C-E's predictions, a more thorough treatment of these data is available in References 4-11 and 4-32. A total of [ ] points from the model's development and [ ] points from the independent check are plotted together in Figure 4-15. Note that the data points which are independent of the model are those plotted with open symbols.

As of this writing, four of the recent results from Calvert Cliffs have been modeled and are therefore included in Figure 4-15. The data from all four

FIGURE 4-15

PREDICTED - MEASURED GAS RELEASE VERSUS BURNUP

cycles in Calvert Cliffs illustrate two important aspects of the FATES3 model. All of the points which are near the median, and therefore showing correspondence with measured values, are the rods made with modern, nondensifying fuel. The consistency in these predictions extends from 18 MWd/kg to 42 MWd/kg. Although the model predictions have not been completed, reference to Figure 4-13 shows the relative absence of burnup enhancement to 46 MWd/kg. The points in Figure 4-15, which show an overprediction of up to 10%, are all from rods containing the earlier densifying fuel. It is important to note that the overprediction starts at low burnup and remains consistent throughout the range of burnup tested. The conclusion made by C-E is that this overprediction results from a conservative treatment of the phenomenon affecting gap closure and therefore temperature early-in-life. Increases in burnup do not affect the predictability of FATES3 in either the densifying or nondensifying case.

The data from KWU were obtained from a special assembly irradiated in Obrigheim called "The Loose Lattice Assembly". As shown in Figure 4-15, the correlation of FATES3 predictions with measured values showed many cases of under-prediction, as well as overprediction. There appears to have been considerable uncertainty in the assignment of heat ratings for these rods. Since there were no instruments used, and since these rods were in an assembly with a lattice of higher water-to-fuel ratio than surrounding assemblies, C-E feels that the uncertainties in power history are wider than in the case of Calvert Cliffs, for example, and resulted in the wide scatter between the measured and predicted values.

The data from Petten provide a good check on the model's prediction of fission gas during fast ramps to LHGRs up to 16 kW/ft. As can be seen from the figure, with the exception of one point at low burnup, the predictions are either accurate or somewhat conservative.

Finally, there are the data from Bellamy and Rich, and these are important because of their high levels of burnup. The correlation with measured releases was excellent, including burnups to 48 MWd/kg.

Ongoing Work on Fission Gas Release. Several programs are in progress which will produce more data on gas release to verify the treatment of fission gas release to extended levels of burnup. For normal operating conditions, C-E is currently conducting lead assembly programs in Calvert Cliffs-1 and in Fort Calhoun. A series of fifteen fuel rods, which are part of the EPRI/C-E program, are currently operating in Calvert Cliffs-1 and will be discharged in mid-1982 with peak burnups of 55 MWd/kg. The data from these fuel rods will provide a useful extension of the values shown in Figure 4-13 since these rods are companion fuel rods with burnup as the primary difference.

The lead assembly in Fort Calhoun is part of a DOE program in which lead fuel rods will reach 56 MWd/kg. The addition of these data are expected to enhance the statistical confidence related to the absence of burnup enhancement at low temperatures.

Although data from ramp tests are considerably more difficult to obtain, the range of available burnups is extending there as well. In the follow-on program to Over-Ramp (i.e., Super-Ramp, cf. Section 1.4.8), a rodlet has already been ramped without failure after a burnup of 45.2 MWd/kg. The High Burnup Effects Program being conducted by Battelle Northwest Laboratories (cf. Section 1.4.11) is also expected to yield data on fuel rods with high linear heat ratings and high burnups.

4.1.6.2 Evaluation of Fission Gas Release

The discussion in Section 4.1.6.1 surveys the situation at C-E with respect to the data available and the modeling of fission gas release to extended burnups. Significant strides have been achieved in the area of normal operation and in the area of response to ramps. The conclusions which can be reached at this stage are:

(1) Fuel rods operating in PWRs with helium prepressurization and nondensifying fuel have been examined and consistently found to contain very low levels of released fission gases to burnup levels of 46 MWd/kg. The relative absence of any enhancement due to burnup is now verified by direct measurement.

(2) Fuel rods which were irradiated in a PWR and subsequently ramped to linear heat ratings up to 16 kW/ft show higher releases of fission gas. The amount of fission gas released is strongly dependent on linear heat rating (temperature) and the grain size of the UO_2 pellets. These data display an apparent enhancement of fission gas release due to burnup to at least 25 MWd/kg. As the burnup of these test rodlets increases, the data show a mitigation of burnup enhancement which is probably due to an improved gap conductance resulting from better fuel-clad contact at higher burnups.

(3) Data available to C-E, and reported to the NRC, support the FATES3 model to appropriate levels of burnup. The observed trends in the behavior of UO_2 are gradual and support the orderly extension of the allowable burnups.

(4) Design improvements including helium prepressurization, nondensifying UO_2, reduced pellet-cladding gaps and the use of pellets with larger grain sizes have all shown improved behavior relative to fission gas release.

(5) The programs which are on-going, and which extend the range of applicable data, are expected to further support the orderly extension of allowable burnups.

4.1.7 Fuel Thermal Conductivity

Thermal conductivity of fuel is a principal independent variable which governs many thermal and mechanical parameters of fuel rods. Sufficient in-pile tests have been conducted so that the data on irradiated samples form the current basis for modeling the UO_2 conductivity up to its melting point. These data are usually presented in the form of an integral conductivity. The use of UO_2 thermal conductivity in this form has become universal because of its mathematical convenience and ease of use for a fuel rod geometry (4-42).

C-E submitted a fuel thermal conductivity model to the NRC in 1974 (4-1). That model was based on the relationship published by Ogawa et al. (4-43). Recently, the model was revised to take into account [

] Only the important features of the model are highlighted in the following section. The thermal conductivity model is embodied in the FATES3 (4-11) fuel evaluation code.

4.1.7.1 Modeling of Fuel Thermal Conductivity

In thermal analyses performed by FATES3, the value of the integral of the UO_2 thermal conductivity for 95% TD fuel is 93 W/cm over the range of 0 to 2800°C. Thermal conductivity as a function of temperature is taken from Reference 4-43 and is given by:

$$K_{95} = 38.24/(402.4+T) + 6.12 \times 10^{-13} (T+273)^3$$

where:

K_{95} = thermal conductivity of fuel of 95% TD, W/cm-°C
T = fuel temperature, °C.

For analyzing fuels other than of 95% TD, [

]

[

]

4.1.7.2 Effect of Extended Burnup

Defects introduced by radiation are known to degrade thermal conductivity of crystalline solids. In UO_2, this effect is pronounced at low temperatures (<500 °C) and reaches saturation rapidly at low burnups (4-42). This early-in-life, low temperature degradation has little practical consequence in the applications to operating fuel rods as most of the fuel operates at temperatures above 500 °C. In the operating temperature regime of PWR fuel rods, the irradiation-induced defects anneal out rapidly and, therefore, do not cause a measurable degradation of the thermal conductivity of the fuel (4-42).

Thus, only phenomena which are known to significantly affect fuel thermal conductivity are those which change [ ] In the C-E model, the effects of these phenomena are taken into account through the [ ] Therefore, no abrupt reduction in thermal conductivity is expected by increasing the discharge burnup of fuels beyond the current levels.

4.1.7.3 Evaluation of Fuel Thermal Conductivity

Experimental in-reactor data that are available on fuel thermal conductivity are limited to low burnups. However, the current state of knowledge of the effect of irradiation damage on thermal conductivity indicates that the intrinsic effect of irradiation damage is not significant for operating fuel rods. Gross changes in fuel attributes, such as [ ] have stronger effects on fuel thermal conductivity. The effects of these factors are modeled in the current FATES3 fuel evaluation code.

In addition, it is important to note that extended-burnup fuel has a significantly reduced power capability compared with a fuel at lower burnup. Therefore, the change in fuel thermal conductivity as a function of burnup is not a limiting effect to the licensing of extended-burnup fuel.

4.1.8 Fuel Melting Temperature

Under PWR normal operation, the fuel operates at heat ratings which are far below the value required to cause fuel melting. However, to ensure that fuel damage is avoided during anticipated transients, the absence of fuel melting is included as one of the Specified Acceptable Fuel Design Limits (SAFDLs). Fuel melting temperature is therefore modeled in C-E's fuel performance licensing codes. The above criterion is satisfied by appropriately restricting the peak linear heat rating to preclude the occurrence of fuel melt.

4.1.8.1 Modeling of Fuel Melting Temperature and Effect of Increased Burnup

Based on a review of the results of several experimental investigations on the melting point of unirradiated UO_2 and of UO_2 irradiated to below 10 MWd/kg, 2865 $\pm$ 15°C (5190 $\pm$ 27°F) was recommended by Lyons et al (4-42) as the best estimate value for the melting point of unirradiated UO_2 having exact stoichiometry. The melting point of UO_2 is known to decrease due to the presence of impurities and/or due to a deviation from exact stoichiometry. Considering the above, a lower value of 5080°F is taken in the C-E model as the melting point of unirradiated UO_2 of compositions which are normally used in the fabrication of PWR fuel rods.

The effect of burnup on the melting point of UO_2 was investigated by Christensen (4-46). The melting point was observed to decrease with burnup up to approximately 50 MWd/kg, and the largest rate of measured decrease was about 58°F per 10 MWd/kg. In contrast, no significant reduction in the melting point of UO_2 due to irradiation was reported by Reavis and Green (4-47). In addition, the rate of decrease of the melting point of mixed oxides irradiated up to 85 MWd/kg (4-48) was found to be a factor of 2 to 3 times lower than the largest rate of decrease for UO_2 reported by Christensen. Despite the varying experimental results, as a conservative approach, the melting point of UO_2 is reduced with irradiation in the C-E model, and the rate of [

] Thus, the melting point is calculated as a function of burnup using the following expression:

[ ]

where

T_{melt} is the melting point in °F, and burnup is in MWd/kg.

It is noted that the melting point of unirradiated UO_2 used in the C-E model is [ ] than the value used in MATPRO (4-49). [ ]

4.1.8.2 Evaluation of Fuel Melting Temperature

As discussed in the previous section, despite nonconclusive evidence on the presence of any effect of burnup on the melting point of UO_2, the fuel melting temperature is reduced with burnup in the C-E model as a conservative approach. The criterion of no fuel melting is not considered to adversely affect the extended burnup operation beyond the current target burnups because of the following considerations:

(1) The peak linear heat rating of the fuel is expected to decrease with burnup because of depletion of the inventory of fissile atoms.

(2) The fuel centerline temperature attained at a specific linear heat rating is expected to decrease with increasing burnup beyond the onset of contact between fuel and cladding. The lowering of fuel temperature is caused by the improvement in gap conductance with increasing fuel cladding interfacial pressure. Thus, the peak fuel center line temperatures, which are calculated to occur in the lead power rods of a current design PWR during anticipated transients, are expected to remain well below the melting temperature of UO_2 at extended burnups.

4.1.9 Fuel Swelling

The generation of solid and gaseous fission products within the fuel due to fission events causes the fuel to swell. This expansion of fuel volume must be accommodated for the fuel rod to achieve high exposure. The fuel swelling is

included in the C-E fuel performance evaluation and design codes for the following applications: [

] These calculations are integral parts of fuel performance evaluations involving temperature distribution and internal pressure of fuel rods. C-E submitted a swelling model to the NRC in 1974 (4-1). That model was based primarily on the Bettis data (4-50) for plate type fuel elements. Recently, the model was revised by considering the data available in the open literature (4-51) as well as data from measurements of density changes of C-E fuels irradiated in Calvert Cliffs-1 through three cycles (4-52). These data indicated that in the range of interest of PWR operation, the unrestrained swelling rate of fuels is lower than the rate used previously. The technical basis for the modification of the swelling is discussed in detail in Reference 4-11. Only some of the important features of the model are highlighted in the following sections. The modified swelling model is embodied in the FATES3 fuel evaluation code.

4.1.9.1 Modeling of Fuel Swelling

[ ] are implicit parts of the fuel densification model. Therefore, swelling during this period is not distinguished but is included in the terminal densification value that is assumed for a particular fuel type. The densification value is estimated from a qualified thermal resintering test. [

]

When hard contact occurs, [

] The swelling difference between the restrained and the unrestrained rate is used for filling in the internal void volume within the fuel rod.

The use of the above fuel swelling model was justified on the basis of the experimentally based swelling rates that were deduced from post-irradiation immersion densities measured in three types of fuel irradiated in Calvert Cliffs-1 up to [ ] MWd/kg. Recently obtained data from four-cycle Calvert Cliffs-1 fuel rods (4-45) extend the validity of the above swelling rate up to a local pellet burnup of about [ ] MWd/kg. These data also show that a significant fraction of fuel swelling is accommodated by the internal pores of the fuel pellets without causing large outward expansion of the fuel rod diameter.

The integrated swelling model for calculation of fuel rod internal void volume (including accommodation of swelling volume by closed and open pores in the fuel, by the fuel-pellet dishes and by the fuel clad gap) was verified by comparing the void volumes predicted by FATES3 with measurements made at end-of-life (EOL) in the two- and three-cycle Calvert Cliffs-1 fuel rods (4-11). In addition, the EOL internal void volumes calculated by FATES3 for two other groups of high power rods were compared against the measured values. These data were obtained through the Over-Ramp Project (4-37) and from the high burnup RISO rods (4-53,4-54). For both groups of rods, FATES3 calculated void volumes are in good agreement with the experimental data. These evaluations extend the validity of the integrated swelling model in FATES3 up to an EOL rod averaged burnup of [ ] MWd/kg and to heat ratings which are significantly higher than those experienced by fuel rods at extended burnups.

4.1.9.2 Effect of Extended Burnup

Data evaluations (4-45) have established that, under normal steady state operation of PWRs, the swelling mechanisms which are operating in UO_2 fuel at burnup levels to 50 MWd/kg are gradual. There is evidence that swelling is accommodated by the open pores of the UO_2 microstructure. No abrupt swelling phenomenon has been observed which would limit the life of UO_2 fuel rods with Zircaloy cladding.

Void volumes measured in several Over-Ramp (4-37) rods after power ramping at Studsvik show no trend of decreasing void volume with increasing burnups. These observations indicate that swelling is not likely to affect adversely the extended burnup operation of lead power rods in a current design PWR.

4.1.9.3 Evaluation of Fuel Swelling

As discussed in Section 4.1.9.1, well-characterized experimental data are available from fuel rods which have been irradiated in a PWR through four cycles [ ] These data indicate that under normal power reactor operation, UO_2 swelling is a gradual process, and no abrupt phenomena are observed which would limit the life of UO_2 fuel rods with Zircaloy cladding. Performance of fuel rods subjected to power ramping after two and three cycles of irradiation also show that fuel swelling is not likely to be a life-limiting factor for the lead power rod of a current design PWR at extended burnup. Data acquisitions from higher burnup fuel rods subjected to power ramping following their base irradiations will continue. These data are expected to provide added confirmation that fuel swelling is adequately modeled in the C-E fuel evaluation code, FATES3.

4.1.10 Fuel Rod Bow

Fuel and poison rod bowing results in random lateral deflections of the fuel and poison rods. The mechanism causing this bowing is grid restraint coupled with rod axial growth. Thus, the fuel rod behaves like a column with multiple supports at each grid location. The degree of bow is a function of basic design features, of the initial bow resulting during fabrication, and of burnup.

Rod bowing can result in either an increase or a reduction in the subchannel flow area between adjacent fuel (or poison) rods. This change in subchannel geometry can give rise to two effects: (1) an increase in the flow area can cause an increase in the local power for rods in the affected regions and (2) a decrease in the gap between rods can reduce the critical heat flux (CHF) for the affected rods.

4.1.10.1 Fuel Rod Bow Model

C-E has developed generic rod bow methods which account for the effects of fuel and poison rod bowing in 14x14 and 16x16 fuel assemblies. A discussion of the development and application of the current C-E methods is given in Supplement 3 to Reference 4-55. These methods include predictions of fractional channel

closure as a function of assembly-averaged burnup, where channel closure refers to the decrease in the gap between adjacent rods. These channel closure predictions are conservative for all spans between grids in an assembly since the data base used to develop the models included only the channel closure data for the most limiting span of each as-fabricated and each irradiated fuel assembly.

Utilizing data which includes measurements of channel closures, a regression analysis was performed to obtain coefficients for a rod bow model for 14x14 fuel assemblies. The data and predictions from the resultant model are shown in Figure 4-16. The initial data base for model development included data with maximum assembly burnups of [ ] MWd/kg. Curve 1 in Figure 4-16 represents the best fit regression model for channel closure on a one standard deviation basis for this data.

A factor greater than unity is used with the generic 14x14 model to account for the possible variation in channel closure among fuel assemblies resulting from [ ] This [ ] is based upon a statistical analysis of the variances associated with the closure data plotted in Figure 4-16; this factor is included in Curve 2 of Figure 4-16. Curve 2 represents the 14x14 fuel generic model used in licensing calculations. As can be seen in the figure, Curve 2 conservatively bounds all of the model development data for burnups up to [ ] MWd/kg. The generic 14x14 closure model indicates that the magnitude of the channel closure increases as a function of [

] The applicability of this generic 14x14 closure model for higher assembly burnups has been substantiated by recent rod-to-rod gap measurements. These data provide confirmation that the 14x14 model is conservative for burnups up to [ ] MWd/kg. The new data are also shown in Figure 4-16 and are also conservatively bounded by Curve 2.

The generic model for fractional channel closure in the 16x16 fuel assembly is discussed in Supplement 3 of Reference 4-55. The dependency of rod bow among C-E designs was determined, as required by the NRC, by comparing the ratio of [

]

FIGURE 4-16
C-E GENERIC MODEL FOR FRACTIONAL CHANNEL CLOSURE IN A 14x14 DESIGN FUEL ASSEMBLY AND ITS SUPPORTING DATA BASE

[

]

Predictions of fractional channel closure versus burnup for the 14x14 and 16x16 fuel assembly rod bow models are compared in Figure 4-17. In this figure, Curve 1 is the generic 14x14 model without the addition of a [ ] (this curve is identical to Curve 1 of Figure 4-16). Curve 2 includes the extrapolation factor based on [ ] and Curve 3 includes an additional factor to account for possible [ ] effects in 16x16 fuel assemblies. Curve 3 represents the 16x16 fuel generic model used in licensing calculations.

Other differences between the two models are the intercept value of closure at zero burnup. which is based on differences in measured values of channel closure in as-fabricated fuel assemblies [ ] and the nominal channel values which appear in the denominator of the model equations. These nominal channel values are used to convert the absolute channel closure into fractional channel closure [ ]

Figure 4-17 also includes the first measurement data available on fractional channel closure in a 16x16 fuel assembly design following irradiation. These data were obtained during poolside examination of three fuel assemblies from Arkansas Nuclear One Unit 2 (ANO-2) after their first cycle of irradiation. A single assembly from each of the three fuel batches of the initial core is included. The good agreement of these data with Curve 1 (the 14x14 model) rather than Curve 2 (the 16x16 model) indicates that the appropriate analytical extrapolation among different assembly designs should be based on an [ ] rather than an [ ] comparison as explained in Reference 4-55. These ratios provide extrapolation factors of [ ] respectively, for the ANO-2 assemblies. Thus, the [ ] dependence suggests that similar channel closure should occur in the ANO-2 and in 14x14 fuel assemblies, which is confirmed by the data. The [ ] factor is being maintained in the generic 16x16 fuel assembly model at this time, however, to comply with NRC requirements.

The channel closure models described above are applicable to channels between adjacent fuel rods and guide tubes, and between adjacent fuel rods and [

FIGURE 4-17
CONFIRMATION OF THE C-E GENERIC MODEL FOR FRACTIONAL CLOSURE IN A 16x16 DESIGN FUEL ASSEMBLY BY COMPARISON WITH FIRST CYCLE DATA FROM ARKANSAS NUCLEAR ONE, UNIT 2

] At present, only [ ] poison rods are being considered for use in C-E 14x14 and 16x16 fuel assembly designs.

4.1.10.2 Effect of Extended Burnup on Rod Bow

Data evaluation has indicated that the channel closure resulting from fuel rod bow is dependent on [

] Furthermore, since the radial peak is generally not limiting in fuel assemblies with extended burnup, the increased penalties applied to account for rod bow in the extended-burnup assemblies will have little impact on core thermal margin.

4.1.10.3 Evaluation of Rod Bow

As explained in Section 4.1.10.1, the rod bow closure model has yielded conservative predictions of channel closure when compared with measurements from 14x14 fuel assemblies at burnups up to [ ] MWd/kg. Further confirmatory channel closure data will be obtained for 14x14 and 16x16 fuel assembly designs. In a DOE sponsored program to demonstrate the extended burnup operation of C-E's 14x14 fuel assembly design (cf. Section 1.4.5), a single Batch D assembly is being irradiated through six reactor cycles at Fort Calhoun. The projected assembly average burnup of this assembly is 52 MWd/kg. Rod-to-rod gap measurements are to be performed on this Batch D assembly after final discharge. Also, in a continuation of a fuel performance program with EPRI, gap measurements will be made on representative ANO-2 fuel assemblies after two and three cycles of irradiation (cf. Section 1.4.3).

Extended burnup fuel does not have power peaks near the limiting peak of lower burnup fuel because of its lower reactivity and lower fissile content. Thus, in general, lower burnup assemblies will be at higher power levels and will be limiting for thermal margin calculations. Therefore, additional data on channel closure is not essential for the licensing of an extended-burnup cycle.

4.1.11 Fretting Wear

Spacer grids are used to maintain the fuel rod lattice geometry within an assembly during irradiation by providing positive restraint to lateral fuel rod

motion but only frictional restraint to axial fuel rod motion. Each cell of a spacer grid contains two leaf springs and four arches. The springs press the rod against the arches to restrict relative motion between the grids and fuel rods. Fretting, or wear, may occur on the fuel rod surfaces in contact with the spacer grid due to a reduction in the spring load (caused by irradiation induced stress relaxation and creepdown) in combination with small amplitude, flow-induced vibratory forces.

C-E's grid design is based upon the results of extensive development programs conducted since the early 1970s, which have included out-of-pile tests such as fatigue tests, autoclave vibration tests, and dynamic flow tests over a wide range of simulated reactor operating conditions (4-57 through 4-59). Many of these tests have employed full size fuel assemblies of either the 14x14, 15x15 or 16x16 design. A rigorous quality control program is routinely conducted during spacer grid and fuel assembly fabrication to assure that design dimensional requirements are maintained and that fuel rods are tightly held by each spacer grid. The successful in-reactor performance of the grid design has been confirmed through extensive post-irradiation surveillance programs conducted since 1973.

4.1.11.1 Design Approach

The amount of lateral restraint or force exerted on a fuel rod by a spacer grid spring is controlled by the as-fabricated grid "preset" value. This value may be viewed as a measure of the interference fit between the fuel rod and grid cell at the beginning-of-life (BOL). [

] These tests have shown that changes in [

] within representative limits do not significantly alter fretting characteristics. The key observation from these tests is that fretting proceeds at a [ ] rate following a brief break-in period at a slightly [ ] rate. No significant fretting has been observed in any fuel rods supported by grids set to cover the anticipated range of BOL and EOL conditions. Based on these results, the maximum anticipated depth of clad wear has conservatively been estimated at approximately [ ] mils which is only [ ] of the initial clad wall thickness. The only instances of wear greater than this value occurred in special tests of off-nominal conditions in the [ ] grid in which the fuel rods were totally unrestrained laterally.

4.1.11.2 Effect of Extended Burnup

Extending burnup beyond current levels is not expected to adversely affect the occurrence of fretting wear. This conclusion is based on three considerations, namely:

- The results of extensive inspections of fuel rods and assemblies with burnups up to [ ] MWd/kg have confirmed the absence of any significant wear regardless of burnup.
- The degree of stress relaxation and fuel rod creepdown changes very little after one operating cycle (cf. Section 4.2.5).
- The results of the out-of-pile testing program show that significant fretting would occur early in life if it were to occur at all.

4.1.11.3 Evaluation of Fretting Behavior

Since 1973, C-E has conducted over 20 inspection programs at several commercial power reactors as part of its fuel performance surveillance activities (cf. Table 4-3). Approximately [ ] fuel assemblies with average burnups up to [ ] MWd/kg have been visually examined by C-E using either underwater closed circuit television or periscopes. No evidence of abnormal fuel rod wear or perforations due to fretting have been observed in any of these examinations. Approximately [ ] individual fuel rods have also been examined either in connection with jointly sponsored fuel performance evaluation programs or as part of reconstitution campaigns to prepare assemblies for continued operation (4-29 through 4-31 and 4-60 through 4-63). These rather

TABLE 4-3

Summary of C-E Fuel Inspection Programs

Which Provided Data on Fretting Wear

Reactor	Cycle	Fuel Assemblies Examined		Individual Fuel Rods Examined	
		Number	Max.Avg. Burnup (MWd/kg)	Number	Lead Avg. Burnup (MWd/kg)
[redacted]					

**Examinations were performed under contract with DOE and OPPD (cf. 4-61)

***Examinations were performed as part of a joint EPRI/C-E Fuel Performance Evaluation Program (cf. 4-30, 4-31, 4-60).

detailed examinations have also confirmed the absence of unusual wear regardless of fuel rod burnup. In 1975, two fuel rods with the most severe wear marks found at Maine Yankee during an inspection program performed following reactor Cycle 1 were taken to the Battelle (BMI) hot cell facility for further examination. Metallography on these atypical rods showed that the deepest wear mark was relatively superficial with a maximum penetration of only [ ] (4-60).

Another source of information on the behavior of C-E fuel rods with respect to fretting may be obtained indirectly from the current fuel performance levels in operating C-E plants. By examining the operation of these plants with respect to coolant iodine activity levels, estimates of the number of leaking fuel rods may be made. Table 1-4 (cf. Section 1.3) summarizes C-E fuel performance as a function of burnup and indicates excellent reliability with increasing burnup. This would not be the case if significant fretting were occurring in C-E reactors or if fretting wear were adversely affected by increased exposure.

As in the past, C-E will continue to verify satisfactory fuel rod performance in both 14x14 and 16x16 fuel assembly designs through a variety of different fuel performance evaluation programs and surveillance activities. However, based on our extensive experience to date, fuel rod fretting is not anticipated to be a significant concern for extended-burnup operation.

4.1.12 Pellet/Cladding Interaction

Irradiation exposure in fuel rods causes the fuel cladding gap to close due to fuel pellet relocations and swelling, and cladding creepdown. In addition, gaseous fission products are generated and released into the free volume of the fuel rod. After gap closure has occurred, an increase in power causes tensile stresses in the clad because of the differential thermal expansion between the fuel pellet and cladding. These stresses, if sufficiently large, in the presence of sufficient amounts of certain corrosive fission products (such as iodine or cesium) can cause pellet/cladding interaction (PCI) fuel failures.

Combustion Engineering has been engaged in an extensive PCI research program both independently and in cooperation with Kraftwerk Union (KWU) of Germany. This program has included many PCI ramp tests on C-E and KWU fuel rods, thus providing a large body of information on the cause and prevention of PCI failures.

As a result of the evidence of PCI failures, C-E has prepared and recommended operating guidelines to C-E plant operators which are designed to minimize the potential for PCI. These guidelines have been updated and revised as required to reflect the advancing understanding of PCI which has been gained through analytical and experimental research programs.

4.1.12.1 Fuel Design Characteristics That Affect Pellet/Cladding Interaction

In addition to operating guidelines, there are many fuel rod design techniques that can be and are being used by C-E to minimize PCI. The most important are discussed below.

Fuel Rod Internal Prepressurization . For nearly a decade, C-E has internally prepressurized its fuel rods with helium. Highly prepressurized rods with a gas having high thermal conductivity accomplishes several important objectives. First, for a given power or incremental power level, fuel temperatures, thermal expansion, and corresponding clad stresses are reduced. The reduced temperature causes a corresponding reduction in fission gas release which in turn results in reduced quantities of corrosive species. Thus, prepressurization with helium improves PCI performance from both the stress and environment points of view.

[

]

Fuel Pellet Configuration . C-E has performed many calculations using finite element and other analytical techniques and has performed in-pile experiments to assess the effect of pellet configuration on PCI. [

]

[

]

Finite element analyses have shown that,[

]

Dish volume also impacts PCI performance. C-E fuel pellets have a large dish at each end. Throughout life,[

]

[

]

Pellet Clad Gap . As mentioned previously, fuel rods are fabricated with a small gap between the fuel pellets and cladding which in C-E designs is filled with pressurized helium. As the rods are irradiated, the pellets relocate and swell, and the cladding creeps inward.

Eventually, the pellet and cladding come into intimate contact. During power excursions after contact, the differential thermal expansion between pellet and clad causes stresses to be built up in both components. During power excursions before contact, some portion of the differential thermal expansion fills the remaining pellet/clad gap. Therefore, a portion of the incremental power rise does not cause stresses in the cladding thereby providing improved PCI performance. This enhancement is evident in most PCI testing. For C-E fuel designs, pellet/cladding contact under normal operation typically occurs at [ ] MWd/kg burnup. After contact, when all of the differential thermal expansion is effective in causing cladding stress, the gap no longer affects PCI performance. The additional effect of a closed gap at extended burnups is that of stabilized heat transfer characteristics. Since elevated temperatures are needed to release the fission products, the heat rating required to promote this release remains high. Thus, even at extended burnups, there will be no deterioration in PCI performance due to this design characteristic.

4.1.12.2 Evaluation of Pellet/Cladding Interaction

The design characteristics of C-E fuel rods which are most important relative to PCI have been briefly discussed above. The design analyses which have been performed to date have the objective of producing fuel rods with reliable PCI performance throughout the life of the fuel. Design features of C-E fuel rods were selected to minimize the propensity for PCI throughout life; some provide PCI advantages to very high burnups[ ]

[ ]

As mentioned earlier, C-E has been involved in many ramping experiments and has collected a considerable amount of PCI data. The data plotted in Figure 4-18

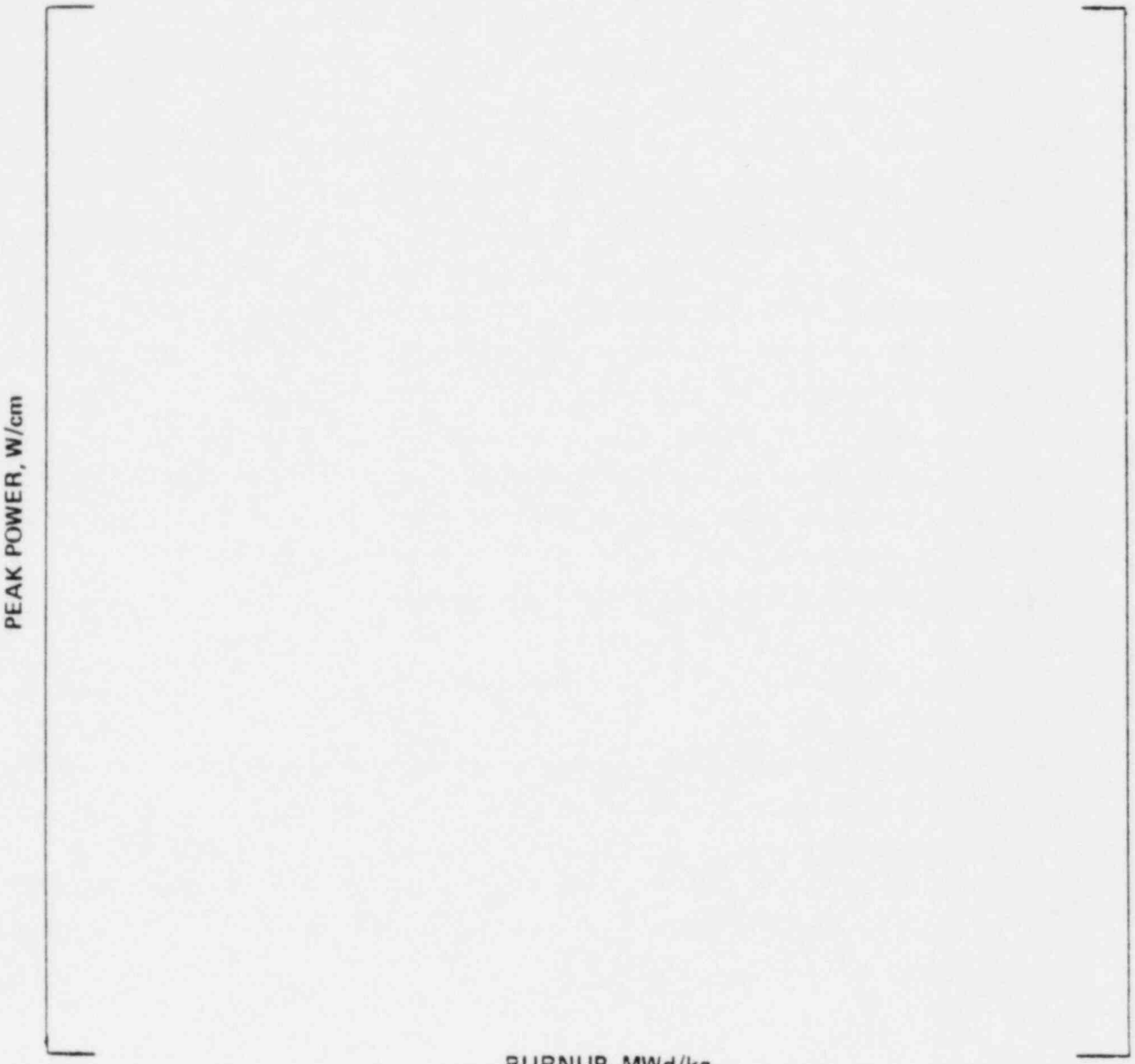

FIGURE 4-18
PEAK POWER VERSUS BURNUP FOR
C-E/KWU PCI RAMP EXPERIMENTS

comes from rodlets pre-irradiated at Obrigheim and ramped at either the Petten or Studsvik test facilities in Europe (4-37,4-64,4-65,). The data shown are only from rodlets using the standard C-E or KWU designs. Other data available in the literature has not been shown because of design differences. These differences would in some cases be expected to produce a PCI sensitivity to burnup. It is important to recognize that comparisons between experimental PCI results are only valid when the important design variables are consistent. All of these rods were preconditioned in a PWR at similar power levels and were ramped under PWR conditions at relatively fast and consistent rates (50-110 W/cm/min). Data is also available at slower ramp rates. The slower ramps are less severe and give improved PCI performance. The data available for burnups less than 20 MWd/kg show a burnup dependence, but this is due to [

] In addition, as burnup increases, the capability of the fuel to reach the power levels needed for PCI failure is diminished. This fact, in conjunction with the insensitivity of PCI to burnup as demonstrated by the data, suggests that the overall probability of PCI failures may in fact decrease with burnup when extended to the 52 MWd/kg range.

4.1.13 Cladding Deformation and Rupture

The acceptability of fuel rod behavior following postulated accidents is based on meeting certain radiological release limits defined in the Code of Federal Regulations (CFR) (4-66 through 4-68). The source of radioactivity from the fuel is based on the assumption that certain conditions are indicative of fuel failure and on assumptions regarding release of radioactive material once failure has occurred. For a postulated LOCA, acceptance criteria for transient fuel rod behavior are prescribed in 10CFR50.46 (4-66). Additionally, required and acceptable features of evaluation models are specified in 10CFR50 Appendix K (4-69) and must be used in analyzing fuel rod behavior. A requirement for each evaluation model is to account for cladding deformation and rupture. This requirement is contained in Section I.B of Reference 4-69 and is as follows:

"Each evaluation model shall include a provision for predicting cladding swelling and rupture from consideration of the axial temperature distribution of the cladding and from the difference in pressure between the inside and outside of the cladding, both as functions of time. To be acceptable, the swelling and rupture calculations shall be based on applicable data in such a way that the degree of swelling and incidence of rupture are not underestimated. The degree of swelling rupture shall be taken into account in calculations of gap conductance, cladding oxidation and embrittlement, and hydrogen generation."

At the NRC's request, a change has been proposed to the portions of the C-E ECCS evaluation model which respond to these requirements (4-70). These proposed changes include the implementation of cladding deformation and rupture models of NUREG-0630, "Cladding Swelling and Rupture Models for LOCA Analyses" (4-71). The NRC models were developed from a relatively large out-of-pile data base and some in-pile data at low burnup. Using available data at higher burnup, it will be shown that these models still satisfy the Appendix K criteria and therefore can be used to evaluate extended burnup for current fuel designs.

4.1.13.1 Modeling of Cladding Deformation and Rupture

During a postulated LOCA transient, rod internal gas pressure varies due to changes in the fuel temperature, cladding temperature and fuel rod free volume. Since the primary system depressurizes during a LOCA, the pressure difference across the cladding reverses, resulting in a net outward load. Cladding strength and ductility also change as the temperature varies during the transient. The combined effects of the differential pressure and cladding temperature variations during the transient may produce deformation and rupture the cladding. The models which predict cladding rupture temperature and circumferential burst strain are shown in Figure 4-19. The model that predicts rupture temperature is a function of rod-to-coolant pressure difference (hoop stress) and heating rate preceding rupture. The model that predicts circumferential burst strain is a function of rupture temperature and heating rate preceding rupture. These models were developed from unirradiated or low burnup cladding burst tests; therefore, these models contain no explicit burnup dependence.

In the proposed changes to the C-E ECCS evaluation model, [

]

Extended burnup influences cladding deformation and rupture during a postulated LOCA transient in several ways which can be accounted for without specific model changes. [

] The impact of extended burnup on these parameters as they relate to cladding deformation and rupture is discussed below.

4.1.13.2 Effect of Extended Burnup on Cladding Deformation and Rupture

Burnup effects that are considered to influence cladding deformation and rupture during a LOCA are summarized in Table 4-4. The list is subdivided into burnup effects for the fuel and cladding and indicates whether the effect is of primary or secondary importance. Cladding deformation and rupture are discussed first with regard to extended-burnup effects for the fuel and then for the fuel rod cladding.

Fuel Burnup Effects . [

] are identified in Table 4-4 as important parameters for consideration at extended burnups and are discussed individually in other sections of this report. These burnup dependent parameters influence the cladding temperature and internal rod pressure response during a LOCA, and subsequently affect the cladding deformation and rupture behavior. [

TABLE 4-4

BURNUP EFFECTS FOR CLADDING DEFORMATION AND RUPTURE

Burnup Effect	Burnup Dependence
[	]

] These fuel parameters are considered to have a primary influence on cladding deformation and rupture at extended burnups.

A number of fuel burnup effects that are listed in Table 4-4 are only a minor consideration in calculating cladding deformation and rupture at extended burnups. These parameters, however, are presented here for completeness. During normal reactor operation, [

] These effects are expected to result in relatively small changes in heat transfer characteristics at extended burnups and are not considered a significant influence on cladding deformation and rupture.

Cladding Burnup Effects. [ ] are the two primary effects listed in Table 4-4 which may be important in modeling deformation and rupture at extended burnups. [

] This burnup effect, therefore, does not impact the Appendix K requirement that the degree of swelling not be underestimated.

[ ]

As was the case for a number of fuel parameters, there are several cladding parameters which are burnup dependent but which are only of minor importance to deformation and rupture during a LOCA. [

] A more detailed discussion of this effect can be found in Reference 4-72. [

] Therefore, this failure mechanism is not considered for LOCA cladding deformation or rupture.

4.1.13.3 Evaluation of Cladding Deformation and Rupture

The effects of extended burnup on cladding deformation and rupture are evaluated in this section. An extension of the cladding deformation data presented in Reference 4-73 is provided first. Next, the adequacy of C-E's modeling of high burnup effects for cladding deformation and rupture is summarized.

Recent Cladding Deformation and Rupture Data . A number of research programs which test fuel rods under LOCA conditions were summarized in Reference 4-73. Since that report, recent experiments dealing with cladding deformation and rupture have been reported (4-75,4-76) employing fuel rods with prior irradiation. This section summarizes these tests and presents key results. The tests discussed were conducted at the Power Burst Facility (PBF) and in the FR-2 reactor at the Kernforschungszentrum Karlsruhe (KfK) facility.

Three LOCA experiments using irradiated rods have been conducted at PBF (4-75,4-77,4-78). The fuel rods employed had an active length of 36 inches, an outside diameter of 0.391 in., and a wall thickness of 0.023 in. These tests were designed to investigate cladding deformation during the blowdown phase of a LOCA. Each experiment was performed using four separately shrouded fuel rods

of a typical PWR assembly. Two of the rods had been previously irradiated in the Saxton reactor to a burnup of about 16 MWd/kg and two rods were unirradiated. One unirradiated and one irradiated rod were pressurized with helium to a cold pressure typical of beginning-of-life conditions, 350 psia, and the other two were pressurized with helium to a cold pressure typical of end-of-life, 700 psia. This test configuration enabled the effects of internal rod pressure and irradiation on fuel rod behavior to be examined separately.

The PBF results generally show that previously irradiated rods have larger rupture strains than fresh rods. Additionally, the cladding strain of the irradiated rods was more uniformly distributed around the cladding circumference. The deformation of the irradiated rods was also larger than that of the unirradiated rods over the heated length. If it is assumed that these single rod tests are representative of multirod behavior, then these results indicate that during blowdown experiments, the potential for coplanar blockage in a bundle of irradiated rods is greater than in an unirradiated bundle. [

]

In the FR-2 reactor, 39 in-pile tests (4-76) have been completed to date. These tests were designed to investigate cladding deformation and rupture during the reflood phase of a LOCA. The test rods for these experiments had a heated length of 19.7 inches and had an outside diameter of 0.423 in. with a wall thickness of 0.0285 in. Tests were conducted with unirradiated as well as irradiated rods with burnups ranging from zero to about 35 MWd/kg to determine cladding deformation and rupture characteristics. In comparison to PBF results, the FR-2 test results do not show any significant influence of irradiation on the mechanisms of fuel rod failure. The rupture data of the in-pile tests lie within the data spread of out-of-pile tests. No influence of burnup was reported.

An explanation for the difference in PBF and FR-2 experiments is related to the LOCA conditions of each experiment. The PBF tests were conducted during the

blowdown phase of a LOCA where the fuel was initially at high power and the fuel and cladding were in good contact. As mentioned earlier, some burnup dependent parameters such as [ ] are extremely sensitive to this situation. During the blowdown, more uniform circumferential temperatures around the cladding were reported in the irradiated rods compared to the unirradiated rods, which accounts for the difference in strains. In comparison, the FR-2 experiments were conducted at low powers during reflood conditions and without good fuel cladding contact. Circumferential temperatures for these test rods may have been similar for all burnups, and no observed difference in cladding strain was apparent due to burnup. This leads to the conclusion that the amount of strain obtained is not significantly dependent on burnup but rather on the uniformity of circumferential heating of the fuel rod. C-E has proposed use of the NRC models of NUREG-0630 (4-70) which encompass data having a broad range of circumferential temperature gradients.

Adequacy of High Burnup Models . Based on these test results and the results of experiments reported in Reference 4-11, it is concluded that [ ] Additionally, there is nothing in the data base generated thus far which would indicate any need to restrict the burnup levels to which the currently available models can be applied.

Cladding circumferential rupture strains, rupture temperature, and rupture pressure for the PBF and FR-2 experiments are compared with rupture/deformation criteria from the C-E ECCS Evaluation Model (which incorporates the proposed changes) in Figure 4-19. The data shown are generally encompassed by the C-E model. The results of these experiments for fuel rods with burnups to 35 MWd/kg indicate that the C-E ECCS Evaluation Model for cladding deformation and rupture will satisfy the NRC Appendix K requirement that the degree of swelling may not be underestimated in LOCA analysis.

In summary, the important burnup considerations for LOCA licensing are [ ] These models

FIGURE 4-19
COMPARISON OF C-E RUPTURE TEMPERATURE AND BURST STRAIN MODELS WITH PBF AND FR-2 EXPERIMENTAL RESULTS

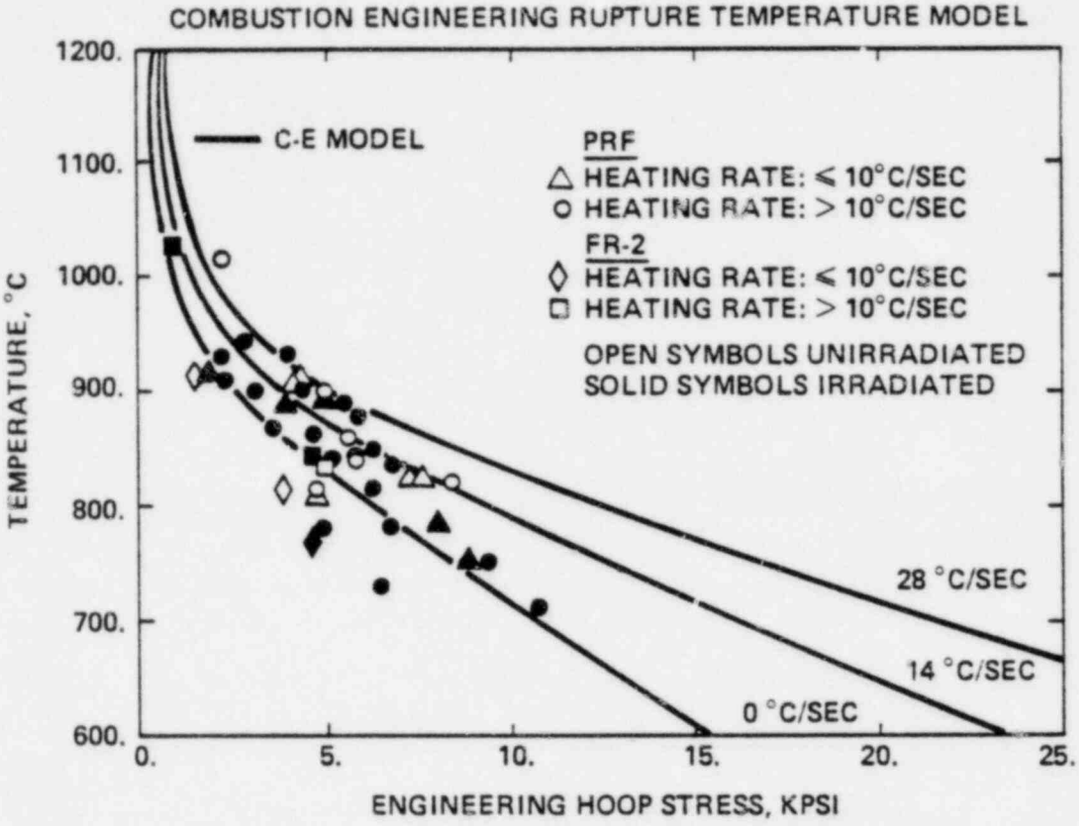

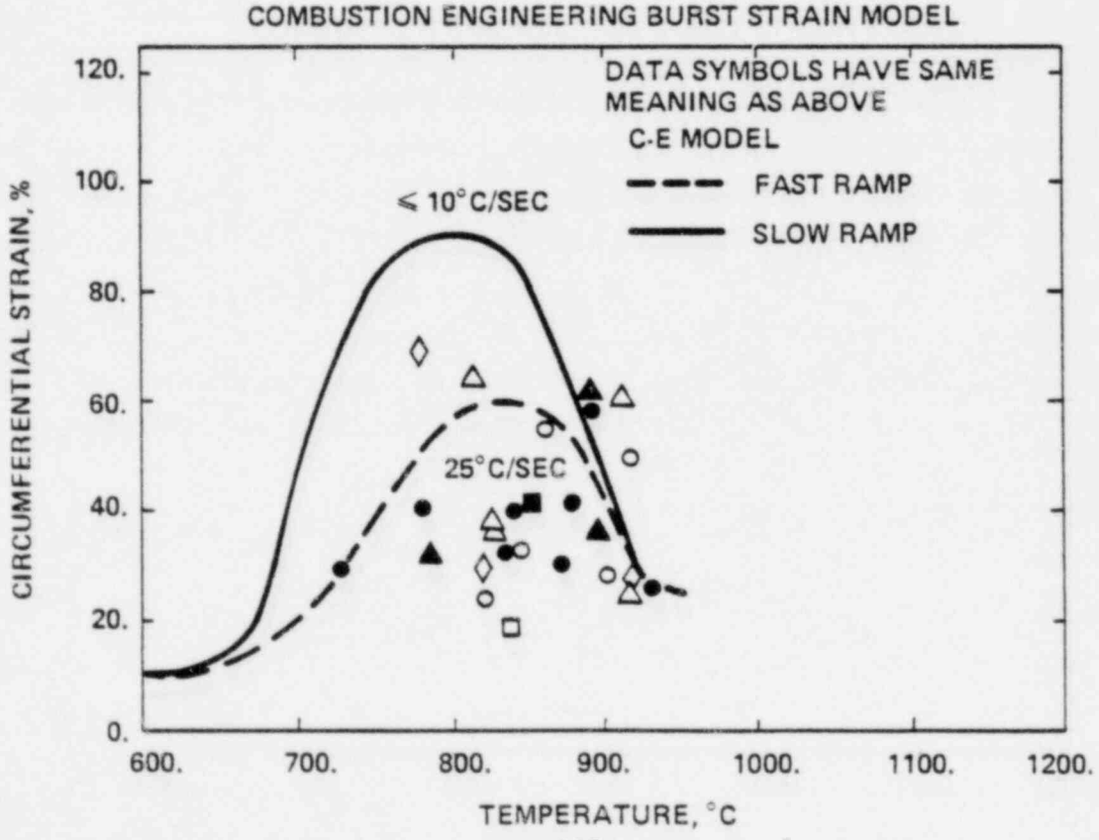

have been reviewed within this report for use at extended burnups and are considered adequate for use along with cladding deformation and rupture models. The decrease in power with burnup for fuel beyond conventional exposure levels is also a determining factor in LOCA analyses and is accounted for where necessary. [

] The overall conclusion of this evaluation is that LOCA licensing models for cladding deformation and rupture are not restricted by burnup level.

4.1.14 Fuel Rod Growth

It has been well established that continued exposure to a neutron flux causes axial elongation or growth of Zircaloy-4. Within the last few years, a substantial amount of growth data has been obtained on PWR fuel rods of modern design (i.e., pressurized rods with nondensifying fuel) at burnups in excess of 35 MWd/kg. This information has been used to verify existing fuel rod growth models originally developed with data obtained at lower fluences and from rods of older design (densifying fuel with lower initial pressurization levels). Within the next several months, growth data will be available to burnups approaching[ ]MWd/kg.

Knowledge of the growth of Zircaloy-4 clad fuel rods is needed to design a fuel assembly with sufficient clearance between the top of the fuel rods and the bottom of the upper end fitting flow plate (shoulder gap) to accommodate fuel rod growth without interference at end-of-life. The amount of clearance allowed in the initial design depends on the anticipated lifetime of the fuel assembly and is a function of the expected fuel rod growth and growth of the Zircaloy-4 guide tubes which form the assembly structure. Together the expected dimensional changes for these two components constitute a major consideration in designing fuel assemblies for extended-burnup operation.

4.1.14.1 Modeling of Fuel Rod Growth

It is known that the overall elongation of a Zircaloy clad fuel rod is due to several contributing mechanisms including stress-free irradiation growth of the Zircaloy cladding, mechanical interaction between the UO_2 fuel pellets and

the Zircaloy cladding, and a net positive growth component due to creepdown of the cladding under the external coolant pressure (4-80). Each of these contributing mechanisms are related to the time of operation through accumulated burnup or fluence. Rather than account for individual contributions from each mechanism, overall fuel rod growth is measured and empirically modeled for design purposes.

The correlation developed by C-E to determine fuel rod growth as a result of irradiation exposure or fluence was described in Reference 4-80. Growth strain versus fluence (E > 0.821 MeV) is linear on a log-log plot. The functional form of such an equation is:

$$\varepsilon = A\,(\phi\tau)^n$$

Where ε = strain, in./in.

$\phi\tau$ = neutron fluence, n/cm^2 (E> 0.821 MeV) x 10^{-21}

A and n = constants, as shown below.

A regression analysis, described in Reference 4-80, was used to determine the value of the constants A and n and resulted in the following growth equations:

[

]

The growth data used in this analysis, which is summarized in Reference 4-80, covered a fluence range of [

]

4.1.14.2 Effect of Extended Burnup

Measurements of rod length obtained to fast fluences over [

] have shown continuous and well-behaved growth with increasing exposure (4-29 through 4-31,4-63). These data have confirmed that no acceleration in the rate of growth or other abrupt changes occur up to the exposure levels at which rods have been examined.

Furthermore, fuel rod growth at higher burnups appears to be relatively insensitive to slight design differences. [

] does not contribute as much to the overall growth rate at higher exposures as would be inferred from measurements after only one or two operating cycles. This observation is supported by measurements taken over 4 reactor cycles as part of a fuel performance evaluation program jointly sponsored by EPRI and C-E at Calvert Cliffs-1 (4-31).

4.1.14.3 Evaluation of Fuel Rod Growth

Figure 4-20 shows growth measurements obtained on C-E fuel rods over the past few years compared to the C-E fuel rod growth model developed in 1975 and described in Reference 4-80. Data from 14x14 fuel rods at Calvert Cliffs-1 have been obtained up to a fluence of [ ] while data from 16x16 fuel rods at ANO-2 have been obtained to a fluence of [

]

The growth data from the Calvert Cliffs-1 fuel rods have also been used in a recent analysis of growth published by Franklin which involved more than 700 fuel rod length measurements (Reference 4-81). This analysis confirmed the well-behaved nature of fuel rod growth at high fluence and [

]

Since 1973, C-E has examined hundreds of fuel assemblies in which the existing C-E fuel rod growth correlation was used in the design process to establish the desired shoulder gap clearance between the top of the fuel rods and the bottom of the upper end fitting flow plate. No instances of interference between the fuel rods and flow plate have ever been observed. In fact, the conservatism of the C-E design methodology has resulted in sufficient margin to allow the irradiation of lead assemblies to burnups in excess of [ ] MWd/kg with adequate margin.

In 1982, C-E will acquire additional growth data from 14x14 fuel rods at Fort Calhoun and Calvert Cliffs-1 to rod average burnups of approximately [ ]

FIGURE 4-20
RECENT FUEL ROD GROWTH MEASUREMENTS COMPARED TO THE
C-E ZIRCALOY FUEL ROD GROWTH MODEL

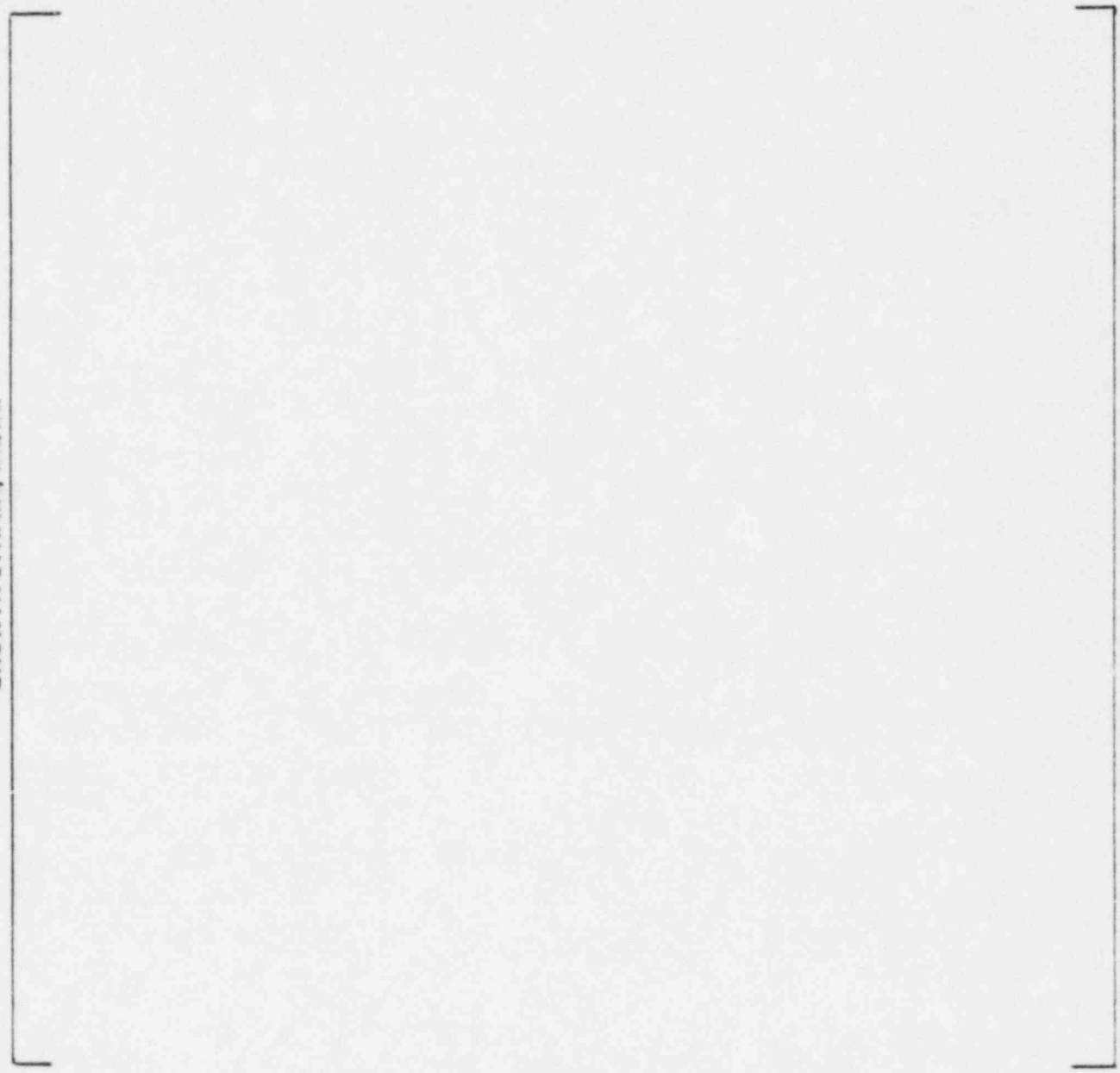

MWd/kg. The growth behavior of 16x16 fuel rods thus far appears consistent with that of 14x14 fuel rods but will be monitored in any case as part of existing joint programs with EPRI and DOE at ANO-2 (cf. Sections 1.4.3 and 1.4.4).

4.2 FUEL ASSEMBLY

The fuel performance topics that are associated with the overall behavior of a fuel assembly and/or its structural components are discussed in this section. A list of these topics was given in Table 1-2 and includes those that describe the behavior of guide tubes, holddown springs, spacer grids, and poison rods for a typical current design PWR. The ordering of these topics is arbitrary and has no particular significance.

4.2.1 Guide Tube Wear

In December 1977, localized wear of the Zircaloy guide tubes was observed in the fuel of several C-E reactors at positions which corresponded to the control rod tip elevations. The wear was caused by small amplitude motion of the control rods. Subsequent to this, a series of submittals were made (e.g., Reference 4-82) describing the results of inspections for this problem and justifying the continued operation of C-E plants.

A two-phase program was initiated in response to the detection of guide tube wear. The first phase involved the development of a chrome-plated, stainless steel sleeve to reinforce or protect the guide tubes of existing fuel. The sleeve was designed such that it could be inserted into a fuel assembly guide tube to either reinforce a worn tube or to act as a wear-resistant surface along the guide tube length where long term control rod contact was expected. The sleeve is described in Reference 4-83. All fuel assemblies with significant guide tube wear were reinforced with this sleeve, and none had to be discharged or reconstituted as a result of guide tube wear.

The second phase of the program involved a series of test programs whose objectives were to obtain sufficient data to gain an understanding of the causes of the control rod motion and to develop a long term solution for the guide tube wear problem. The second phase resulted in three reactor

demonstration programs (4-84 through 4-86) two of which are still in progress. The demonstration programs utilize unsleeved fuel assemblies.

4.2.1.1 Modeling of Guide Tube Wear

Based on the inspections of the original design guide tubes, the out-of-reactor test programs, and the completed reactor demonstration program, guide tube wear [ ] (4-87). The actual rate of wear is a function of both the materials involved and the magnitude of the control rod motion. The magnitude of motion [ ]

4.2.1.2 Effect of Extended Burnup

The effect of extended-burnup operation of the fuel will be to increase the residence time for fuel assemblies in control rod locations, thereby increasing the wear volume produced on either the wear sleeves or unsleeved guide tubes.

4.2.1.3 Evaluation of Guide Tube Wear

Because of the short term and long term approaches taken on the solution to guide tube wear, the evaluations of these two topics are discussed separately.

Fuel Assembly Performance With Wear Sleeves . Reference 4-87 documents the results of eddy-current inspections of several hundred wear sleeves following one cycle of operation in plants using C-E's 14x14 fuel design. The same reference also describes the destructive metallographic examination of a one-cycle sleeve from a high wear location in a C-E plant. Since the issue date of that document, several inspections have been performed on sleeves that have been located in control rod positions for two cycles. These have been reported on a plant-by-plant basis (e.g., Reference 4-88).

The conclusion drawn from all of these inspections is that long term operation of control rods in the 14x14 fuel design containing wear sleeves has produced only an insignificant amount of wear. Since wear volume [ ] it is expected that performance of the

wear sleeves will continue to be satisfactory for the extended burnup fuel (the fuel residence lifetime is approximately 35% longer).

Recent eddy-current inspections performed after one cycle of operation (4-89) have indicated that the guide tube sleeve design for the 16x16 fuel assembly design is also performing satisfactorily, since no wear was detected on any of the sleeves.

Unsleeved Fuel Assembly Performance. Several potential long term solutions to the guide tube wear problem were investigated by C-E in out-of-pile flow testing. The procedure used in the testing was to expose, for modest periods of time, one or more full scale control rod assemblies and prototype fuel assemblies to flow and temperature conditions representing reactor extremes. The guide tubes were then scanned for wear by an eddy-current device. The cases with the most severe wear were measured by destructive examination for best accuracy. The resulting wear volumes[ ] in order to judge the effectiveness of the designs in mitigating long term guide tube wear. The geometries tested included the 14x14, 16x16, and 16x16 System 80 fuel assembly designs, and their associated control rods and reactor internals, since each fuel type has unique features which were expected to affect the propensity for wear.

The best results were obtained for unsleeved fuel assembly designs which had modified guide tubes. A reactor demonstration program was conducted during 1978 and 1979 using this design (4-84) in order to confirm that there were no unanticipated factors in the reactor that would lead to more guide tube wear than was predicted from the out-of-pile testing. Twelve unsleeved 14x14 fuel assemblies were placed in core locations where standard fuel assemblies had resided prior to the discovery of the wear problem. This enabled a direct comparison to be made between the performance of standard and modified guide tubes.

Reference 4-87 summarizes the results of the demonstration program. There was a dramatic reduction in the degree of guide tube wear with the modified design compared to the original guide tube design for 14x14 fuel. Furthermore, the method of extrapolation of the worst out-of-pile wear result from its

relatively short test time to a full reactor cycle proved to be reasonably conservative for the core locations that were tested.

Because of the loading pattern for the reload fuel, the demonstration program discussed in References 4-84 and 4-87 [ ] based on data from the original unsleeved fuel. Therefore, another demonstration program (4-85) is now being conducted [ ] In addition, a minor change was made to the design of some of the fuel assemblies in this program. The wear measurements will be available during 1982. The data will provide the support for operation of unsleeved 14x14 fuel assemblies in all core locations.

A similar demonstration program for the 16x16 fuel assembly will take place in 1982 and 1983 (4-86). In the case of C-E System 80 fuel, the out-of-pile testing was favorable enough to support operation without guide tube wear sleeves in any of the fuel (4-90).

For extended-burnup operation, the defense of the unsleeved fuel assembly design [ ] Based on the expected results from the 14x14 and 16x16 fuel demonstration programs, and on extrapolation of the System 80 fuel flow test results, the increased volumes should easily be accommodated.

4.2.2 Fuel Assembly Length Change

Fuel assembly length change results from two distinct mechanisms in the Zircaloy guide tubes: irradiation induced growth and compressive creep. Growth is produced by radiation effects on the Zircaloy crystalline structure, and causes the guide tubes to elongate. Compressive creep is the permanent reduction in length of the guide tubes in response to the fuel assembly holddown forces.

Change in guide tube length affects the fuel assembly engagement with the reactor internals, as well as the net holddown force on the assembly, and the shoulder gap (the distance between the top of the fuel rods and the bottom of the upper end fitting). The length change is important in the evaluation of criteria pertaining to each of these aspects of fuel performance.

Since the holddown force is a function of fuel assembly length, irradiation induced guide tube growth causes an additional compression of the upper end fitting springs, increasing the compressive load on the guide tubes. The higher load in turn causes an increased compressive creep rate of the guide tubes. Therefore, the net fuel assembly length change at a given time during operation depends on the combined effects of irradiation growth and creep up to that point in time.

4.2.2.1 Modeling of Assembly Length Change

Growth and creep characteristics are dependent on the metallurgical state of the Zircaloy guide tubes. As presently planned, all 14x14 fuel assemblies that will be irradiated to extended burnups will have [ ] The extended burnup 16x16 fuel assemblies will have [ ] The guide tube growth models for the two types of guide tubes are summarized in Table 4-5. The guide tube axial creep models for low stress applications (stress < 5000 psi) are summarized in Table 4-6.

Dimensional changes of fuel assembly guide tubes are analytically predicted by the SIGREEP computer code, which is described in Reference 4-91. The code utilizes a computerized Monte Carlo technique for establishing resultant joint probability density functions by randomly selecting combinations of input values to be used in a time history analysis of dimensional changes. Inputs assigned statistical uncertainties include component dimensions, the assembly uplift force, the guide tube growth coefficients, and the guide tube creep coefficient.

In the analysis which predicts fuel assembly length change, the SIGREEP computer code generates a set of randomly selected values for the input parameters that have been assigned uncertainty distributions, and then uses that set of inputs to perform a time history analysis of the length changes. When the analysis reaches the specified operating time or burnup, the dimensional change prediction for the fuel assembly is complete. A single value of assembly length change is the result of the time history calculation. The same steps are repeated (starting with a different set of randomly selected values for the input parameters) until a sufficient number of values (typically

TABLE 4-5

GUIDE TUBE IRRADIATION GROWTH MODELS

Equation Form: $\epsilon = A (\phi\tau)^n$

Where: ϵ = axial strain, in./in.

A = coefficient, as shown below

Axial Strain Coefficient (A)

[

]

$\phi\tau$ = fluence, n/cm^2 ($E > 0.821$ MeV) x 10^{-21}

n = constant = [

=

]

[

]

TABLE 4-6

GUIDE TUBE AXIAL CREEP MODELS

Equation Form: $\dot{\varepsilon}_Z = \alpha\beta\sigma_Z$

where: $\dot{\varepsilon}$ = principal strain rate, hr^{-1}, in the axial direction

α = coefficient as shown below

Axial Strain Rate Coefficient (α)

[redacted]

σ_Z = axial guide tube stress

$\beta = \phi^{.85} \exp(-6000/RT)\,(AK \exp(-Kt) + C)$

ϕ = fast neutron flux, n/cm^2 - sec (E > 1.0 MeV)

R = 1.987, cal/mol°K

T = temperature, °K

A = constant = [redacted]

t = time, hr

K = constant = [redacted]

C = constant = [redacted]

[redacted]

2000) have been generated to define a probability histogram of length change at end of life (EOL). The resultant histogram represents the statistical variation of EOL length change which can be attributed to the uncertainties of the input parameters. Values can be chosen from the histogram at desired probability levels for comparisons to actual data or appropriate design criteria. Figure 4-21 presents a typical histogram of fuel assembly length change.

As described in Reference 4-91, the SIGREEP computer code can also be utilized to calculate probability histograms for shoulder gap (space between the top of the fuel rod and the bottom of the upper end fitting). In the shoulder gap analysis, fuel assembly length change is calculated by SIGREEP exactly as described above. Corresponding to each time history case for fuel assembly length change, fuel rod length change is simultaneously calculated using values for the growth coefficient and beginning of life (BOL) dimensions that have been randomly selected from the probability distributions for these parameters. The statistical model of the growth coefficient for fuel rods was discussed in Section 4.1.14. Both the 14x14 and 16x16 fuel rod designs use SRA fuel rod cladding.

When the time history case reaches the specified time or burnup, shoulder gap change is calculated as the difference in fuel rod and fuel assembly length changes. A single value of shoulder gap change is the end product of the time history calculation. The calculation is repeated until a sufficient number of values (again typically 2000) have been generated to define a probability histogram of shoulder gap at EOL.

Reference 4-91 was submitted to the NRC in September 1981, and approval is expected early in 1982. The method described in the reference and summarized above is intended to be used for all future length change analyses on standard- and extended-burnup fuel.

4.2.2.2 Effect of Extended Burnup

As stated in the preceding sections, fuel assembly length change is the net change resulting from irradiation induced growth and compressive creep of the guide tubes. Since growth is fluence dependent and compressive creep is time and flux dependent, assembly length change and shoulder gap are affected by

FIGURE 4-21

TYPICAL PROBABILITY HISTOGRAM FOR FUEL ASSEMBLY LENGTH CHANGE

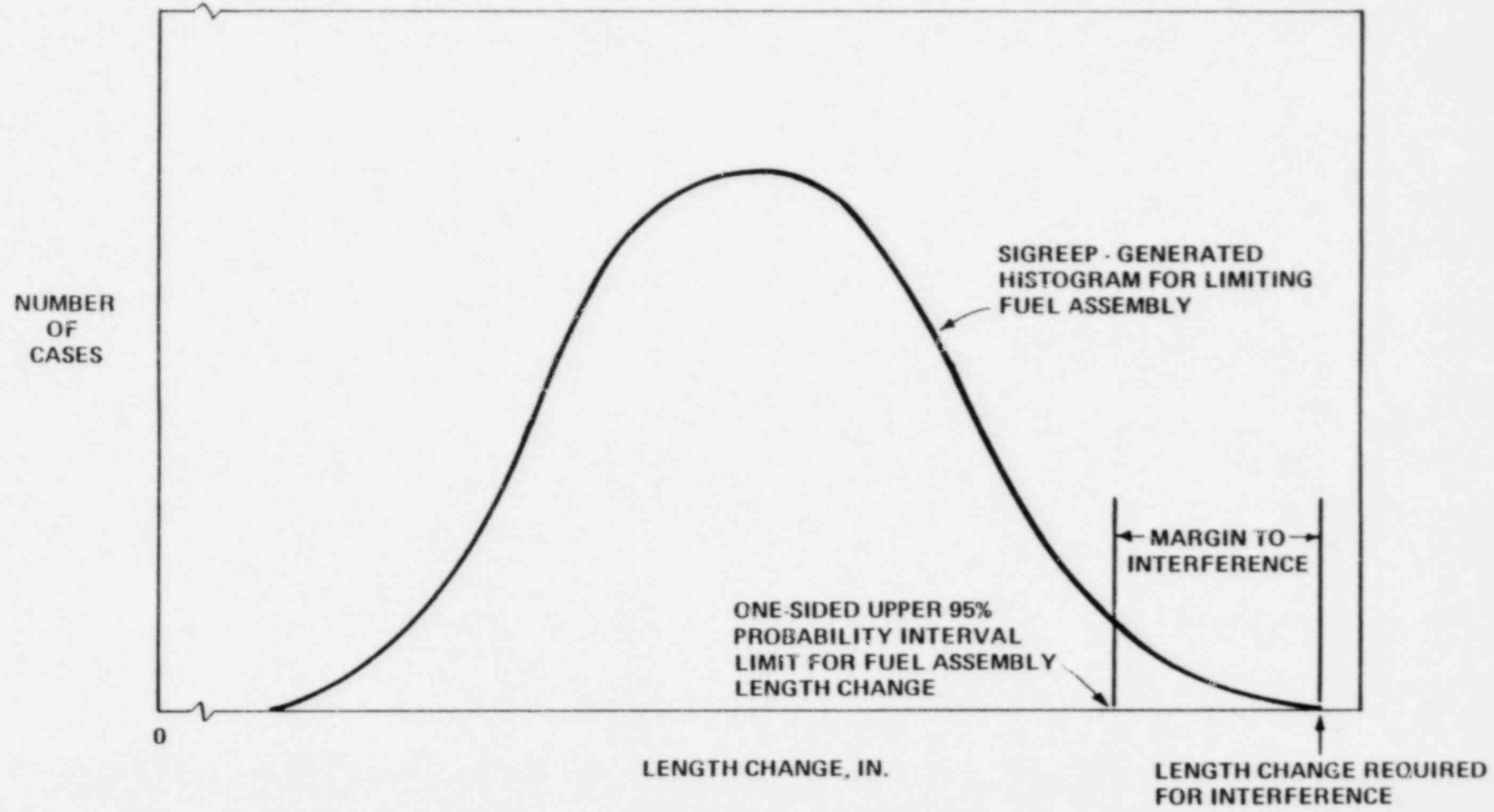

extended burnup. In general, higher burnups are expected to result in greater increases in assembly length, greater holddown spring compression, and larger changes in shoulder gap. The extent of these changes will be evaluated based on the specific extended burnup operating conditions and the particular fuel assembly design.

4.2.2.3 Evaluation of Assembly Length Change

In support of the methodology described in Section 4.2.2.1, Reference 4-91 compared SIGREEP predictions of shoulder gap change and fuel assembly length change to actual data from Maine-Yankee Cycles 1 and 1A and from Calvert Cliffs-1 Cycles 1, 2, 3 and 4. The upper and lower 95% probability limits on the SIGREEP predictions were found to be conservative for design purposes. The predictions enveloped the highest burnup data (46 MWd/kg assembly average burnup). The data are representative of 14x14 fuel assemblies[

] Therefore, it was concluded that the analytical model (the SIGREEP computer code) is acceptable for use in predicting the irradiation induced dimensional changes for extended-burnup fuel using the current 14x14 fuel assembly design.

Shoulder gap change measurements and assembly length change measurements have been obtained after one cycle for 16x16 assemblies with[

]in the Arkansas Nuclear One, Unit 2 reactor. SIGREEP computer runs have been made based on the actual operating conditions, and comparisons made to the measured data (cf. Figures 4-22 and 4-23). The comparisons show that the upper and lower 95% probability predictions envelop the data.

Figures 4-22 and 4-23 demonstrate that the analytical model produces acceptable predictions of the irradiation induced dimensional changes in 16x16 fuel assemblies[ ] While the burnup levels corresponding to the 16x16 fuel assembly data are limited, the 14x14 fuel assembly data reported in Reference 4-91 have shown that the SIGREEP code predicts the trends of dimensional change with increasing burnup. Since the length change mechanisms are the same for both fuel types, it is concluded that the model is appropriate for the 16x16 extended-burnup fuel assembly design in addition to the 14x14 fuel assembly design.

FIGURE 4-22

COMPARISON OF ARKANSAS NUCLEAR ONE UNIT 2, END OF CYCLE 1
ASSEMBLY LENGTH CHANGES TO SIGREEP PREDICTIONS

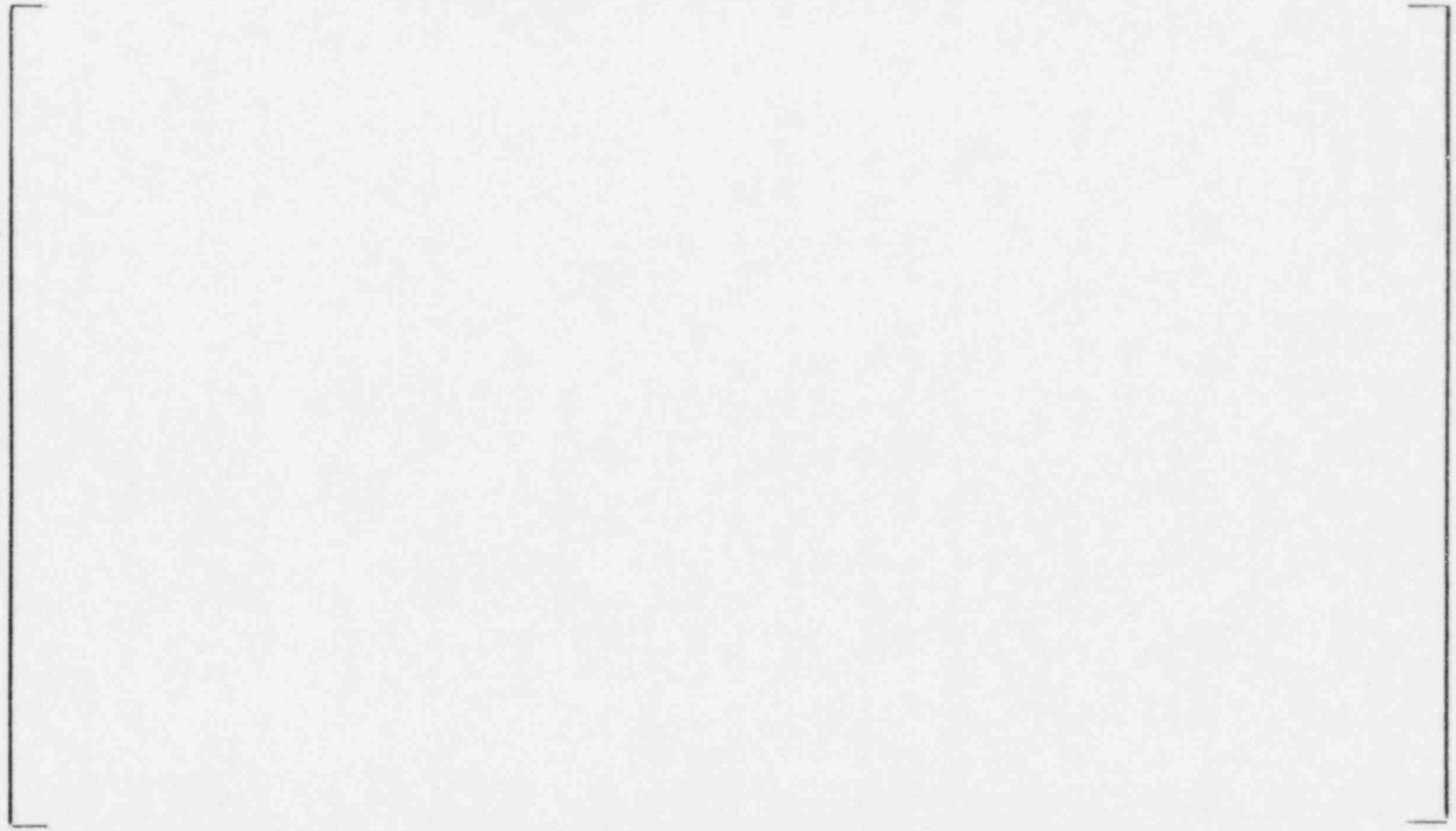

FIGURE 4-23

COMPARISON OF ARKANSAS NUCLEAR ONE UNIT 2, END OF CYCLE 1
SHOULDER GAP CHANGES TO SIGREEP PREDICTIONS

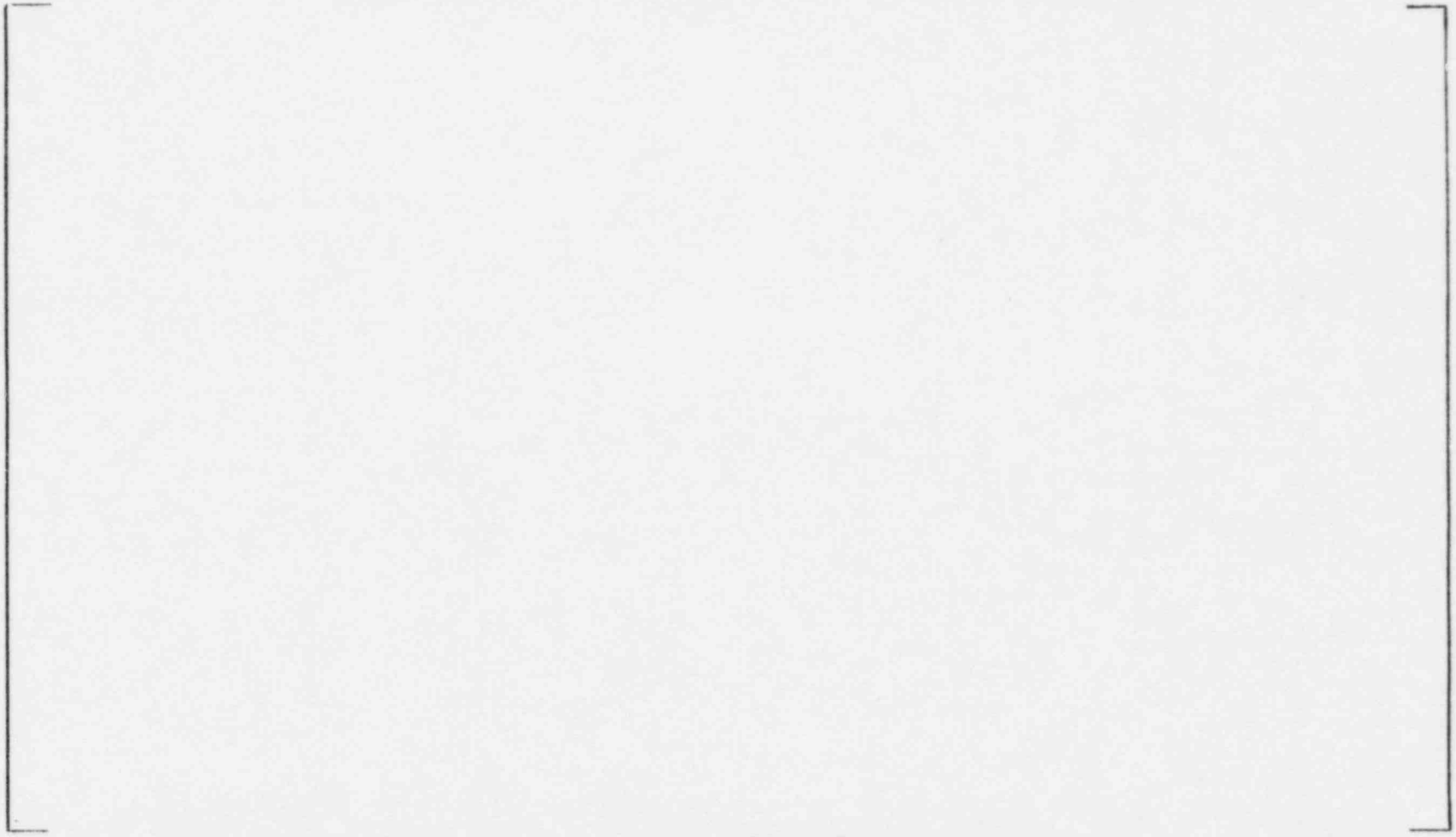

4.2.3 Fuel Assembly Holddown

The fuel assembly must be restrained from lifting off its support surface in response to the hydraulic forces which are produced by coolant flow. The restraining force is termed fuel assembly holddown.

Fuel assembly holddown is provided by a combination of assembly wet weight and (if necessary) the force from the upper end fitting holddown springs. Assembly wet weight is strictly a function of dry weight, displaced volume, and moderator density. The amount of holddown spring force depends on the spring constant and spring compression. The compression is a function of the distance between the core support plate and the fuel alignment plate, the length of the fuel assembly components, and the free length of the holddown springs.

As noted in Section 4.2.2, assembly length change and holddown force are interdependent to some degree. Therefore, the holddown force at any time during operation depends on how the irradiation growth, creep, and spring relaxation have interacted during operation up to that time.

4.2.3.1 Modeling of Holddown Spring Force

Section 4.2.2 describes how dimensional changes of fuel assembly guide tubes

are analytically predicted by the SIGREEP computer code. Because of the interdependence of assembly length change and holddown spring force, calculation of spring force is an integral part of the SIGREEP code. At each increment in the time history analysis, the holdown spring force is adjusted to account for the change in spring compression due to assembly length change and spring relaxation during the previous time step. The Inconel spring relaxation correlation used by SIGREEP was obtained from Reference 4-92. No direct measurement of spring relaxation has been made, but the literature indicates that it is modest at the fluence levels of interest for standard burnup levels (about 4.0×10^{19} nvt). Furthermore, Reference 4-92 indicates that spring relaxation increases by only a small amount for the additonal fluence associated with extended burnup.

[

]

4.2.3.2 Effect of Extended Burnup

Section 4.2.2.2 noted that assembly length is expected to increase with extended burnup for all of the C-E designs. This produces an increase in holddown spring compression. At the same time, extended burnup produces greater fluence and therefore more stress relaxation of the holddown springs, which causes a reduction in spring compression. The net change in spring compression will be evaluated by performing a time-history analysis as described above.

4.2.3.3 Evaluation of Assembly Holddown

Providing the proper holddown force at BOL is a relatively straightforward

design procedure. During the fuel lifetime, ensuring the proper holddown spring force depends on the ability to model the time dependent and irradiation dependent phenomena taking place in the assembly components. The SIGREEP method has been shown to accurately model holddown force changes for all C-E extended burnup fuel assembly designs.

4.2.4 Grid Irradiation Growth

The fuel rod spacer grids in C-E plants are fabricated from Zircaloy-4. The changes in the grid dimensions resulting from growth under irradiation must be accounted for by setting a maximum size in the initial design of the grids. The overall dimensions of the grid must be such that enough clearance is provided between fuel assemblies in the reactor core at BOL to ensure that interference will not occur between assemblies later in the fuel lifetime.

One method of accommodating grid growth would be to fabricate the grids with the smallest possible dimension. However, the minimum size of the spacer grids must also be limited. [

]

4.2.4.1 Modeling of Grid Irradiation Growth

The spacer grids are fabricated [

] The current C-E model for irradiation growth strain of Zircaloy-4 grids is the same as that [ ] In the model, growth strain is a function of fast neutron fluence.

To evaluate the clearance within the core during a cold shutdown, the SIGMA computer code (Reference 4-17) is used to prepare a histogram of the available space across a row of fuel assemblies in the core. Uncertainties which are input to the SIGMA analysis include the tolerance on the width

between the core shroud plates on either end of the row, the tolerance on the beginning of life spacer grid width, and the variation in values of grid growth corresponding to the axial strain coefficients listed [ ] in Table 4-5.

[ ]

The output of the SIGMA code is a histogram that shows the variation in clearance across a row of assemblies which is attributable to the uncertainties in dimensions and irradiation growth. The criterion applied to the histogram is that clearance must be demonstrated at the 95% probability level.

4.2.4.2 Effect of Extended Burnup

The effect of extended burnup is to increase the spacer grid growth due to the increase in neutron fluence. This causes the cold clearance between fuel assemblies to decrease at extended burnup.

4.2.4.3 Evaluation of Grid Irradiation Growth

Grid growth on a four-cycle assembly discharged from Calvert Cliffs-1 has been directly measured at the Battelle Columbus Hot Cell Facility. Three grids, representing the regions of highest fluences, were measured, and the measurements were compared to their pre-irradiation values. Figure 4-24 displays a single data point from these measurements which represents the average grid growth at a fluence of 9.0×10^{21} n/cm^2 (E>0.821 MeV). The grid growth data point agrees well with all other growth measurements [ ] The point also reflects about 90% of the target fluence for extended-burnup operation.

The grid growth model described above will be used to ensure that the clearance criterion stated in Section 3.3 will be satisfied for extended burnup designs.

FIGURE 4-24
COMPARISON OF MEASURED GUIDE TUBE AND SPACER GRID GROWTH STRAINS

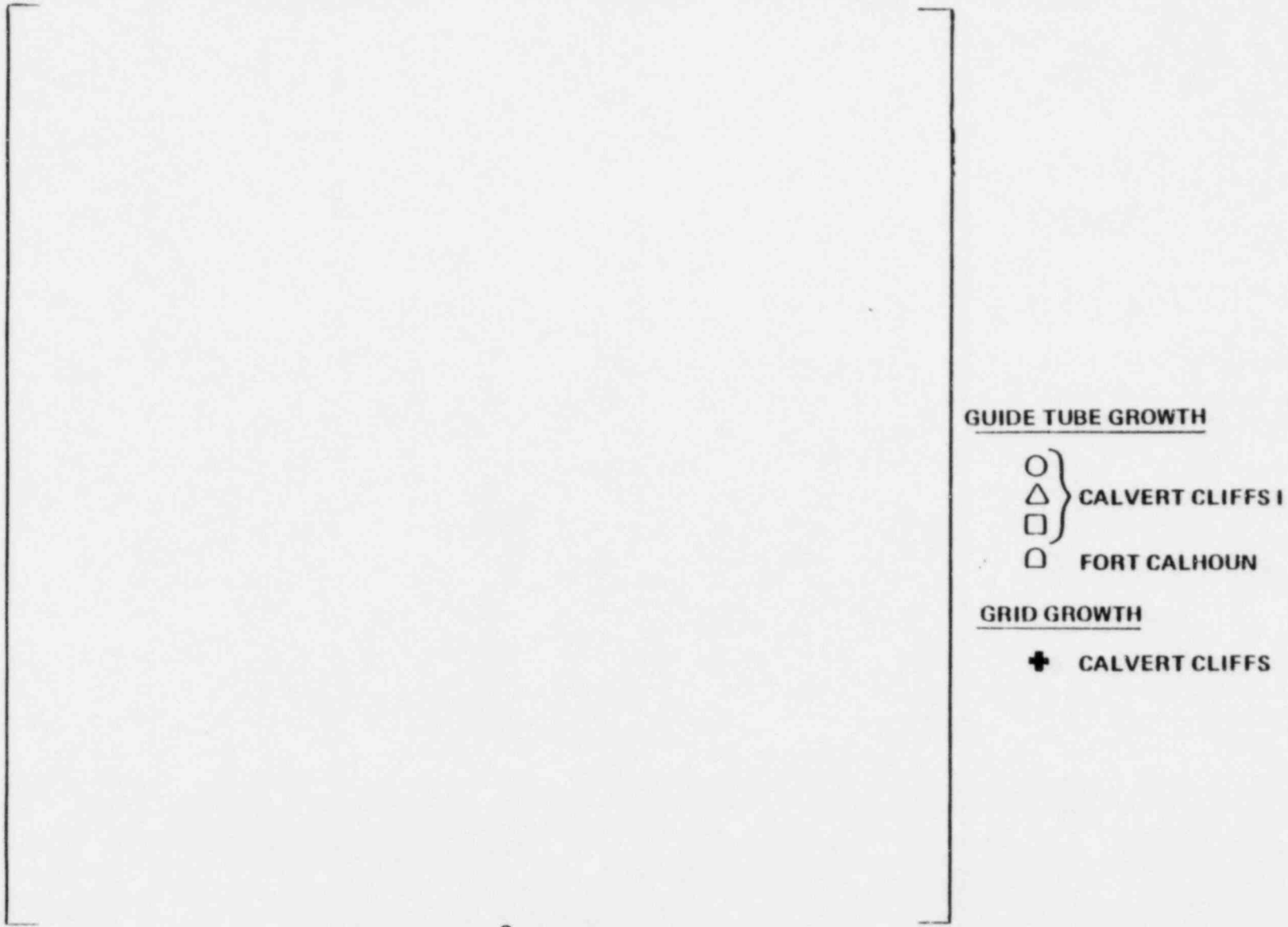

4.2.5 Spacer Grid Relaxation

The spacer grids are necessary to support and locate the fuel and poison rods axially and radially within the fuel assembly. There are two types of spacer grids in each fuel assembly. The lowermost grid is fabricated from Inconel 625 and the remaining grids are fabricated [ ] In both types of grid, each rod is supported between two sets of rigid arches and flexible spring tabs such that there are two orthogonal sets of contact forces on the rods.

The choice of the initial contact force between the grid springs and the rods is constrained by two factors. The force must be small enough to permit installation and replacement (i.e., assembly reconstitution) of rods without damage and to minimize the contribution of axial restraint to rod bowing. However, the BOL contact force decreases with burnup due to relaxation of the Inconel and Zircaloy grid springs, and to a lesser extent due to dimensional changes of the rods and grids. Inadequate contact between the rods and the grid springs can contribute to increased fretting. The initial interference must therefore be large enough to ensure adequate radial restraint to prevent fretting following grid spring relaxation.

4.2.5.1 Modeling of Spacer Grid Relaxation

Relaxation models for the Inconel and Zircaloy grids are taken from Reference 4-92. Relaxation is modeled as a function of stress, temperature, and fluence. The models indicate that the Zircaloy grid springs will relax to a very light contact condition at modest fluence accumulations, while the Inconel grid springs will maintain significant contact forces for high fluence values. Both materials exhibit a decreasing rate of relaxation as fluence increases.

4.2.5.2 Effect of Extended Burnup on Grid Relaxation

Extended burnup will have little or no effect on spacer grid relaxation. The Zircaloy grids will essentially retain their contact geometry since they have relaxed completely, grid growth exhibits saturation (cf. Section 4.2.4), and the fuel rod diameter has stabilized (cf. Section 4.1.3). The effect on the Inconel grid will be small since there is only a small relaxation rate at high fluence values.

4.2.5.3 Evaluation of Spacer Grid Relaxation

The predicted trends of relaxation have been observed directly during fuel assembly reconstitution. A load cell placed between the fuel rods and the lifting device was used to monitor rod withdrawal force at Calvert Cliffs-1 over the course of several cycles. The same fuel assembly (BT03) was reconstituted several times as part of a fuel performance program. The load cell detected a positive "breakaway" force corresponding to rod withdrawal from the Inconel grid. Little or no additional friction force change was observed as the rod passed out of each Zircaloy grid.

The grid interference conditions with the rods were entirely satisfactory at Calvert Cliffs-1 since no fretting was observed on any of the rods. This observation is particularly important because of the high burnup (46 MWd/kg) in the BT03 assembly and the fact that the contact geometry between the fuel rods and spacer grids was affected by the reconstitution procedure (e.g., the new orientation of the slightly oval fuel cladding would either increase or decrease the interference with the grid springs when the rod is replaced in the assembly).

The empirical behavior of the C-E fuel rod support system has also been discussed in Sections 4.1.10 and 4.1.11. Based on the conclusions presented in these sections, it is apparent that the grid contact forces and geometries have been properly selected to minimize both fuel rod bow and fretting. The observation of superior performance of the grids in the extended-burnup demonstration programs confirm the fact that the relaxation of fuel assembly materials is not of concern in extended-burnup operation.

4.2.6 Corrosion of the Fuel Assembly Structure

The C-E fuel assembly structure (cage) includes five Zircaloy-4 guide tubes welded to (eight to eleven) Zircaloy-4 grids (depending on the specific plant) and one bottom Inconel 625 grid attached to an Inconel 625 skirt. The effect of extended-burnup operation on corrosion, i.e., the oxidation and hydriding, of these Zircaloy components while in a pressurized water reactor environment is considered in this section.

4.2.6.1 Modeling of Corrosion of the Fuel Assembly Structure

Based on the known out-of-reactor corrosion data and the recent corrosion data from a 14x14 fuel assembly cage after 4 cycles of exposure in Calvert Cliffs-1, the following model is used to estimate the corrosion of the Zircaloy structure at extended burnup.

The corrosion conditions for the Zircaloy structure are different from those for the Zircaloy fuel cladding. A heat flux exists across the fuel cladding but not across the Zircaloy cage components. Therefore, the corrosion model used for the Zircaloy structure is different from that for the Zircaloy cladding. The corrosion of the Zircaloy structure is represented by a simple isothermal model without the complication of the presence of a thermal heat flux. The oxidation model (4-93) is:

[ ]

The value of the radiation enhancement factor K was estimated from the measured values of oxide thickness from the Calvert Cliffs 14x14 fuel assembly cage components after 4 exposure cycles.

The hydrogen uptake in the metal (Zircaloy) was estimated on the basis of the following model:

$$Zr + 2H_2O \longrightarrow ZrO_2 + 2H_2$$

The amount of hydrogen produced can be estimated based on this reaction. For every eight weight units of weight change due to oxidation, one weight unit of hydrogen is evolved. Since the hydrogen atoms are very mobile (due to small atomic size), most of the evolved hydrogen escapes and only a small fraction gets absorbed by the metal. The hydrogen pickup fraction was estimated to be [ ] from the 14x14 fuel assembly cage hydriding data after 4 cycles of exposure. These values of hydrogen pickup fraction are consistent with the observed pickup fractions (4-5) for several metallographic specimens from fuel rods irradiated in different reactors.

The cage of fuel assembly BT03 was examined at the Battelle Hot Cells after 4 cycles of exposure in Calvert Cliffs 1. The assembly had experienced 1472 effective full power days (EFPD), and the fuel rods had accumulated a burnup of 43 MWd/kg. The assembly was under hot flow conditions for 1900 days. The core average exit coolant temperature was 312.8°C. The cage was subjected to visual examination and destructive metallographic examination to reveal the oxide layer thickness and extent of hydriding [ ] of the spacer grids and guide tubes. The results are presented in Table 4-7 along with the predicted values. [

] gave good agreement between the measured and predicted values shown in Table 4-7. A decrease in the hydrogen pickup fraction with increasing oxide thickness is consistent with the trends observed with fuel rods from other reactors (4-5).

4.2.6.2 Effect of Extended Burnup

The effect of extended burnup on the corrosion of Zircaloy-4 structures in different reactors can be estimated from Equations (1) through (4). At extended burnup, it is expected that corrosion will increase monotonically with

TABLE 4-7

CORROSION OF BTO, ZIRCALOY-4 STRUCTURE AFTER 4 CYCLES

[ ]

time. However, the corrosion rate will decrease nonlinearly with decreasing temperature. Since for most fuel cycles the assembly power decreases with increasing burnup beyond conventional levels, the associated decrease in coolant temperature will result in a concomitant decrease in the corrosion rate.

4.2.6.3 Evaluation of Corrosion of the Fuel Assembly Structure

The available data on corrosion and hydriding of Zircaloy-4 cage components are from the recently completed examination of the BT03 fuel assembly cage. These results are summarized in Table 4-7. Since the fuel assembly BT03 was subjected to typical coolant conditions (chemistry and temperature) of Calvert Cliffs 1 to an assembly average burnup of 43 MWd/kg, the BT03 results are directly applicable to evaluate extended burnup behavior.

The hot cell examination of BT03 after 4 cycles of exposure demonstrated that the cage is in excellent condition, and it was concluded that for coolant conditions typical of Calvert Cliffs 1, the corrosion resistance of Zircaloy structurals is sufficient to achieve an assembly average burnup of at least 52 MWd/kg. [

]

Two important aspects of hydriding of Zircaloy structurals are the hydrogen concentration level and hydride orientation. Hydrides oriented normal to the stress axis are more detrimental to the ductility than those oriented parallel to the stress axis (4-27,4-94). [

]

The amount of hydrogen necessary to cause embrittlement of Zircaloy is a function of deformation temperature. Watkins et al. (4-28) have concluded that for prehydrided irradiated and unirradiated Zircaloy-2 specimens, up to 800 ppm hydrogen reduces ductility at 70°F but has no effect on the ductility at 572 °F. Mehan and Wiesinger (4-95) have shown that up to 500 ppm of hydrogen in unirradiated Zircaloy-2 reduces ductility without affecting the yield strength over the temperature range 77 to 600 °F. The reduction in ductility is more significant at lower temperatures.

Considering the [ ] hydrogen pickup in BT03 after four cycles of exposure, it is concluded that, for coolant conditions typical of Calvert Cliffs-1, hydrogen embrittlement resulting from the presence of hydride platelets in the Zircaloy cage components (at temperatures up to reactor operating temperatures) is not expected during extended-burnup operation. At reactor operating temperatures, the solubility of hydrogen in Zircaloy is significant (~ 100 ppm) [

]

Summarizing, on the basis of BT03 cage hot cell examinations, it is concluded that for the coolant conditions typical of Calvert Cliffs-1, the corrosion on the Zircaloy structure will not limit the operation of C-E fuel assemblies to burnups of 52 MWd/kg and probably beyond. The corrosion and hydriding of the Zircaloy cage in plants with higher operating temperatures are not expected to limit extended-burnup operation.

4.2.7 Burnable Poison Rod Behavior

Burnable poison rods are placed in selected fuel assemblies to reduce the beginning-of-life reactivity of those assemblies and/or the corewide moderator temperature coefficient of reactivity. Because these rods are deployed in fixed lattice positions (replacing fuel rods), they will reside within the assembly until it is discharged. The performance of the burnable poison rods, therefore, is of interest in the context of the extended burnup capability of the C-E fuel assembly.

The fluence and time increments between standard and extended burnups induce physical changes in the poison rod components. Although the small quantity of boron-10 contained within the burnable poison pellets will be virtually 100 percent depleted prior to completion of the residence time associated with standard burnup, the poison rod cladding will continue to elongate and creepdown (if unsupported by the pellets), and the burnable poison pellets will continue to swell. In addition, the rod void volume changes produced by these effects will continue to change the rod internal pressure. Each of the individual performance mechanisms affected by extended burnup is modeled as a function of fluence or time to show compliance with the cladding strain and clearance criteria listed in Section 3.3. These models are combined into a rod internal pressure analysis method to verify acceptable performance under the internal pressure criteria also listed in Section 3.3.

4.2.7.1 Modeling of Burnable Poison Rod Behavior

This section is divided into discussions of the individual performance mechanisms listed above that are important in modeling burnable poison rod behavior. Each model is supported by a data base derived from the postirradiation examination (PIE) programs which have been performed by Combustion Engineering over the past several years.

The reference burnable poison rod designs for extended-burnup operation differ in some regards from the designs represented by the data base. The differences result from design improvements made as a result of operating experience. A design comparison is presented in Table 4-8. Differences in the designs will be addressed in each section below when appropriate.

Al_2O_3-B_4C Pellet Swelling . The swelling of the burnable poison material, induced by irradiation, results in dimensional changes which can affect cladding strain and poison rod void volume. The neutron absorber material employed in the poison rods is in a pelletized form and consists of a hot-pressed dispersion of boron carbide (B_4C) particles in an alumina (Al_2O_3) matrix. The B_4C content is established by core neutronic requirements and has ranged to levels on the order of 3 wt%. The dimensional changes of the pellet are predicted by a model which assumes [

] Thus, one of the parameters in the model is the B_4C content of the pellet.

In relating pellet swelling to irradiation exposure, it is assumed [

] The B_4C swelling rate used is the same as in C-E's model for B_4C swelling in a control element assembly (CEA) as described in Reference 4-3, i.e., a volumetric swelling of 0.3% per percent B-10 burnup. The Al_2O_3 swelling behavior is based on the high fluence data reported by Keilholtz and Moore for high density (>99% TD) pellets (4-96). Because Al_2O_3 swelling is caused by fast neutron irradiation damage, Keilholtz and Moore correlated their observed Al_2O_3 volume increases with fast fluence (E > 1 MeV).

Since the Al_2O_3 swelling is the dominant contributor to pellet swelling at high exposure, the Al_2O_3-B_4C swelling is related to fast fluence in the model. It is recognized, however, that the swelling of B_4C is a function of thermal flux to the extent that it depends upon the B-10 (n, α) Li-7 reaction.

The model assumes that swelling is independent of temperature since poison pellets are not expected to exceed an operating temperature of 500°C in PWR

TABLE 4-8

Burnable Poison Rod Details

Parameter	Early 14x14 Design	Extended Burnup 14x14 Design	Early 16x16 Design	Extended Burnup 16x16 Design
Pellet O.D., in.	0.376-0.379	0.362	0.310	0.307
Pellet Length, in.	[			]
Pellet End Condition				
Pellet Open Porosity, %*				
Pellet Density, % TD				
Cladding O.D., in.	0.440	0.440	0.382	0.382
Cladding I.D., in.	0.388	0.384	0.332	0.332
Prepressure Level, psig	[			]

*Expressed as a percent of the total pellet volume

applications. Further, Keilholtz and Moore found no significant temperature dependency for Al_2O_3 swelling in the range of 300 to 600°C.

In constructing the Al_2O_3-B_4C model, it was found desirable to first establish an Al_2O_3 pellet swelling model. A review of the data reported by Keilholtz and Moore (4-96) indicates that a two-stage swelling rate model is an appropriate representation for Al_2O_3 swelling. Above a fast fluence of approximately 2.6 x 10^{21} n/cm^2, the swelling of Al_2O_3 is enhanced by microcracking and grain boundary separation which causes a sharp increase in the apparent swelling rate. Thus, the swelling of Al_2O_3 is represented as the sum of two components corresponding to swelling below and above the fast fluence level of 2.6 x 10^{21} n/cm^2. Assuming isotropic behavior, the volumetric increase data reported by Keilholtz and Moore were used to develop the following expressions for the diametral swelling of Al_2O_3:

[

]

For the Al_2O_3-B_4C pellet swelling model, a similar [ ] model is used. [

] Again, assuming isotropic behavior, the volumetric swelling rate for B_4C (i.e., 30% at 100% B-10 depletion) was used in conjunction with Equations (1) and (2) for Al_2O_3 to arrive at the following expressions for the diametral swelling of the composite Al_2O_3-B_4C pellet:

[

]

The above relationships for swelling as a function of fluence for Al_2O_3 and Al_2O_3-B_4C (at the 3 wt% and 5 wt% B_4C levels) are plotted in Figure 4-25. Also plotted are diametral swelling data which were obtained in C-E sponsored post-irradiation examination (PIE) programs to verify the performance of the Al_2O_3 and Al_2O_3-B_4C pellets. These data consist of direct diameter measurements on 42 whole Al_2O_3-B_4C pellets and 16 whole Al_2O_3 pellets which were removed from poison rods discharged after 1 cycle of exposure. In addition, indirect diametral swelling data were obtained, after higher exposure, by profilometry measurements on unpressurized burnable poison rods discharged after 2, 3 and 4 cycles of reactor irradiation. The pellet diametral swelling in these rods was inferred by conservatively assuming that the Zircaloy-4 cladding had crept down to contact the pellets. This approach had the advantage of directly determining the mechanical performance characteristics of interest at high fluence: (1) the cladding strain as affected by pellet swelling and (2) by inference, the restrained swelling behavior of the Al_2O_3-B_4C pellets. It was found that even after 4 cycles of reactor operation, the average cladding strain was still negative, exhibiting only a slight tendency to be less negative than the 1-cycle value. Moreover, after 4 cycles, the cladding had completely crept down to contact the pellets and conformed to the pellet shapes. The inferred Al_2O_3-B_4C pellet swelling in these rods, shown in Figure 4-25, was calculated from the irradiated diameter profiles, the as-fabricated cladding wall thickness, and the as-fabricated pellet diameter.

FIGURE 4-25
SWELLING OF $Al_2O_3 \cdot B_4C$

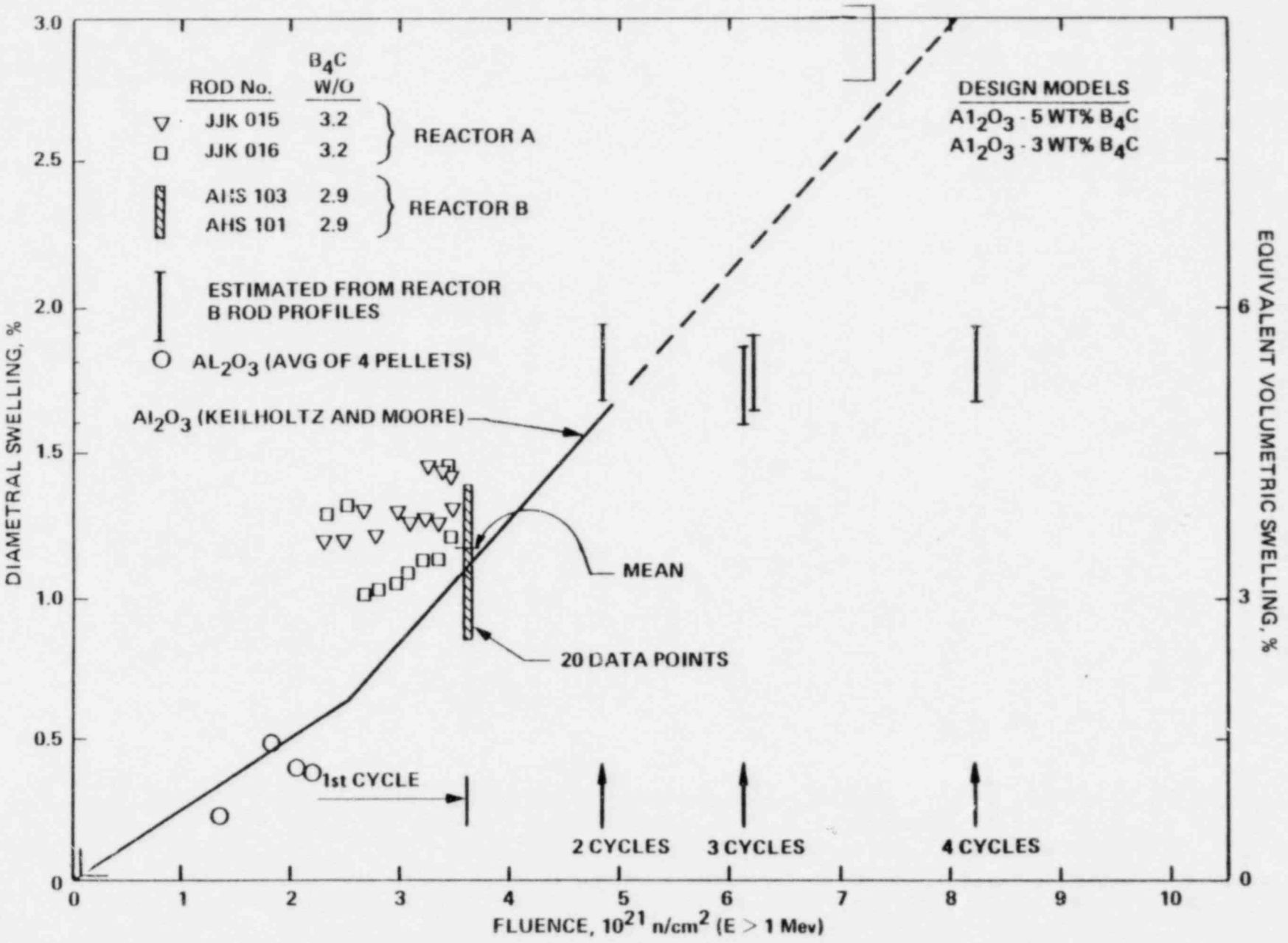

It should be noted that, because of the different measurement techniques, the 1-cycle pellet data represent an unrestrained condition, while the higher exposure data derived from rod profiles represent a restrained condition. It is also noteworthy that the results of the post-irradiation examination of the 1-cycle exposed Al_2O_3-B_4C pellets substantiated the assumption of isotropic swelling behavior (i.e., equal axial and diametral swelling rates). It was further found that swelling was independent of initial pellet density in the density range of 85 to 98% TD.

A comparison of the performance data with the model in Figure 4-25 indicates the following:

- The model reasonably predicts the diametral swelling of Al_2O_3-B_4C pellets, as well as that of Al_2O_3 pellets that occurred during the first cycle of irradiation up to a fluence of about 3.5×10^{21} n/cm^2 (E >1 MeV). The data scatter indicates that several 1-cycle Al_2O_3-B_4C pellets apparently swelled more than predicted by the model.

- The diametral swelling of the pellets contained in burnable poison rods exposed to additional irradiation up to 4 cycles, equivalent to 8.2×10^{21} n/cm^2 (E> 1 MeV), is substantially overpredicted by the model.

The reason for the apparent differences between the observed behavior and the model prediction is believed to be related to the following overall swelling behavior mechanism:

(a) B_4C particle swelling caused by the B-10 (n, α) Li-7 reaction induces microcracking and grain boundary separation in the pellet structure.

(b) The resulting early apparent swelling (while the B-10 is depleting) could be enhanced by this void contribution when the pellet is not restrained. (This may account for any underprediction of 1-cycle swelling.)

(c) At higher fluence (i.e., after 100% B-10 depletion) at least some of these new voids, as well as the original voids within the pellet structure, are accommodating the Al_2O_3 matrix swelling, especially under cladding

restraint. As a result of such internal swelling accommodation, the pellet diameter changes under the restrained higher exposure conditions are overpredicted by the model.

Gas Release. In addition to the initial helium fill gas introduced during the fabrication of the burnable poison rod, helium generated by the B-10 (n, α) Li-7 reaction also contributes to internal rod pressure. The gas released from the Al_2O_3-B_4C pellets during irradiation exposure consists of a small fraction of this generated helium. The gas release model is empirically-based and establishes an upper bound value for the total fractional helium release expected during the life of the burnable poison rod.

The gas release model assumes that the helium is released early in the exposure, i.e., while the (n, α) reaction is proceeding and the pellets are operating at their highest temperature because of the energy deposited by this reaction. At higher exposures, after the B-10 has been depleted and the operating temperature is reduced, no additional helium is released. These assumptions recognize the role of the two mechanisms responsible for helium release from the B_4C particles dispersed in the Al_2O_3 matrix: recoil and diffusion. The recoil process is a consequence of the high energy (2.8 MeV) produced by the (n, α) reaction. It results in the high velocity ejection of helium ions (α-particles) from the B-10 nuclei, such that some of the helium ions are driven out of the B_4C particles. Recoil can only contribute directly while the B-10 is depleting, whereas diffusion through the B_4C and Al_2O_3 is temperature dependent and would be favored by the higher temperatures early in life.

Data which support these assumptions and which are used as a basis for a design gas release model were obtained from C-E sponsored PIE programs. The results of fractional helium release measurements on standard poison rods from 14x14 fuel assemblies exposed up to 4 cycles are shown in Table 4-9. The release data for the series of unpressurized rods from Reactor B, irradiated for 1, 2, 3 and 4 cycles confirm that no significant additional release occurred after the first cycle. The data on the 1-cycle pressurized rods from Reactor A confirm that helium prepressurization does not significantly affect the fractional release. The somewhat lower release levels for both the unpressurized and pressurized rods in Reactor A may be indicative of a

TABLE 4-9

Summary of Burnable Poison Rod Helium Release Data From C-E Sponsored Examinations

Rod No.	Pressurized	% B_4C	Plant	No. of Cycles Exposed	% B-10 Depletion	Fractional Helium Release, %
QAF-199	No	2.9	Reactor B	1	99.2	2.3
QAF-173	No	2.9	Reactor B	2	100	[
QAF-172	No	2.9	Reactor B	3	100	
QAF-149	No	2.9	Reactor B	4	100	]
UAC-039	No	2.9	Reactor A	1	63.5	1.3
JJD-044	Yes	3.2	Reactor A	1	99.8	0.9
JJK-011	Yes	3.2	Reactor A	1	99.9	1.2

generally lower operating temperature history than experienced in Reactor B. More importantly, a helium release fraction of [ ] bounds all of the data for the particular design represented in Table 4-9. This design is associated with a calculated maximum (BOL) operating temperature of 640°F, while higher peak BOL temperatures are calculated for the designs to be used for extended burnup. To establish an upper bound limit for helium release in these newer designs, a temperature dependency relationship based on helium release data for B_4C reported by Russcher and Pitner (4-97) and Homan (4-98) was applied to the [ ] value.

The newer designs may utilize somewhat higher B_4C loadings than represented by the data base of Table 4-9. The principal effect, however, is to increase the heat generation rate which is accounted for by invoking the temperature dependency. Other differences, such as the higher pellet density and lower open porosity of the new designs (cf. Table 4-8), would tend to reduce the actual release fractions.

Poison Rod Axial Growth . For the reference burnable poison rod designs which will undergo extended-burnup operation, axial growth will not exceed that of the fuel rods. (The fuel rod growth model was described in Section 4.1.14.)

The original 14x14 poison rod design (cf. Table 4-8) had a substantial growth component due to mechanical interaction between the poison pellets and the cladding. However, the reference designs for extended burnup include higher helium fill pressure, thicker cladding, greater diametral gap, and pellet geometry improvements, all intended to minimize the degree of interaction.

The effect of the pellet geometry improvements after one cycle of operation is depicted in Figure 4-26 where shoulder gap change data from a recent PIE program on 16x16 fuel are plotted. For comparison purposes, shoulder gap change data from the original 14x14 poison rod designs would have been significantly larger than that for fuel rods. The 16x16 poison rod data represent the burnable poison rod design labeled "Early 16x16" in Table 4-8. As is evident by comparing this rod design to that labeled "Extended Burnup 16x16", the designs are essentially the same from a mechanical interaction viewpoint.

FIGURE 4-26

SHOULDER GAP CLOSURE HISTOGRAMS FOR
16 x 16 FUEL RODS AND POISON RODS

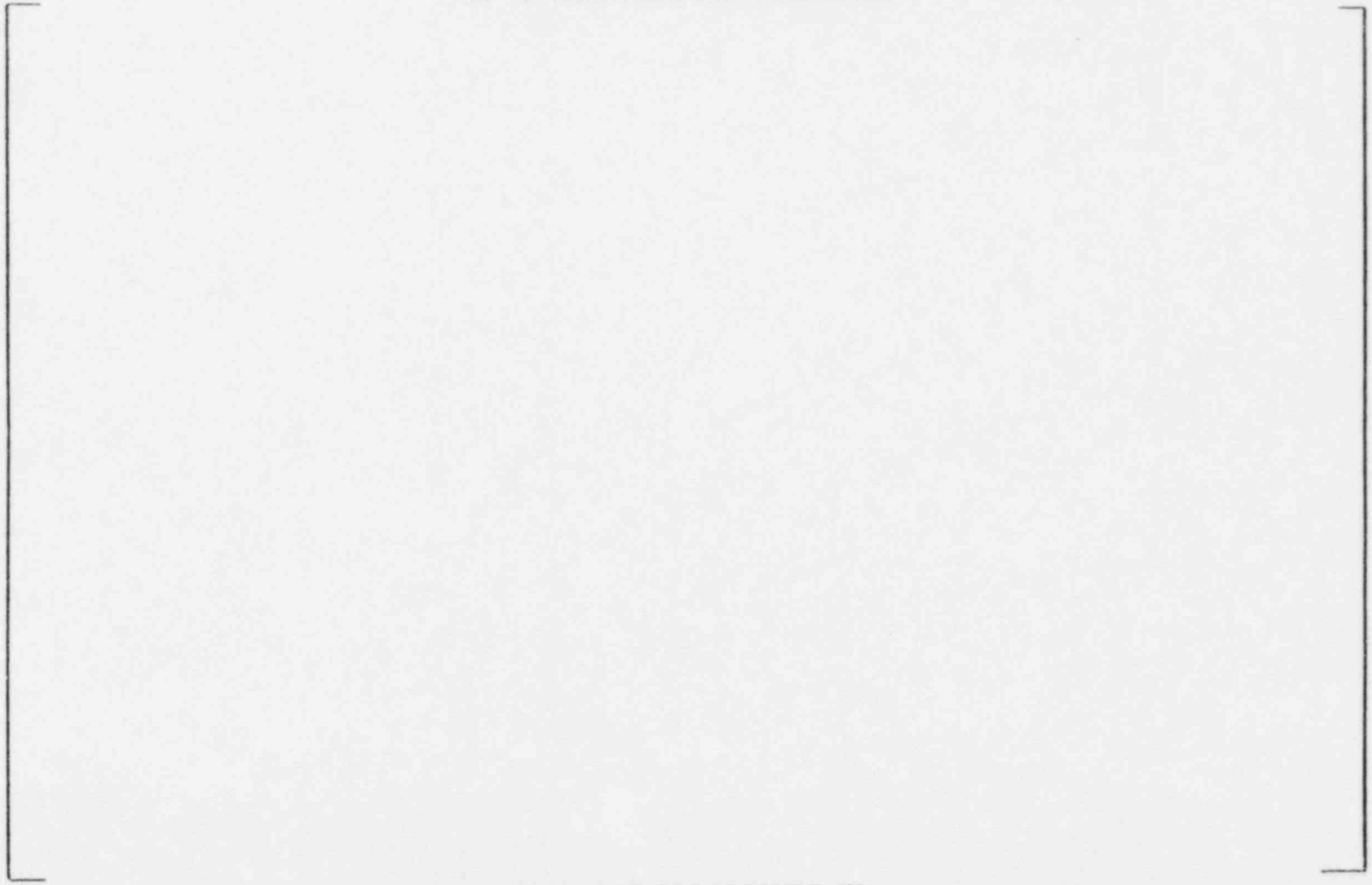

The diametral gap between the poison pellets and the cladding in both 16x16 designs has been sized such that no significant interaction is predicted as the poison pellets swell and the cladding creeps down. Therefore, the growth behavior of the 16x16 poison rods will continue to be comparable to or less than that of the fuel rods. The same considerations were made in the design of the 14x14 poison rod design for extended burnup.

Since the poison rods will grow at the same rate as the fuel rods, the SIGREEP analysis method described in Section 4.2.2 is used to ensure that sufficient clearance exists between the poison rods and the upper end fitting.

Poison Rod Cladding Creep. Poison rod cladding is produced under the same specifications as those used for fuel rod cladding. The creep model described for the fuel rod (Section 4.1.3) is also used for the case of the poison rod cladding.

Poison Rod Internal Pressure. The BOL internal pressure at operating conditions is predicted by a straightforward analysis involving the calculation of the poison rod void volume and gas temperature at operating conditions. Each of the models discussed above represents a time-dependent or fluence-dependent mechanism which will produce changes in the poison rod internal pressure through changes in the void volume.

Calculation of the EOL internal pressure is predicted for appropriate EOL conditions which include the number of moles of helium (prepressure plus gas released from the pellets), gas temperature (the 100% depleted poison pellets produce only a small amount of heat flux due to gamma heating), and the void volume (reflecting changes due to different temperatures, pellet swelling, poison rod growth, and cladding creepdown). The combined accuracy of the models describing the fluence-dependent and time-dependent aspects of poison rod behavior is demonstrated by Figure 4-27. The figure shows that the predicted rate of volume decrease is larger than that of the actual measured rods, prior to full diametral contact between the pellets and cladding. This results in a conservative prediction of rod internal pressure during this period of operation. For the extended burnup poison rod designs, full diametral contact is not predicted.

FIGURE 4-27

EFFECTIVE VOID VOLUME VERSUS FLUENCE

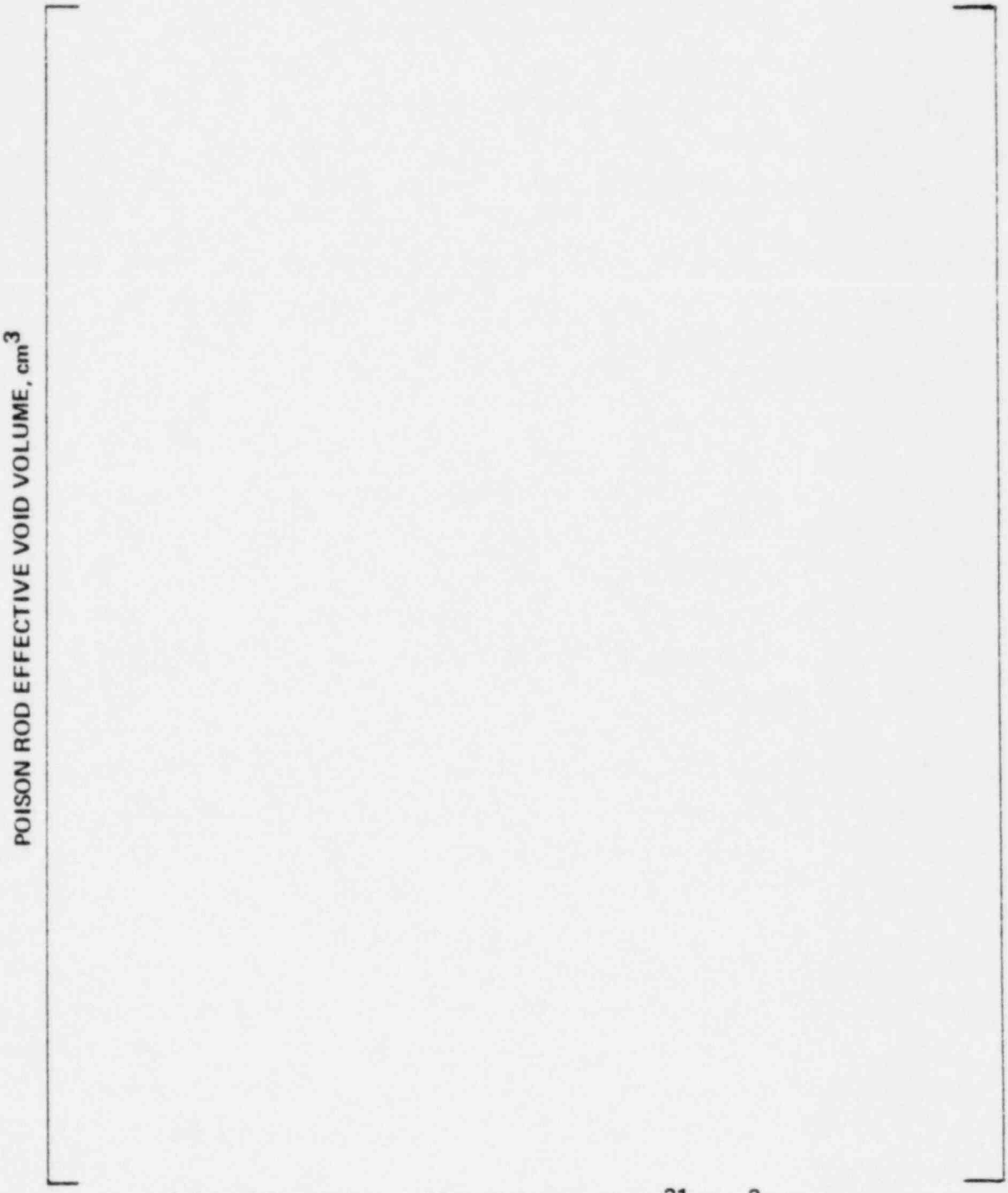

Also, for the extended-burnup reference designs, pellet open porosity at BOL is nonexistent (Table 4-8). The contribution to EOL void volume from the pellet porosity exposed through pellet microcracking behavior is ignored for conservatism. The poison pellet material should tend to develop microcracks with increasing exposure, which would make available a substantial amount of additional void volume to accommodate gas release from the pellets.

4.2.7.2 Effect of Extended Burnup on Burnable Poison Rod Behavior

Al_2O_3-B_4C Pellet Swelling . The swelling of Al_2O_3-B_4C pellets is strongly fluence dependent; therefore, the mechanical behavior of the burnable poison rod is affected by extended burnup. While the cladding may not be strained because of the large diametral gap in the new designs and the internal swelling accommodation characteristics of the pellets, the rod void volume will be decreased by the diametral and axial swelling of the pellets. The present Al_2O_3-B_4C swelling model appears to predict swelling conservatively so that it can be used reliably to ensure that poison rods will not exceed internal pressure limits in extended-burnup applications.

Gas Release . As discussed in the preceding section, helium is generated and released primarily in the first cycle of irradiation, when the poison rod is operating at its highest temperature. Extended burnup, therefore, will not result in significant additional helium release. This behavior has already been verified by gas release measurements on burnable poison rods exposed for up to 4 cycles.

Axial Growth and Diametral Creep . Extended-burnup operation will result in additional elongation of the burnable poison rods. Since the growth is proceeding at the same rate as that in fuel rods, the same amount of clearance with the upper end fitting is required for the two types of rods at BOL in order to support the target exposure levels.

The increment of diametral cladding creep associated with extended-burnup operation should be extremely small due to the low cladding temperatures and low differential pressure across the cladding during this period of time. Full diametral contact between the pellets and cladding is not predicted so there will be no outward creep of the cladding.

Rod Internal Pressure . Internal pressure will increase during extended-burnup operation due to a reduced void volume within the rod caused principally by pellet swelling. Rod growth and creepdown will be second order effects on the void volume compared to pellet swelling, but will be accounted for. No additional gas release from the pellets is predicted.

4.2.7.3 Evaluation of Burnable Poison Rod Behavior

Well defined models exist for all fluence-dependent and time-dependent aspects of burnable poison rod behavior. When used in combination with the design improvements in the extended-burnup poison rod designs, they will demonstrate that there is margin to the strain, clearance, and internal pressure criteria for the poison rods.

Section 5

CONCLUSIONS

5.1 OVERALL CONCLUSIONS

The objective of this report is to provide a basis for the generic licensing approval of C-E's fuel performance models to support the operation of standard 14x14 and 16x16 fuel assembly designs to batch-averaged discharge burnups of 45 MWd/kg (maximum rod-averaged burnups of 52 MWd/kg). To accomplish this objective, fuel performance topics affected by increased burnup or residence time have been reviewed and the models (or submodels) used by C-E to address these topics have been described with emphasis placed on showing how burnup is included. The data base that supports these models has been presented to demonstrate the adequacy of the models to the target burnup values.

The major conclusions from this examination of fuel performance topics and their modeling can be summarized by the following points:

- Present licensing guidelines and/or requirements are adequate for extended-burnup applications.

This conclusion is based, in part, on the work performed in preparing this report and, in part, on previous work to assess the licensability of extended-burnup fuel (5-1). This same conclusion has apparently been reached by the NRC after reflecting on the information presented during the generic extended-burnup meetings (5-2). Therefore, reload analyses for extended-burnup cycles can be accomplished within the current licensing framework.

- There are no discontinuous effects or abrupt limitations which are a function of burnup up to the target exposures addressed in this report, and C-E modeling of fuel performance parameters reflects this behavior.

This conclusion is supported by the extended-burnup experience achieved to date which is summarized in Section 1.3 and discussed in greater detail under the individual fuel performance topics in Section 4. The extended-burnup research, development and demonstration programs currently in place will supply further verification of this conclusion for C-E fuel designs to increasingly higher exposure levels during the next few years.

- A considerable amount of fuel performance data already exists to extended-burnup levels for normal operation in commercial power reactors and more data will be available over the next several years as ongoing fuel demonstration programs are completed.

C-E is currently participating in six separate extended-burnup fuel demonstration programs in commercial power reactors. These programs are primarily directed at obtaining data in the areas of dimensional stability, Zircaloy corrosion, fission gas release, and pellet/cladding interaction.

- Although fuel performance data for conditions of power ramping at extended burnups is more limited than the data from normal operation at the present time, there are several ramp test programs already in place that will provide such data during the next few years. Data presently available (covering a burnup range to 45 MWd/kg) indicates essentially no change in ramp performance at extended burnups.

C-E is obtaining data on fuel performance during power ramping from six distinct research and development (R&D) programs being conducted in various test reactors. The data being obtained in these R&D programs are primarily in the areas of fission gas release, pellet/cladding interaction, and fuel and cladding microstructural characteristics.

- All currently used fuel performance models that exhibit a significant dependence on burnup, neutron fluence, or residence time are explicitly modeled as such and appropriately reflect the effect of burnup.

This conclusion is supported by the discussions presented for each fuel performance topic in Section 4 of this report and by appropriate comparisons between model predictions and observed data summarized therein.

- C-E incorporates burnup-dependent effects in each reload analysis; therefore, acceptable results from safety and licensing analyses will demonstrate acceptable performance at extended burnups.

Thus, no additional licensing effort beyond a straightforward extension of that already being accomplished for standard burnups is needed for extended-burnup reload cycles for batch-averaged discharge burnups of up to 45 MWd/kg (maximum rod-averaged burnups of 52 MWd/kg).

5.2 CONCLUSIONS ON INDIVIDUAL FUEL PERFORMANCE TOPICS

In the previous section, the overall conclusions of the topical report were presented. In this section, the conclusions for each individual fuel performance topic are given. To a large extent, they represent a collection of the significant points from the evaluation subsection for each topic.

5.2.1 Fatigue

The fatigue analysis method used at C-E results in a series of cladding strain range values covering the fuel lifetime. The cumulative fatigue damage fraction is determined by summing the ratios of the number of cycles in a given strain range to the permitted number at that range. This method of calculating fatigue damge will remain applicable for extended-burnup operation since the individual components of the method (e.g., cladding creep, fuel swelling) are

modeled adequately as discussed in Section 4 of this report. While longer residence times with the assumption of continued daily power cycling would tend to increase calculated fatigue damage, the increased damage is typically offset in the analysis by the use of actual plant operating history for previous exposure. Realistically, extended burnup will result in only a few additional power cycles on the fuel.

5.2.2 Cladding Corrosion

Cladding corrosion is primarily dependent on the temperature at the metal/oxide interface, which in turn depends on the oxide thickness, as well as the heat flux and the thermal conductivity of the oxide layer. As the oxide layer thickness increases for a constant power level, the temperature at the metal/oxide interface increases, driving up the corrosion rate. This, in turn, can increase the oxide layer thickness further. Thus, at higher burnups and longer residence times when oxide layers are thicker, the corrosion rate may increase unless the decrease in power that accompanies increasing burnup is sufficient to offset this effect. For current operating C-E reactors, corrosion does not appear to be a limit in achieving burnups of up to 55 MWd/kg. This conclusion is based on experimental data representative of current C-E plants. C-E has several irradiation test programs which will provide experimental confirmation of the extended-burnup performance of its fuel. These programs will monitor corrosion and allow the model predictions to be verified to burnups in excess of 55 MWd/kg for both 14x14 and 16x16 fuel assembly designs.

5.2.3 Cladding Creep

The fuel rod dimensional behavior is complex after contact occurs between the fuel pellet and the cladding, which is anticipated early in life at relatively low burnups between 10 and 20 MWd/kg. Since the cladding creep behavior mechanisms for extended burnup operation are expected to be the same as those for normal burnup operation, and since the cladding diameter is not expected to change significantly during extended-burnup operation to a burnup of about 50 MWd/kg, the cladding creep model is judged to be applicable to the range of burnups covered by this topical.

5.2.4 Cladding Collapse

Cladding collapse is a creep-related phenomenon. The longer residence times associated with extended-burnup fuel will increase the amount of creep of unsupported cladding. The increased creep strain will be accounted for in the analysis of the ability of the fuel rod design to resist cladding collapse. The criterion for collapse will be that the most limiting rod in the core will have at least a 95% probability that its predicted time to collapse exceeds the reactor operating time during its residence. The SIGPAN model, which is currently under review by the NRC, will be used to demonstrate that this criterion has been satisfied.

5.2.5 Embrittlement of Fuel Cladding

For design purposes, it is conservatively assumed that the elevated temperature yield strength is unaffected by irradiation. Since the elevated temperature yield strength of cladding material actually increases with fluence and is unaffected by hydrogen level, the margin over the unirradiated yield strength increases with extended burnup. The material ductility at operating temperatures is slightly reduced initially by irradiation but then remains relatively constant. Increasing the burnup to levels beyond the first irradiation cycle does not affect the ductility. The ductility at operating temperatures does not appear to be infuenced by hydrogen concentrations of up to 800 ppm; these levels should not be reached even for extended burnups. Thus, it is concluded that extended burnup will have no detrimental effect upon cladding yield strength or ductility.

5.2.6 Fission Gas Release

Modern design fuel rods from operating PWRs have been found to contain consistently very low levels of released fission gases to burnup levels of 46 MWd/kg. The relative absence of any enhancement due to burnup is now verified by direct measurement. Current design fuel rods which have been irradiated in a PWR and subsequently ramped to high linear heat ratings (up to 16 kW/ft) show

higher releases of fission gas. The amount of fission gas released is strongly dependent on linear heat rating (temperature) and the grain size of the UO_2 pellets. The apparent enhancement of fission gas release due to burnup up to about 25 MWd/kg reverses at higher burnups. The data show a mitigation of burnup enhancement which is probably due to an improved gap conductance resulting from better fuel-clad contact at higher burnups. Data available to C-E and reported to the NRC support the fission gas release model incorporated into the FATES3 code to the target burnup levels.

5.2.7 Fuel Thermal Conductivity

The only phenomena which are known to significantly affect fuel thermal conductivity are those which change the density of the fuel (i.e., in-reactor densification and gaseous fission product swelling). In the C-E model, the effects of these phenomena are taken into account through a porosity correction factor. Data on C-E fuel show that for normal operating conditions of PWRs, fuel swelling remains linear up to burnups of at least 50 MWd/kg. Therefore, no abrupt change in thermal conductivity is expected by increasing the discharge burnup of fuels beyond the current levels. The effects of the phenomena which change the density of the fuel are modeled in the current FATES3 fuel evaluation code.

5.2.8 Fuel Melting Temperature

Despite non-conclusive evidence of the presence of any effect of burnup on the melting point of UO_2, the fuel melting temperature is reduced with burnup in the C-E model as a conservative approach. The rate of decrease used in the model is $58^{\circ}F$ per 10 MWd/kg, which is the maximum rate of decrease measured. This conservative approach is not expected to adversely affect extended-burnup operation because: (1) the peak linear heat rating of the fuel is expected to decrease with burnup and (2) the fuel centerline temperature attained at a specific linear heat rating is expected to decrease with increasing burnup beyond the onset of pellet-clad contact.

5.2.9 Fuel Swelling

Data evaluations have established that, under normal operation of PWRs, the swelling mechanisms which are operating in UO_2 fuel at burnup levels to 50 MWd/kg are gradual. There is evidence that swelling is accommodated by the open pores of UO_2 microstructure. No abrupt swelling phenomena have been observed which would limit the life of UO_2 fuel rods with Zircaloy cladding to extended burnups. Performance of fuel rods subjected to power ramping after two and three cycles of irradiation also suggest that the fuel swelling is not likely to be a life-limiting factor for a current-design PWR fuel rod at extended burnup. Data from higher burnup fuel rods subjected to power ramping will continue; these data are expected to provide added confirmation that fuel swelling is adequately modeled by FATES3 to extended burnups.

5.2.10 Fuel Rod Bow

Data evaluations have indicated that the channel closure resulting from fuel rod bow is dependent on the square root of burnup. Thus, the rate of increase of channel closure with burnup will lessen as burnup increases. This rod bow closure model has yielded conservative predictions of channel closure when compared with measurements of 14x14 fuel assemblies at burnups up to 45.3 MWd/kg. Data after one cycle of irradiation for 16x16 fuel indicates that the C-E generic channel closure model is conservative for this fuel design. Since the radial power peak is generally not limiting in fuel assemblies with extended burnup, the penalty factors applied to account for rod bow in extended burnup fuel will have little impact on core thermal margin calculations.

5.2.11 Fretting Wear

Extended burnup beyond current levels is not expected to adversely affect the occurrence of fretting wear. This conclusion is based on three considerations: (1) the results of extensive inspections of fuel rods and assemblies with burnups up to 40 MWd/kg have confirmed the absence of any significant wear regardless of burnup, (2) the degree of stress relaxation and fuel-rod creepdown changes very little after one operating cycle, and (3) the results of out-of-pile testing programs show that significant fretting wear would occur very rapidly early in life if it were to occur at all.

5.2.12 Pellet/Cladding Interaction

Design features of C-E fuel rods have been selected to minimize the propensity for PCI throughout life; some provide PCI advantages to very high burnups (e.g., large fuel pellet dishes). The data available for burnups less than 20 MWd/kg show a burnup dependence, but this is due to gap closure mechanisms. Based on the data for burnups greater than 20 MWd/kg, there is no apparent PCI dependence on burnup for C-E fuel designs. Furthermore, the PCI performance of C-E fuel at 45 MWd/kg is as good as the performance at 20 MWd/kg. In addition, as burnup increases, the capability of the fuel to reach the power levels needed for PCI failure is diminished. This fact, in conjunction with the insensitivity of PCI to burnup, suggests that the overall probability of PCI failures may, in fact, decrease with increasing burnup.

5.2.13 Cladding Deformation and Rupture

The important burnup considerations for cladding deformation and rupture are: (1) fission gas release, (2) fuel swelling, (3) fuel power generation, (4) cladding oxidation, and (5) irradiation growth. Based on the data available, it is concluded that burnup considerations are adequately modeled for extended-burnup analyses of cladding deformation and rupture. Additionally, there is nothing in the data base which would indicate any need to restrict the burnup levels to which the currently available models can be applied. The C-E ECCS evaluation model which includes the NUREG-0630 models for cladding deformation and rupture satisfies the 10CFR50 Appendix K requirement that the degree of swelling may not be underestimated in LOCA analysis.

5.2.14 Fuel Rod Growth

Measurements of rod length obtained to average burnups of up to 46 MWd/kg have shown continuous and well-behaved growth with increasing exposure. These data have confirmed no acceleration in the rate of growth or other abrupt changes occurring up to the exposure levels at which rods have been examined. C-E has examined hundreds of fuel assemblies in which the existing fuel rod growth correlation was used in the design process to establish the desired shoulder-gap clearance. No instances of interference between the fuel rods and the flow

plate have ever been observed. In fact, the conservatism of the C-E design methodology has resulted in sufficient margin to allow the irradiation of lead assemblies to burnups in excess of 50 MWd/kg. This experience verifies the adequacy of the C-E rod growth model to extended burnups.

5.2.15 Guide Tube Wear

Guide tube wear is believed to proceed[ ] The actual rate of wear is a function of both the materials involved and the magnitude of the control rod motion (i.e., vibrations). The effect of extended-burnup operation of the fuel will be to increase the residence time for fuel assemblies in control rod locations, thereby increasing the wear volume produced on either wear sleeves or on unsleeved guide tubes. C-E has taken two approaches to solving guide tube wear: (1) the use of wear sleeves and (2) the use of modified guide tubes. The conclusion that can be drawn from the use of wear sleeves is that only an insignifiant amount of wear now occurs. Extrapolating this performance to longer residence times, it is expected that the performance of the wear sleeves will continue to be satisfactory for extended-burnup fuel. The use of modified guide tubes results in a dramatic reduction in the degree of guide tube wear compared to that with the original guide tube design. Based on the expected results from ongoing fuel demonstration programs and on extrapolation of flow test results, the guide tube wear volumes associated with extended-burnup operation should easily be accommodated.

5.2.16 Fuel Assembly Length Change

Since Zircaloy growth is fluence dependent and compressive creep is time and flux dependent, assembly length change and shoulder gap are affected by extended burnup. In general, higher burnups are expected to result in greater increases in assembly length and larger changes in shoulder gap. The SIGREEP code is used to predict these two design parameters. The upper and lower 95% probability limits on the SIGREEP predictions were found to be conservative for design purposes to the highest burnup data (46 MWd/kg assembly average burnup) for 14x14 fuel assemblies. It is therefore concluded that the SIGREEP methodology is acceptable for use in predicting the irradiation induced dimensional changes to extended burnups for the current 14x14 fuel assembly

design. Shoulder gap and assembly length change measurements have been obtained after one cycle for the 16x16 fuel assembly design. SIGREEP predictions have been made based on actual operating conditions and comparisons made to the measured data. These comparisons show that the upper and lower 95% probability predictions envelop the data. Since the length change mechanisms are the same for both fuel assembly designs, it is concluded that the SIGREEP model is also appropriate for the 16x16 fuel assembly design to extended burnups.

5.2.17 Fuel Assembly Holddown

As discussed previously, fuel assembly length is expected to increase with extended burnup for all of the C-E designs; this produces an increase in the holddown spring compression. At the same time, extended-burnup produces greater fluence and therefore more stress relaxation of the holddown springs, which causes a reduction in the spring compression. The net change in spring compression is evaluated by performing a time history analysis using the SIGREEP code. Providing the proper holddown force at BOL is a relatively straightforward design procedure. During the fuel lifetime, ensuring the proper holddown spring force depends on the ability to model the time dependent and irradiation dependent phenomena taking place in the assembly components. The SIGREEP method has been shown to accurately model holddown force changes for all C-E fuel assembly designs that will be used for extended-burnup applications.

5.2.18 Grid Irradiation Growth

An increase in the neutron fluence will cause the fuel assembly spacer grids to grow. This results in a decrease in the cold clearance between fuel assemblies at increasing burnup levels. Spacer grid growth measurements from four-cycle fuel shows good agreement with all other growth measurements on recrystallization annealed Zircaloy. Thus the grid growth model, as embodied in the SIGMA code, adequately predicts spacer grid growth. This model will be used to ensure that the criterion on clearance between fuel assemblies will be satisfied for extended-burnup applications.

5.2.19 Spacer Grid Relaxation

Extended-burnup will have little or no effect on spacer grid relaxation. The Zircaloy grids will essentially retain their contact geometry since they have relaxed completely at relatively modest fluence values, since grid growth exhibits saturation, and since the fuel rod diameter has stabilized. This conclusion is supported directly by data obtained during reconstitution of a fuel assembly with a burnup of 46 MWd/kg.

5.2.20 Corrosion of the Fuel Assembly Structure

The model used to estimate the corrosion of the Zircaloy structure at extended burnups was developed based on out-of-reactor corrosion data and the recent in-reactor corrosion data of a fuel assembly cage after four cycles of irradiation. The effect of extended burnup is to increase the corrosion monotonically with time. However, corrosion rate will decrease nonlinearly with decreasing temperature. Since the assembly power typically decreases with increasing burnup beyond conventional levels, the associated decrease in coolant temperature will result in a concomitant decrease in the corrosion rate. Based on the data available from operating C-E plants, it is concluded that the corrosion on the Zircaloy structure will not be limiting for operation of C-E fuel assemblies to burnups of 52 MWd/kg and probably beyond. The corrosion and hydriding of the Zircaloy cage in plants not yet in operation but which have higher coolant temperatures are not expected to limit extended-burnup operation.

5.2.21 Burnable Poison Rod Behavior

Well-defined models exist for all fluence-dependent and time-dependent aspects of burnable poison rod behavior. When used in combination with the design improvements in the extended-burnup poison rod designs, they will demonstrate that there is margin to the strain, clearance, and internal pressure criteria for the poison rods.

Section 6

REFERENCES

Section 1 References

1-1 "Historical Survey of Nuclear Fuel Utilization in U.S. LWR Power Plants," SSA-122 and DOE/ER/1020-T1, Southern Science Applications, Inc., August 1979.

1-2 R. A. Matzie et al., "Uranium Resource Utilization Improvements in the Once-Through PWR Fuel Cycle," CEND-380, Combustion Engineering, Inc., April 1980.

1-3 Memorandum for W. V. Johnston (Core Performance Branch, Division of Systems Integration, USNRC) from M. Tokar (Core Performance Branch, DSI, USNRC), "Extended Burnup Fuel - Generic Kickoff Meeting," February 18, 1981.

1-4 Letter from L. S. Rubenstein (Core and Containment Systems, Division of Systems Integration, USNRC) to A. E. Scherer (Combustion Engineering) dated June 2, 1981.

1-5 Letter, A. E. Lundvall, Jr. (BG&E) to R. W. Reid (USNRC), "BG&E Application for Cycle 4 Reload," dated February 23, 1979.

1-6 Letter, A. E. Lundvall, Jr. (BG&E) to R. A. Clark (USNRC), "Calvert Cliffs Nuclear Power Plant Unit No. 1, Docket No. 50-317 Amendment to Operating License DPR-53, Fifth Cycle License Application," dated September 22, 1980.

1-7 D. Franklin et al., "LWR Core Material Performance Program: Progress in 1979-1980," EPRI NP-1770-SR, Electric Power Research Institute, March 1981.

1-8 Letter from L. C. Corsetti (C-E) to D. C. Franklin (EPRI), EPRI/C-E Contract RP586-1: Transmittal of a Letter Report on the Hot Cell Examination of the BT03 Fuel Assembly Cage and Request for Limited Publication of the Results," TDF-82-009, dated January 5, 1982.

1-9 E. J. Ruzauskas et al., "C-E/EPRI Fuel Performance Evaluation Program, RP 581-1 Task A: Examination of Calvert Cliffs-1 Test Fuel Assembly After Cycle 4," CENPSD-146, Combustion Engineering, Inc., October 1981.

1-10 S. R. Pati and N. Fuhrman, "Densification, Swelling and Microstructures of LWR Fuels Through Extended Burnups," ANS International Topical Meeting, LWR Extended Burnup - Fuel Performance and Utilization, April 4-8, 1982, Williamsburg, Virginia.

1-11 R. G. Weber et al., "EPRI/C-E Fuel Performance Evaluation Program, RP 586-1 Task B: Examination of Arkansas Nuclear One Unit 2 Characterized Fuel Assemblies After Cycle 1," CENPSD-174, Combustion Engineering, Inc., to be issued.

1-12 U. Decher, "The Evaluation and Demonstration of Methods for Improved Nuclear Fuel Utilization - First Semi Annual Progress Report: January-June 1980," DOE/ET/340113-1 and CEND-384, Combustion Engineering,Inc., October 1980.

1-13 U. Decher, "The Evaluation and Demonstration of Methods for Improved Nuclear Fuel Utilization - Second Semi Annual Progress Report: July 1 to December 31, 1980," DOE/ET/34013-2 and CEND-388, Combustion Engineering, Inc., April 1981.

1-14 U. Decher, "The Evaluation and Demonstration of Methods for Improved Fuel Utilization - First Semi Annual Progress Report: October 1979 - March 1980," COO-34010-1 and CEND-382, Combustion Engineering, Inc., June 1980.

1-15 U. Decher, "The Evaluation and Demonstration of Methods for Improved Fuel Utilization - Third Semi Annual Progress Report: October 1, 1980 to March 31, 1981," DOE/ET/34010-4 and CEND-390, Combustion Engineering, Inc., June 1981.

1-16 F. Garzarolli et al., "C-E/KWU/EPRI Waterside Corrosion of Zircaloy Clad Fuel Rods, RP 1250-1 Interim Report: Review of PWR Fuel Rod Waterside Corrosion Behavic·," CENPSD-79, Electric Power Research Institute, June 1979.

1-17 F. Garzarolli, "C-E/KWU/EPRI Waterside Corrosion of Zircaloy Clad Fuel Rods, RP 1250-1 Interim Report: Recent PWR Waterside Corrosion Data Acquisition and Review of Clad Surface Temperature Calculation," CENPSD-140, Combustion Engineering, Inc. June 1981.

1-18 T. E. Hollowell et al., "The International OVER-RAMP Project at Studsvik," ANS International Topical Meeting, LWR Extended Burnup - Fuel Performance and Utilization , April 4-8, 1982, Williamsburg, Virginia.

1-19 S. R. Pati et al., "Fission Gas Release from PWR Fuel Rods Under Conditions of Normal Operation and Power Ramping," ANS International Topical Meeting, LWR Extended Burnup - Fuel Performance and Utilization, April 4-8, 1982, Williamsburg, Virginia.

1-20 H. Mogard, "The Status of International Fuel Performance Programs: C. SUPER-RAMP, DEMO-RAMP I, DEMO-RAMP II," ANS International Topical Meeting, LWR Extended Burnup - Fuel Performance and Utilization , April 4-8, 1982, Williamsburg, Virginia.

1-21 Letter from Mr. Holzer and Dr. Stehle (KWU) to Dr. R. O. Meyer (USNRC), "Power Ramp Testing of HFR Petten KWU/C-E Test Data," dated February 13, 1981.

1-22 J. C. LaVake an N. Gaertner, "High Burnup PWR Ramp Test Program: First Semi-Annual Progress Report for the Period October 1980 to March 1981,", DOE/ET/34030-1 and CEND-395, Combustion Engineering, Inc., October 1981.

1-23 M. D. Freshley, "The Investigation of High Burnup Effects in Sintered UO_2 Pellet Fuel with Emphasis on Fission Gas Release - Program Plan (Revision 3)," Battelle Pacific Northwest Laboratories, May 1981.

1-24 "OECD Halden Reactor Project Quarterly Progress Report January to March 1975," HPR 181, Institutt for Atomenergi, OECD Halden Reactor Project, May 1975.

1-25 R. A. Matzie et al., "Licensing Assessment of PWR Extended-Burnup Fuel Cycles," CEND-381, Combustion Engineering, Inc., March 1981.

Section 2 References

2-1 "System 80™ Standard Safety Analysis Report, Final Safety Analysis Report (CESSAR FSAR)," STN-50-470F, Combustion Engineering, Inc., October 1978.

2-2 "Calvert Cliffs Nuclear Power Plant, Final Safety Analysis Report for Units 1 and 2," Docket No. 50-317, Baltimore Gas and Electric Company, September 10, 1971.

Section 3 References

3-1 "Standard Review Plan (SRP), Section 4.2, Fuel System Design," NUREG-0800, U.S. Nuclear Regulatory Commission, July 1981.

3-2 "System 80™ Standard Safety Analysis Report, Final Safety Analysis Report (CESSAR FSAR)," STN-50-470F, Combustion Engineering, Inc., October 1978.

3-3 "Structural Analysis of Fuel Assemblies for Seismic and Loss of Coolant Accident Loading," CENPD-178-P, Rev. 1-P, Combustion Engineering, Inc., August 1981.

Section 4 References

4-1 "C-E Fuel Evaluation Model Topical Report," CENPD-139 with its revisions and supplements, Combustion Engineering, Inc., July 1974.

4-2 S. S. Manson, "Fatigue: A Complex Subject - Some Simple Approximations," Experimental Mechanics, 11 (2), 193, July 1965.

4-3 System 80™ Standard Safety Analysis Report Final Safety Analysis Report (CESSAR FSAR), STN-50-470F, Combustion Engineering, Inc., October 1978.

4-4 F. Garzarolli et al., "C-E/KWU/EPRI Waterside Corrosion of Zircaloy Clad Fuel Rods, RP 1250-1 Interim Report: Review of PWR Fuel Rod Waterside Corrosion Behavior," June 1979, CENPSD-79, Combustion Engineering, Inc., to be reprinted as an EPRI publication.

4-5 F. Garzarolli et al., "C-E/KWU/EPRI Waterside Corrosion of Zircaloy Clad Fuel Rods, RP 1250-1 Interim Report: Recent PWR Waterside Corrosion Data Acquisition and Review of Clad Surface Temperature Calculation," CENPSD-140, Combustion Engineering, Inc., June 1981.

4-6 U. Decher, "The Evaluation and Demonstration of Methods for Improved Fuel Utilization - First Semi Annual Progress Report: October 1979 - March 1980," COO-34010-1 and CEND-382, Combustion Engineering, Inc., June 1980.

4-7 D. Franklin et al., "LWR Core Material Performance Program: Progress in 1979-1980," EPRI NP-1770-SR, Electric Power Research Institute, March 1981.

4-8 U. Decher, "The Evaluation and Demonstration of Methods for Improved Nuclear Fuel Utilization - First Semi Annual Progress Report: January-June 1980," DOE/ET/340113-1 and CEND-384, Combustion Engineering,Inc., October 1980.

4-9 W. R. Smalley, "Evaluation of Saxton Core III Fuel Materials Performance," WCAP 3385-57, Westinghouse Electric Corporation, Nuclear Fuel Division, July 1974.

4-10 W. R. Smalley, "Saxton Core II Fuel Performance Evaluation, Part I: Materials," WCAP-3385-56, Part 1, Westinghouse Electric Corporation, Nuclear Fuel Division, September 1971.

4-11 "Improvements to Fuel Evaluation Model," CEN-161(B)-P, Combustion Engineering, Inc., July 1981.

4-12 D. E. Bessette et al., "C-E/EPRI Fuel Performance Evaluation Program: RP 586-1 Task A, Examination of Calvert Cliffs I Test Fuel Assemblies at End of Cycles 1 and 2," CENPSD-72, Combustion Engineering, Inc., September 1978.

4-13 E. J. Ruzauskas et al., "C-E/EPRI Fuel Performance Evaluation Program: RP 586-1 Task A, Examination of Calvert Cliffs I Test Fuel Assembly After Cycle 3," CENPSD-87, Combustion Engineering, Inc., September 1979.

4-14 E. J. Ruzauskas et al., "C-E/EPRI Fuel Performance Evaluation Program: RP 586-1 Task A, Examination of Calvert Cliffs I Test Fuel Assembly After Cycle 4," CENPSD-146, Combustion Engineering, Inc., October 1981.

4-15 "CEPAN Method of Analyzing Creep Collapse of Oval Cladding," CENPD-187, Combustion Engineering, Inc., March 1976.

4-16 "Statistical Approach to Analyzing Creep Collapse of Oval Fuel Rod Cladding Using CEPAN," CEN-182(B), Combustion Engineering, Inc., September 1981.

4-17 F. J. Berte, "The Application of Monte Carlo and Bayesion Probability Techniques to Flow Prediction and Determination", TIS-5122, Combustion Engineering, Inc., February 1977.

4-18 J. F. Mclehan, "Yankee Core Evaluation Program, Final Report," WCAP-3017-6094, Westinghouse Atomic Power Division, January 1971.

4-19 R. L. Knecht and P. J. Pankaskie, "Zircaloy 2 Pressure Tubing," BNWL-746, Battelle Pacific Northwest Laboratory, December 1968.

4-20 L. M. Howe and W. R. Thomas, "The Effects of Neutron Irradiation on the Tensile Properties of Zircaloy 2," AECL-809, Atomic Energy of Canada Ltd., March 1959.

4-21 J. E. Irvin, "Effects of Irradiation and Environment on the Mechanical Properties and Hydrogen Pickup of Zircaloy," Zirconium and Its Alloys, Electrochemical Society, New York, NY, 1966.

4-22 W. A. Pavinich and T. P. Papazoglou, "Hot Cell Examination of Creep Collapse and Irradiation Growth Specimens - End of Cycle 3," LRC-4733-8, Babcock and Wilcox Co., March 1980.

4-23 F. A. Nichols, "Evidences for Enhanced Ductility During Irradiation Creep," Mater. Sci. Eng, 6, 167 (1970).

4-24 E. F. Ibrahim and C. E. Coleman, "The Effect of Stress Sensitivity on Stress Rupture Ductility of Zircaloy 2 and Zr-2.5 wt% Nb," Can. Met. Quart., 12, 285 (1973).

4-25 E. F. Ibrahim, "Creep Ductility of Cold-Worked Zr-2.5 wt% Nb and Zircaloy-2 Tubes In-Reactor," J. Nucl. Mat., 96, 297 (1981).

4-26 D. S. Wood, "High Deformation Creep Behavior of 0.6 in. Diameter Zirconium Alloy Tubes Under Irradiation," ASTM-STP-551, 274 (1974).

4-27 W. Evans and G. W. Parry, "The Deformation Behavior of Zircaloy-2 Containing Directionally Oriented Zirconium Hydride Properties, " Electrochem. Tech., 4, 225 (1966).

4-28 B. Watkins et al., "Embrittlement of Zircaloy-2 Pressure Tubes," Applications Related Phenomena for Zirconium and Its Alloys, ASTM-STP-458, 1968.

4-29 D. E. Bessette et al., "CE/EPRI Fuel Performance Evaluation Program RP586-1 Task A: Examination of Calvert Cliffs I Test Fuel Assemblies at End of Cycles 1 and 2," CENPSD-72, Combustion Engineering, Inc., September 1978.

4-30 E. J. Ruzauskas et al., "C-E/EPRI Fuel Performance Evaluation Program: RP 586-1 Task A, Examination of Calvert Cliffs I Test Fuel Assembly After Cycle 3," CENPSD-87, Combustion Engineering, Inc., September 1979.

4-31 E. J. Ruzauskas et al., "CE/EPRI Fuel Performance Evaluation Program, RP586-1 Task A: Examination of Calvert Cliffs I Test Fuel Assembly After Cycle 4," CENPSD-146, Combustion Engineering, Inc., October 1981.

4-32 S. R. Pati et al., "Fission Gas Release From PWR Fuel Rods Under Conditions of Normal Operation and Power Ramping," ANS Topical Meeting, LWR Extended Burnup-Fuel Performance and Utilization, April 4-8, 1982, Williamsburg, Virginia.

4-33 H. Zimmermann, "Investigation of Swelling and Fission Gas Retention on Oxide Nuclear Fuel Under Neutron Irradiation," Kernforschungszentrum, Karlsruhe, KFK-2467, June 1977.

4-34 H. Zimmermann, "Investigation of Swelling and Fission Gas Behavior in Uranium Dioxide," J. Nucl. Mat., 75, 154 (1978).

4-35 S. R. Pati, "C-E/EPRI Fuel Performance Evaluation Program, RP 586-1 Task A: Gas Release and Microstructural Evaluation of One- and Two-Cycle Fuel Rods from Calvert Cliffs I," CENPSD-75, Combustion Engineering, Inc., December 1980.

4-36 S. R. Pati, "C-E/EPRI Fuel Performance Evaluation Program, RP 586-1 Task A: Gas Release and Microstructural Evaluation of Three-Cycle Fuel Rods from Calvert Cliffs I," CENPSD-119, Combustion Engineering, Inc., December 1980.

4-37 T. Hollowell et al., "The International Over-Ramp Project at Studsvik," ANS Topical Meeting, LWR Extended Burnup-Fuel Performance and Utilization, April 4-8, 1982, Williamsburg, Virginia.

4-38 American Nuclear Society Licensing Group 5.4 and U.S. Nuclear Regulatory Commission, "Background and Derivation of ANS 5.4 Standard Fission Product Release Model," compiled by Southern Science Applications, Inc., NUREG/CR-2507, January 1982.

4-39 F. Sontheimer et al., "Correlating Fission Gas Release Due to Power Ramping with Observed Microstructural Changes in the Fuel by Use of a Simple Diffusion Model," paper presented at The Enlarged Halden Programme Group Meeting on Water Reactor Fuel Performance, June 14-19, 1981 (Proprietary).

4-40 J. B. Ainscough et al., "Isothermal Grain Growth Kinetics in Sintered UO_2 Pellets," J. Nucl. Mat., 49, 117 (1973/74).

4-41 R. G. Bellamy and J. B. Rich, "Grain-Boundary Gas Release and Swelling in High Burnup Uranium Dioxide," J. Nucl. Mat.,33, 64 (1969).

4-42 M. F. Lyons et al., "UO_2 Properties Affecting Performance," Nuclear Engineering and Design, 21, 167 (1972).

4-43 S. Y. Ogawa, E. A. Lees and M. F. Lyons, "Power Reactor High Performance UO_2 Program - Fuel Design Summary and Program Status," GEAP-5591, Nuclear Fuels Department, General Electric Co., January 1968.

4-44 C. R. Hann et al., "GAPCON-Thermal-1: A Computer Program for Calculating the Gap Conductance in Oxide Fuel Pins," BNWL-1778, Battelle Pacific Northwest Laboratories, September 1973.

4-45 S. R. Pati and N. Fuhrman, "Densification, Swelling and Microstructure of LWR Fuels Through Extended Burnups," ANS International Topical Meeting: LWR Extended Burnup - Fuel Performance and Utilization, April 4-8, 1982, Williamsburg, Virginia.

4-46 J. A. Christensen et al., "Melting Point of Irradiated Uranium Dioxide," Trans. Am. Nucl. Soc., 7 (2), 390 (1964).

4-47 J. G. Reavis and J. L. Green, "Transformation Temperatures of Irradiated UO_2-PuO_{22} Fast Reactor Fuels," Trans. Am. Nucl. Soc.

4-48 J. L. Krankota and C. N Craig, "Melting Point of High Burnup PuO-UO_2," Trans. Am. Nucl. Soc., 11, 132 (1968).

4-49 D. L. Hagrman et al., "MATPRO-Version 11 (Revision 1) - A Handbook of Materials Properties for Use in the Analysis of Light Water Reactor Fuel Rod Behavior," NUREG/CR-0497, TREE-1280, Rev. 1, R3 and R4, EG&G Idaho, Inc., Idaho Falls, Idaho, February 1980.

4-50 R. C. Daniel et al., "Effects of High Burnup on Zircaloy Bulk UO_2 Plate Fuel Element Samples," WAPD-263, Westinghouse Electric Corporation, September 1962.

4-51 H. Assmann and R. Manzel, "The Matrix Swelling Rate of UO_2," J. Nucl. Mat., 68, 360 (1977).

4-52 N. Fuhrman and P. A. VanSaun, "Densification annd Swelling Behavior of Two- and Three-Cycle UO_2 Fuels From Calvert Cliffs I," CENPSD-135, Combustion Engineering, Inc., March 1961.

4-53 P. Knudsen and C. Bagger, "Power Ramp and Fission Gas Performance of Fuel Pins M20-1B and T9-3B, "Riso National Laboratory (Denmark) Report Riso-M-2151, December 1978.

4-54 C. Bagger, H. Carlsen and P. Knudsen, "Details of Design, Irradiation and Fission Gas Release for the Danish UO_2-Zr Irradiation Test 022," Riso National Laboratory (Denmark) Report Riso-M-2152, December 1978.

4-55 "Fuel and Poison Rod Bowing," CENPD-225-P and Supplements, Combustion Engineering, Inc., October 1976.

4-56 "Responses to First Round Questions on CENPD-225-P, Fuel and Poison Rod Bowing," Attachment to LD-81-073, letter from A. E. Scherer (C-E) to R. L. Tedesco (NRC) dated October 2, 1981.

4-57 Florida Power and Light Company, St. Lucie Plant - Unit No. 1, Final Safety Analysis Report, Volume 5, Section 4.2 "Mechanical Design".

4-58 Final Safety Analysis Report, San Onofre Nuclear Generating Station, Units 2 and 3, Section 4.2 "Fuel System Design".

4-59 A. J. Anthony, "Results of the Flow Test of a 16x16 Fuel Assembly," PED 76-003P, Combustion Engineering, Inc., December 1976.

4-60 N. Fuhrman et al., "Evaluation of Fuel Rod Performance in Maine Yankee Core 1 - Task C," EPRI NP-218, Electric Power Research Institute, November 1976.

4-61 J. C. LaVake and G. P. Smith, "Evaluation and Demonstration of Methods for Improved Fuel Utilization - Fort Calhoun Fuel Inspection Programs, End-of-Cycles 4 and 5," DOE/ET/34010-2, CEND-383, Combustion Engineering, Inc., August 1980.

4-62 L. V. Corsetti et al., "Maine Yankee EOC-4; Summary of Fuel Inspection Results," CENPSD-99-P, Combustion Engineering, Inc., March 1980.

4-63 R. G. Weber et al., "EPRI/C-E Fuel Performance Evaluation Program, RP586-1 Task B: Examination of Arkansas Nuclear One Unit 2 Characterized Fuel Assemblies After Cycle 1," CENPSD-174, Combustion Engineering, Inc., to be issued.

4-64 "Agreement on the Studsvik Super-Ramp Project Through the Period April 1, 1980 to December 31, 1982," Studsvik Energiteknik AB, Sweden, December 1980.

4-65 J. C. LaVake annd M. Gaertner, "DOE High Burnup PWR Ramp Test Program - Topical on Background Ramp Test Data," DOE/ET/34030-3, Combustion Engineering, Inc., to be issued.

4-66 "Standard for Protection Against Radiation," United States Nuclear Regulatory Commission, Rules and Regulations, Title 10, Chapter 1, Code of Federal Regulations - Energy, Part 20, May 1977.

4-67 "Licensing of Production and Utilization Facilities," United States Nuclear Regulatory Commision, Rules and Regulations, Title 10, Chapter 1, Code of Federal Regulations - Energy, Part 50, May 1977.

4-68 "Reactor Site Criteria," United States Nuclear Regulatory Commission, Rules and Regulations, Title 10, Chapter 1, Code of Federal Regulations - Energy, Part 100, May 1977.

4-69 "Licensing of Production and Utilization Facilities," United States Nuclear Regulatory Commission, Rules and Regulations, Title 10, Chapter 1, Code of Federal Regulations - Energy, Part 50, Appendix K, "ECCS Evaluations Models," May 1977.

4-70 Enclosure 1-P of Letter LD-81-095, from A. E. Scherer (C-E) to Mr. J. R. Miller (NRC) dated December 15, 1981.

4-71 D. A. Powers and R. O. Meyer, "Cladding Swelling and Rupture Models for LOCA Analyses," NRC report NUREG-0630, April 1980.

4-72 STRIKIN-II, A Cylindrical Geometry Fuel Rod Heat Transfer Program (Modifications)," CENPD-135P, Supplement 2, Combustion Engineering, Inc., February 1975.

4-73 R. A. Matzie et al., "Licensing Assessment of PWR Extended-Burnup Fuel Cycles," CEND-381, Combustion Engineering, Inc., March 1981.

4-74 P. Hofman, "Influence of Iodine on the Strain and Rupture Behavior of Zircaloy-4 Cladding Tubes at High Temperatures," Zirconium in the Nuclear Industry, ASTM STP 681, American Society for Testing and Materials, 409 (1979).

4-75 J. M. Broughton et al., "PBF LOCA Test Series, Test S LOC-3 and LOC-5, Fuel Behavior Report," NUREG/CR-2073, EGG-2094, June 1981.

4-76 E. H. Karb et al., "KFK In-Pile Tests on LWR Fuel Rod Behavior During the Heatup Phase of a LOCA," KFK 3028, October 1980.

4-77 T. R. Yackle et al., "An Evaluation of the Thermal-Hydraulic Response and Fuel Rod Thermal and Mechanical Behavior During the Power Burst Facility Test LOC-3," ANS Fuel Topical Meeting, April 1980, Knoxville, Tennessee.

4-78 P. E. MacDonald, R. K. McCordell, "Results of Power Burst Facility Appendix K Tests," Ninth Water Reactor Safety Research Information Meeting, October 1981, Gaithersburg, Maryland.

4-79 "Calculational Methods for the C-E Large Break LOCA Evaluation Model," CENPD-132-P Sup. 1, Combustion Engineering, Inc., February 1975.

4-80 "In-Reactor Dimensional Changes in Zircaloy-4 Fuel Assemblies," CENPD-198-P, Combustion Engineering, Inc., December 1975.

4-81 D. G. Franklin, "Zircaloy-4 Cladding Deformation During Power Reactor Irradiation," Fifth Symposium on Zirconium in Nuclear Applications, ASTM, August 4-7, 1980, Boston, MA.

4-82 "Reactor Operation With Guide Tube Wear," CEN-79, Combustion Engineering, Inc., Combustion Engineering, Inc., February 3, 1978.

4-83 "Maine-Yankee Reactor Operation With Modified CEA Guide Tubes," CEN-93(M), Combustion Engineering, Inc., June 21, 1978.

4-84 "Calvert Cliffs II Cycle 2 Reload Submittal Update," CEN-101(B), Combustion Engineering, Inc., August 21, 1978.

4-85 "Description of Modified Assemblies in Calvert Cliffs-1 Cycle 5," CEN-138(B), Combustion Engineering, Inc., September 1980

4-86 Response to Question 231.32 on the San Onofre Units 2 and 3 Final Safety Analysis Report.

4-87 Letter, A. E. Scherer to Robert A. Clark, "Slides From NRC Meeting of April 30, 1980", dated April 30, 1980 (LD-80-019).

4-88 "End of Cycle 4 Eddy Current Inspection Results: 1980 Calvert Cliffs-1 Refueling Outage," CEN-146(B), Combustion Engineering, Inc., December 22, 1980.

4-89 "Arkansas Nuclear One Unit 2 1981 Refueling Outage: Fuel and CEA Eddy Current Inspection Report," CEN-163(A), Combustion Engineering, Inc., September 1981.

4-90 Letter, A. E. Scherer to James R. Miller, "Slides Presented at September 24, 1981 Meeting on System 80 Guide Tube Wear Resolution," October 2, 1981 (LD-81-066).

4-91 "Application of CENPD-198 to Zircaloy Component Dimensional Changes," CEN-183(B), Combustion Engineering, Inc., September 1981.

4-92 B. Z. Hyatt, "Degradation of the Stress Relaxation Properties of Selected Reactor Materials in a Fast-Neutron Flux," WAPD-TM-881(L), Bettis Atomic Power Laboratory, March 1973.

4-93 H. Stehle, W. Kaden and R. Manzel, "External Corrosion of Cladding in PWRs," Nuclear Engineering and Design, 33, 155 (1975).

4-94 R. P. Marshall and M. R. Louthan, Jr., "Tensile Properties of Zircaloy With Oriented Hydrides," Trans. ASM, 56, 693 (1963).

4-95 R. L. Mehan and F. W. Wiesinger, "Mechanical Properties of Zircaloy-2," KAPL-2110, Knolls Atomic Power Laboratory, February 1, 1961.

4-96 G. W. Keilholtz and R. E. Moore, "Irradiation Damage to Aluminum Oxide Exposed to 5×10^{21} Fast Neutrons/Cm^2," Nuclear Applications, 3, 686, November 1967.

4-97 G. E. Russcher and A. L. Pitner, "Empirical Helium Release Function From Thermal Reactor Irradiated Boron Carbide," Nuclear Technology 16, 208, October 1972.

4-98 F. J. Homan, "Performance Modeling of Neutron Absorbers," Nuclear Technology, 16, 216, October 1972.

Section 5 References

5-1 R. A. Matzie et al., "Licensing Assessment of PWR Extended-Burnup Fuel Cycles," CEND-381, Combustion Engineering, Inc., March 1981.

5-2 Letter from L. S. Rubenstein (Core and Containment Systems, Division of Systems Integration, USNRC) to A. E. Scherer (Combustion Engineering) dated June 2, 1981.

COMBUSTION ENGINEERING, INC.